Integrating Multimodal Sensors and Simulation Models for Optimized Dairy Barn Microclimate Management

By

Dimuth V. Panditharatne

A dissertation submitted in partial fulfillment of

the requirements for the degree of

Doctor of Philosophy

(Biological Systems Engineering)

at the

UNIVERSITY OF WISCONSIN-MADISON

2026

Date of final oral examination: 12/10/2025

The dissertation is approved by the following members of the Final Oral Committee:

Christopher Y. Choi, Professor, Biological Systems Engineering

Neslihan Akdeniz Onuki, Assistant Professor, Biological Systems Engineering

Matthew Digman, Assistant Professor, Biological Systems Engineering

Zhou Zhang, Associate Professor, Biological Systems Engineering

DEDICATION

This dissertation is dedicated to my parents, Saliya and Dinusha Panditharatne. Their sacrifices, patience, and unconditional support shaped not only my education but also my character. They encouraged resilience in moments of uncertainty and humility in moments of success. I am deeply grateful for the foundation they provided and for the perseverance they instilled in me. This achievement is as much theirs as it is mine.

ACKNOWLEDGEMENTS

I am deeply indebted to my advisor, Professor Christopher Y. Choi, whose mentorship has defined my graduate experience. His guidance and high standards have not only shaped this research but have also fundamentally influenced my professional growth. I also thank my committee members, Dr. Matthew Digman, Dr. Nesli Akdeniz, and Dr. Zhou Zhang, for their thoughtful critique and steady encouragement.

This work would not have been possible without the support of many dedicated individuals. I specifically thank Kody Habeck and Jeff Nelson from Biological Systems Engineering for their help, as well as the staff at the Emmons Blaine Arlington Dairy Research Center, especially Michael Grott, Tony Ziemke, and Jessica Cederquist, for their essential assistance with animal care and the logistical complexities of our experiments.

I am also grateful for the camaraderie of my colleagues, Sahitha Karapitiya, Trey Standiford, Nilroth Ly, and Hanwook Chung, who made the research group a supportive and inspiring place to work. Also, special thanks to Dr. Younghyun Kim and his group, especially Hien Vu and Unmesh Raskar, for their pivotal support for my work.

Lastly, my deepest thanks go to my wife, Miranda Salazar, and my brother, Naveen Panditharatne. Your unwavering love, patience, and confidence in me gave me the strength to navigate the challenges of this degree. Thank you for making this achievement possible.

ABSTRACT

Heat stress has become a defining constraint for dairy production as herds grow, summers intensify, and expectations for animal welfare and energy stewardship rise. Most ventilation strategies regulate the barn macro-environment, yet the decisive heat and momentum exchanges occur in the animal-occupied zone at the stall and cow scales. This dissertation advances an animal-centric framework for microclimate management that links direct indicators of heat load to targeted airflow delivery. The work integrates sensing, modeling, and ventilation design to direct cooling to the appropriate location and time, with the appropriate intensity, while ensuring practical deployment in working freestall barns.

Chapter 1 introduces the problem space, motivates an animal-based approach to cooling control, and outlines design principles for precision airflow in freestall housing. The principles emphasize three pillars. First, prioritize measurements that reflect the animal's physiological and behavioral state over coarse barn averages. Second, direct momentum towards the stall microenvironment rather than relying on whole-barn air exchange. Third, prepare control logic that can be integrated with commercial hardware and realistic farm workflows.

Chapter 2 develops a sensing and data-integration pipeline that aligns individual-level physiology, behavior, and microclimate. This study combines ultra-wideband localization, inertial data, and computer vision for behavior inference with high-resolution core body temperature and temperature-humidity measurements in the pen. Using behavior inferred through non-invasive sensing, this chapter explores the next step of using these behaviors to detect heat stress in dairy cows as a heat alarm.

Chapter 3 investigates stall-scale airflow management through modifications to stall arrangement to enhance convective cooling at the cow. The work builds on concepts investigated in prior studies, including staggered stall layouts and the use of baffles, and frames them within a design space

accessible to both new construction and retrofits. A retrofit-friendly stall modification is introduced and conceptually compared with the traditional inline configuration, staggered configurations, and arrangements that incorporate baffles. The focus is on how layout choices can steer airflow toward resting cows while remaining compatible with practical constraints in commercial facilities.

Chapter 4 advances precision, cow-level cooling by building and evaluating a positive-pressure plenum ventilation system under real farm conditions. Earlier studies examined targeted jets primarily through computational analyses and prototype trials in controlled environments; this chapter situates the concept in a production dairy during natural summer heat. It defines the system architecture, the jet delivery strategy, and a measurement protocol that maps airflow within the animal-occupied zone while continuously recording microclimate, physiology, and behavior.

Chapter 5 synthesizes the dissertation's contributions and maps a path from research to application. It presents three core assets: a deployable sensing and validation stack that yields direct, cow-level heat stress indicators; a design and evaluation framework for stall-scale airflow management that clarifies how layout and airflow parameters shape conditions in the animal-occupied zone; and an in-barn evaluation of a targeted ventilation concept that establishes the methods and datasets from which smart, individual, cow-centric cooling can emerge, guided by parameters explored in simulation and strengthened by advances in sensing. Together, these elements provide a foundation for intelligent, animal-centric ventilation design and control that is responsive to animals, compatible with operational realities, and oriented toward improved animal welfare and barn energy performance.

CONTENTS

CHAPTER 1: INTRODUCTION

1.1. Background and Motivation

Heat stress is one of the most persistent biological and economic constraints in modern dairy production. When environmental heat load exceeds a cow's capacity to dissipate heat, physiological and behavioral compensations, tachypnea, reduced feed intake, altered time budgets, and shifts in lying and standing translate rapidly into depressed milk yield, impaired reproduction, and elevated health risk (West, 2003; Polsky & von Keyserlingk, 2017). Industry-wide losses have been estimated in the hundreds of millions to billions of dollars annually in the United States alone, underscoring the scope for both welfare and profitability gains from better heat abatement (St-Pierre et al., 2003). These pressures intensify as herds scale up, per-cow milk output rises, and summers trend hotter, raising the practical bar for delivering adequate cooling to all stalls and pens throughout the day. The scientific and extension literature converge on a central insight: managing the macro-environment of a barn is necessary but not sufficient; the decisive exchanges of heat, momentum, and moisture occur in the animal-occupied zone at stall height, where cows rest and ruminate. Improvements in barn-level averages can coexist with pockets of insufficient airflow at the cow, which is precisely where heat load must be relieved.

1.2. Limitations of Conventional Indicators and Cooling Strategies

Conventional practice has long relied on environmental indices, especially the Temperature-Humidity Index (THI), and on downstream production responses such as milk yield to detect and manage heat load. Both are valuable, but they are either lagging or incomplete. THI is constructed from ambient air temperature and relative humidity; it does not include wind speed, solar radiation, or the substantial animal-to-animal heterogeneity that shifts susceptibility thresholds with production level, parity, breed,

and acclimation. Empirically, THI thresholds for performance losses vary by climate, facility, and metric; therefore, meaningful impacts can occur at lower THI in high-producing herds, which means that index-based triggers alone may not protect all cows equally or early enough (Bohmanova et al., 2007; review updates in Yan et al., 2021; Hendriks, 2025). Milk yield itself is a trailing indicator, reflecting accumulated thermal strain after the fact. For early protection, producers need signals that rise with cow-level thermal load before productivity drops. The literature also documents systematic differences between meteorological-station conditions, pen conditions, and the microclimates cows experience at the stall; these gaps become consequential for control when barns are large, and airflow is nonuniform. Thus, the limitations of macro-level environmental triggers motivate a complementary, animal-centric signal path.

At the same time, traditional abatement tools, natural ventilation, tunnel and cross-ventilation, and soaking, remain indispensable but often imprecise at delivering momentum to the animal-occupied zone. Reviews and CFD-validated field studies show that internal obstructions, pen geometry, and fan placement can produce stagnant or bypassed zones at stall level even when barn averages look adequate. Practical design modifications, baffles, deflectors, or changes in stall layout can steer airflow streams toward cows and improve AOZ velocities but must be tuned to each facility's geometry and pressure budget (Van Os, 2019; Pakari & Ghani, 2021; Zhou et al., 2019). The technical challenge, then, is not merely to move large volumes of air but to deliver the proper air speed to the right place at the right time, guided by signals that reflect the animal or stall rather than the barn.

1.3. An Animal-Centric Strategy for Early Detection and Targeted Control

A growing body of work argues for treating the cow as the primary sensor, with the environment as context rather than proxy. Early detection of heat stress is difficult if one relies only on rising THI or falling milk yield, because both can be late relative to the onset of harmful thermal load at the individual

cow. Physiological "gold standards" such as rectal, vaginal, or rumen-reticular temperature can quantify core thermal status but are intrusive to collect manually, can increase handling stress, and are logistically impractical at scale for continuous monitoring in commercial herds; continuous devices like rumen boluses and intravaginal loggers can help in research or select herds but still face adoption constraints and maintenance costs (Idris et al., 2021; Bang et al., 2022; Shu et al., 2021). By contrast, behavior and posture respond quickly to heat: cows stand more, lie less, and alter time budgets as heat load increases, providing timely cues amenable to automation. This motivates a sensing stack that fuses more practical, low-cost modalities, accelerometer, ultra-wideband (UWB) localization, and computer vision, with pen-level environmental data to infer heat stress risk at the cow level and to trigger cooling before performance losses accrue. Recent validations show that accelerometer tags reliably detect rumination, eating, lying, and activity patterns; UWB real-time location systems can resolve pen-level trajectories and lying/standing bouts; and vision models can classify feeding and occupancy non-invasively. A pragmatic composite that blends these sources with THI and other ambient measures can deliver a low-cost, labor-saving pipeline for early warning in working barns.

This dissertation adopts the animal-centric strategy in Chapter 2. We formalize a deployable pipeline that integrates neck or ear-tag accelerometry for behavior, UWB for position and movement context, and computer vision, where feasible, to observe feeding and occupancy, all synchronized with pen-level THI. We justify this mix on three grounds. First, it addresses the practical obstacles to continuous core body temperature measurement in commercial settings while still tracking near-term physiological risk through behavior. Second, it provides granularity at the cow rather than just the pen or barn, counteracting the averaging that can mask vulnerable animals. Third, the stack uses commodity hardware and existing infrastructure, preserving a low cost for barn ownership and minimizing additional labor. Within this framework, we develop and validate an early-warning model that flags

elevated heat risk using behavioral precursors and ambient context rather than waiting for milk yields to fall or THI to breach a single global threshold.

1.4. From Design Physics to Field-Scale Targeted Ventilation

As previously mentioned, cow-level signals need to be translated into airflow that reaches the cows, as explored in Chapter 4, which focuses on targeted cooling of the cow. However, passive cooling strategies are also pivotal, as they require the least farmer intervention when cows are hot. Modified stall arrangements and baffles are passive cooling techniques explored in Chapter 3, along with another innovative passive strategy for existing dairy barns: the use of in-stall deflectors. Chapter 3 uses computational fluid dynamics, validated against measurements, to quantify how stall-scale geometry and flow-redirecting components determine AOZ velocities, uniformity, and static-pressure costs. Across large freestall facilities, both modeling and experiments reveal microenvironments, stagnant pockets, and path-of-least-resistance bypass, that degrade cooling precisely at the stall. We evaluate retrofit-friendly options, including staggered stall alignments, retractable or fixed baffles, and deflectors, to more uniformly steer jets into resting zones. The goal is actionable design guidance that raises stall-level air speeds without wasteful increases in total fan power.

Chapter 4 advances a targeted, positive-pressure precision ventilation (PPPV) approach that decouples cow-level delivery from whole-barn exchange. In PPPV, a pressurized plenum feeds an array of nozzles that meter jet momentum directly into each stall's AOZ. Recent development work and CFD studies show the potential to produce repeatable, perpendicular jets with predictable throw and impingement, thereby reducing dependence on room-scale flow patterns and improving uniformity across pens. Building on Chung (2023), a framework for microclimate control, we design and operate a PPPV system in a working dairy barn and evaluate responses in microclimate, behavior, and production, using energy-normalized metrics to compare with conventional cross- or tunnel-type

systems. This chapter is not a repudiation of established methods; fans and soaking remain essential where appropriate, but a demonstration that precision momentum delivery can complement them, especially for ensuring that every lying cow feels the air.

1.5. Objectives and Significance

The overarching objective of this dissertation is to shift heat stress management in freestall dairies from coarse, barn-level environmental triggers toward animal-centered, sensor-driven control that measures what individual cows experience and delivers cooling where it matters most, namely at the stall and at the cow's body surface (West, 2003; Polsky and von Keyserlingk, 2017). To achieve this, the work builds a pipeline that begins with automated detection of behavior-based heat stress, proceeds through stall-scale airflow design, and culminates in the field evaluation of a targeted, positive-pressure ventilation system.

A central premise of the dissertation is that core body temperature (CBT) is the most direct physiological indicator of heat load, but that continuous internal temperature monitoring is invasive, expensive, and difficult to scale for routine herd management (Atkins et al., 2018; Mondaca and Cook, 2018). Accordingly, CBT is used here as a reference signal and ground truth for model development and evaluation. At the same time, the operational heat alarm relies solely on non-invasive behavioral and microclimate features observable in real time. This distinction is essential: the goal is not to require CBT sensors for deployment, but to use CBT strategically to calibrate and validate behavior-based tools.

Within this overarching framework, the dissertation pursues three specific objectives:

1) Develop and validate a multimodal behavior sensing and integration pipeline for dairy cows. Chapter 2 fuses ultra-wideband (UWB) localization, collar accelerometers, and camera-based occupancy detection into a unified data stream synchronized with barn-level temperature–

humidity index (THI) (Vu et al., 2023; Moravčíková et al., 2024). The first aim is to classify key time-budget behaviors—lying, standing, feeding, and drinking—with high agreement to video labels. The second aim is to use these behavior time budgets, together with THI and spatial context, to train machine-learning models that estimate the probability that an individual cow's CBT will exceed a personalized high-temperature threshold in the near term. In deployment, the heat alarm model uses only behavior and environmental covariates as inputs, while CBT remains a physiology-forward label against which performance is judged.

2) Quantify how stall design influences cow-level convective heat transfer and airflow uniformity. Chapter 3 employs three-dimensional computational fluid dynamics (CFD), validated against barn-scale measurements, to compare conventional in-line stall rows with novel staggered configurations and in-stall deflectors (Mondaca and Choi, 2016; Zhou et al., 2019). The objective is to evaluate how stall geometry alters air-occupied-zone (AOZ) velocities, thermal boundary layers, and convective heat transfer coefficients around resting cows, and to identify practical designs that increase cow-level air speeds and reduce stagnant zones without prohibitive static-pressure penalties.
3) Field-test a positive-pressure plenum ventilation (PPPV) system for targeted cooling under commercial conditions. Chapter 4 designs and deploys a full-scale PPPV system that meters jet momentum directly into each stall via an array of nozzles, superimposed on the barn's existing ventilation infrastructure (Chung, 2023). The objective is to assess whether PPPV can deliver consistently high AOZ air speeds to lying cows across a hot weather event and whether this targeted cooling translates into measurable differences in CBT trajectories, lying behavior, and milk yield compared with an adjacent control pen, while remaining within realistic energy budgets.

Collectively, these objectives are significant for both dairy science and animal welfare engineering. They demonstrate that non-invasive behavior and location data, coupled with microclimate measurements, can serve as a reliable early-warning signal of heat stress, and that the resulting animal-centric metrics can guide stall-scale and pen-scale ventilation design. By integrating sensing, modeling, and field experimentation, the dissertation offers a blueprint for dairy barns in which cooling is triggered by the cows' own responses and delivered directly to where those cows rest and ruminate, rather than by barn-average indices alone (Atkins et al., 2018; Herzog et al., 2021).

References

Atkins, I., Cook, N. B., Mondaca, M. R., & Choi, C. Y. (2018). Continuous respiration-rate measurement of heat-stressed dairy cows and relation to environment, body temperature, and lying time. *Transactions of the ASABE, 61*, 1475–1485.

Bang, N. N., Cai, Z., Barwick, T., & Chen, C. (2022). Application of infrared thermal technology to assess the thermal status of dairy cows: A review. *Journal of Dairy Science, 105*(12), 9756–9773.

Bohmanova, J., Misztal, I., & Cole, J. B. (2007). Temperature-humidity indices as indicators of milk production losses due to heat stress. *Journal of Dairy Science, 90*(4), 1947–1956.

Brezov, D. et al. (2023). Predicting rectal temperature from non-invasive signals via multimodal learning. *Applied Sciences, 13*(20), 11416.

Chung, H. (2023). *Design and control of dairy housing microclimate using sensing and modeling* (Ph.D. dissertation). University of Wisconsin–Madison.

Cook, N. B., Mentink, R. L., Bennett, T. B., & Burgi, K. (2007). The effect of heat stress and lameness on time budgets of lactating dairy cows. *Journal of Dairy Science, 90*(4), 1674–1682.

Hendriks, S. J. (2025). Heat stress amelioration for pasture-based dairy cattle. *Animal Frontiers, 15*(2), 32–42.

Idris, M., Uddin, J., Sullivan, M., & McNeill, D. M. (2021). Non-invasive physiological indicators of heat stress in cattle: A review. *Animals, 11*(1), 71.

Jung, S., Wang, X., & Choi, C. Y. (2023). Using computational fluid dynamics to develop positive-pressure precision ventilation systems for large-scale dairy houses. *Journal of Thermal Biology, 112*, 103420.

McDonagh, J., Ranganathan, N., & Marchant-Ford, P. (2021). Detecting dairy cow behavior using vision technology: A review. *Agriculture, 11*(7), 675.

Mondaca, M. R., Choi, C. Y., & Cook, N. B. (2019). Understanding microenvironments within tunnel-ventilated dairy cow freestall facilities: Examination using computational fluid dynamics and experimental validation. *Biosystems Engineering, 183*, 70–84.

Pakari, A., & Ghani, S. (2021). Comparison of mechanical ventilation systems for dairy cow barns: CFD simulations and field measurements. *Computers and Electronics in Agriculture, 186*, 106207.

Pereira, G. M. et al. (2018). Validation of an ear-tag accelerometer sensor to determine rumination, eating, and activity in grazing dairy cows. *Journal of Dairy Science, 101*(3), 2492–2502.

Polsky, L., & von Keyserlingk, M. A. G. (2017). Invited review: Effects of heat stress on dairy cattle welfare. *Journal of Dairy Science, 100*(11), 8645–8657.

Reuscher, K. J., Stone, A. E., & Bewley, J. M. (2024). Consistent stall air speeds are associated with reduced variation in lying behavior during heat stress. *Frontiers in Animal Science, 4*, 1422937.

Shu, H., Lee, K., & Chung, Y. (2021). Recent advances on early detection of heat strain in dairy cows: A review. *Animals, 11*(5), 1299.

St-Pierre, N. R., Cobanov, B., & Schnitkey, G. (2003). Economic losses from heat stress by US livestock industries. *Journal of Dairy Science, 86*(Suppl), E52–E77.

Van Os, J. M. C. (2019). Considerations for cooling dairy cows with water. *Veterinary Clinics of North America: Food Animal Practice, 35*(1), 157–173.

West, J. W. (2003). Effects of heat stress on production in dairy cattle. *Journal of Dairy Science, 86*(6), 2131–2144.

Wu, D., Han, M., Song, H., Song, L., & Duan, Y. (2023). Monitoring the respiratory behavior of multiple cows based on computer vision and deep learning. *Journal of Dairy Science, 106*(4), 2963–2979.

Yan, G., Ouellet, V., Johansen, S., & Choi, C. Y. (2021). Evaluation of thermal indices as indicators of heat stress in dairy cows. *Animals, 11*(8), 2459.

Zhou, B., Wang, X., Mondaca, M. R., Rong, L., & Choi, C. Y. (2019). Assessment of optimal airflow baffle locations and angles in mechanically ventilated dairy houses using CFD. *Computers and Electronics in Agriculture, 165*, 104930.

Moravčíková, Á. et al. (2024). Validating ultra-wideband positioning systems for dairy cows in barns. *Sensors, 24*(14), 4763.

CHAPTER 2: AUTOMATED HEAT STRESS DETECTION IN DAIRY COWS FROM MULTIMODAL BEHAVIOR MONITORING

2.1. Abstract

This study presents a multimodal, behavior-driven framework for early detection of heat stress in dairy cows using only non-invasive sensors. Core body temperature (CBT) is the most direct physiological indicator of heat stress, but continuous internal temperature monitoring is invasive and impractical for routine use in commercial herds (Burdick et al., 2012; Lee et al., 2015). We therefore developed a cow-level heat-stress alarm that relies solely on behavioral and microclimate features, while using CBT exclusively as ground truth for physiological heat load. Dairy cows were instrumented with ultra-wideband (UWB) tags and accelerometers for continuous monitoring of standing, lying, feeding, and drinking, complemented by barn-level measurements of temperature–humidity index (THI). Video annotations (156 h) provided behavior ground truth, and vaginal CBT loggers provided high-resolution physiological data under naturally occurring summer heat. We first validated sensor-based behavior classification against video labels, achieving high agreement across behaviors. We then quantified how behavior and THI patterns differ between hours with normal vs elevated CBT and trained machine-learning models to classify each cow-hour as heat-stressed or not based solely on behavioral and environmental inputs. The resulting behavior-based alarm detects high-CBT hours by approximately three times the rate of random screening, demonstrating that time budgets for standing, lying, feeding, and drinking, contextualized by THI and UWB-derived location, can reliably flag periods of physiological heat stress without direct temperature sensing. These findings support the use of real-time behavior monitoring as a practical, scalable strategy for early heat-stress detection and targeted intervention in precision dairy systems.

2.2. Introduction

In the dairy industry, cow welfare is of critical importance, not only from an ethical standpoint but also because of its significant economic implications. High-producing dairy cows are frequently exposed to various stressors, with heat stress among the most detrimental. Elevated ambient temperatures adversely affect milk yield, reproduction, and overall health, leading to increased incidences of mastitis, lameness, and other disorders (West, 2003). In such a scenario, dairy farmers are often forced to make difficult culling decisions when cows become unproductive or are compromised by stress (Langford & Stott, 2012). Traditional methods to monitor animal welfare, such as visual observation of behavior (e.g., tracking lying time as an indicator of discomfort), are inherently subjective and labor-intensive. Moreover, these methods are prone to delayed detection, which can result in further deterioration of the animal's condition (Tucker et al., 2021). As herd sizes grow larger due to barn consolidation, the limitations of manual observation become even more pronounced.

The pressing need for rapid, accurate, and continuous monitoring has led to the development of Precision Livestock Farming (PLF) technologies. PLF offers the potential to enhance both animal welfare and farm profitability by providing real-time, objective data on animal behavior and health. Advances in sensor technology have enabled the deployment of devices, such as accelerometers, ultra-wideband (UWB) location trackers, and infrared thermography cameras, across modern dairy barns (Kaur et al., 2023; Rathod & Dixit, 2021). These systems can monitor microclimatic conditions and individual animal responses, which are critical for effective heat-stress management. An overview of the instrumented pen illustrating the sensor technology used throughout the study is provided in **Figure 1**, which shows the actual pen layout with four video cameras, eight UWB anchors, and the ten collar tags (UWB + accelerometer) deployed for this study.

Despite these technological advancements, current PLF systems face significant limitations. Most existing systems either rely on a single modality or focus on a limited subset of behaviors. For instance, while accelerometer-based devices can effectively differentiate between lying and standing, they often struggle to detect short-duration events, such as drinking or subtle changes in feeding behavior, which are critical indicators of an animal's thermal status (Renaudeau et al., 2012). Moreover, traditional weather-based indices, such as the temperature–humidity index (THI), provide only a coarse approximation of the thermal strain experienced by individual cows. These indices fail to capture microclimatic variations within barns and do not account for intrinsic differences in heat tolerance among cows (Milan et al., 2018). As a result, herd-average measures may overlook early signs of distress in susceptible individuals, underscoring a critical research gap: the need for an integrated, automated system that monitors both behavior and physiological responses to heat stress at the individual level.

Recent advances in sensor technology and data analytics offer promising solutions to this challenge. An array of networked sensors, including UWB trackers, accelerometers, and computer vision systems, can now collect continuous, real-time data on each cow's activity, location, and physiological state (Moravcsíková et al., 2024; Shine & Murphy, 2021). However, while these technologies have advanced the field of PLF individually, their integration remains limited. In particular, few studies have combined behavioral data with core body temperature (CBT) measurements to provide an early warning system for heat stress. This gap is significant, as cows are known to modify their behavior (e.g., increasing standing time, reducing lying time, altering feeding and drinking patterns) in response to heat stress, and these behavioral changes are directly related to their internal temperature regulation (Islam et al., 2021).

Machine learning (ML) has emerged as a critical tool in addressing this challenge. ML algorithms excel at processing high-dimensional, multimodal datasets and can uncover complex, nonlinear

relationships that traditional methods often miss. In the context of dairy farming, ML has been successfully applied to classify behaviors and predict health outcomes from sensor data, enabling more proactive and accurate management decisions (Raj & Kos, 2023; Zeng et al., 2014). For instance, recent studies have demonstrated that incorporating comprehensive variables, such as production metrics, individual cow traits, and environmental factors, into ML models significantly improves the prediction of heat-stress indicators, such as respiration rate and core body temperature, outperforming traditional threshold-based approaches (Shu et al., 2023). These advances illustrate the potential of Artificial Intelligence (AI)-driven analysis to not only monitor animal behavior but also to provide actionable insights for early intervention.

Nevertheless, existing PLF systems have notable gaps that motivate further research. Many current sensor systems rely on a single modality, which limits their ability to capture the full spectrum of cow behavior and physiological responses. An accelerometer collar, for example, might accurately detect changes in activity levels or posture but cannot provide context regarding the animal's location or the environmental conditions it experiences. Similarly, a thermal camera might measure skin temperature but cannot distinguish between a cow actively drinking to cool down and one simply passing by a shaded area. Consequently, there is a strong need for an integrated approach that combines data from UWB, accelerometers, and computer vision systems. Multimodal sensor integration not only enhances the accuracy of behavior classification but also enables the cross-verification of data streams, thereby reducing false alarms and providing a more comprehensive picture of an animal's welfare (Benaissa et al., 2023; Barker et al., 2018).

This study aims to develop and evaluate a cow-level, behavior-based heat-stress alarm that is compatible with real-time deployment in commercial dairy barns. We treat CBT as the physiological gold standard for heat load (Burdick et al., 2012; Polsky et al., 2017) but restrict its role to defining the heat-stress label; the alarm itself uses only non-invasive sensor inputs that are feasible to monitor

continuously at scale. Building on the multimodal MmCows platform (Vu et al., 2024), we leverage UWB positioning, accelerometer-derived activity, and barn-level THI to (i) classify key behaviors (standing, lying, feeding, drinking) with high agreement to video ground truth, (ii) characterize how behavior and microclimate patterns differ between physiologically normal and heat-stressed hours, and (iii) train and validate behavior-based models that identify imminent or ongoing heat stress without using CBT as a predictor. In this physiology-anchored yet behavior-driven framework, CBT provides a rigorous reference for evaluating alarm performance. At the same time, the operational decision support relies entirely on behavior and environmental signals that can be captured non-invasively in real time.

Behavior classification with non-invasive sensors has been widely studied – for example, accelerometers for posture/estrus detection and health monitoring (Thorup et al., 2015; Arcidiacono et al., 2020) and computer vision for behavior and respiration monitoring (Wu et al., 2023). Reviews also emphasize the need to turn rich, multimodal data into actionable per-cow decisions (García et al., 2020; Kaur et al., 2023). Our contribution addresses this gap by integrating behavior signals *and* microclimate data with physiological measurements (CBT) to move from recognition to early warning of heat stress. Complementary non-invasive, low-burden physiology sensors (e.g., respiration monitors or ear-tag thermometers) have shown feasibility for heat detection (Atkins et al., 2018; Chung et al., 2023), but few studies combine behavior with CBT to deliver real-time, individual-cow heat alarms in commercial barns. This paper targets that step using behavior sensing based on low-cost, scalable, and non-invasive sensors (UWB, accelerometer, and video) integrated with barn-level THI to enable per-cow, real-time heat-stress alerts – providing farmers with a practical early-warning tool for managing heat stress in their herds.

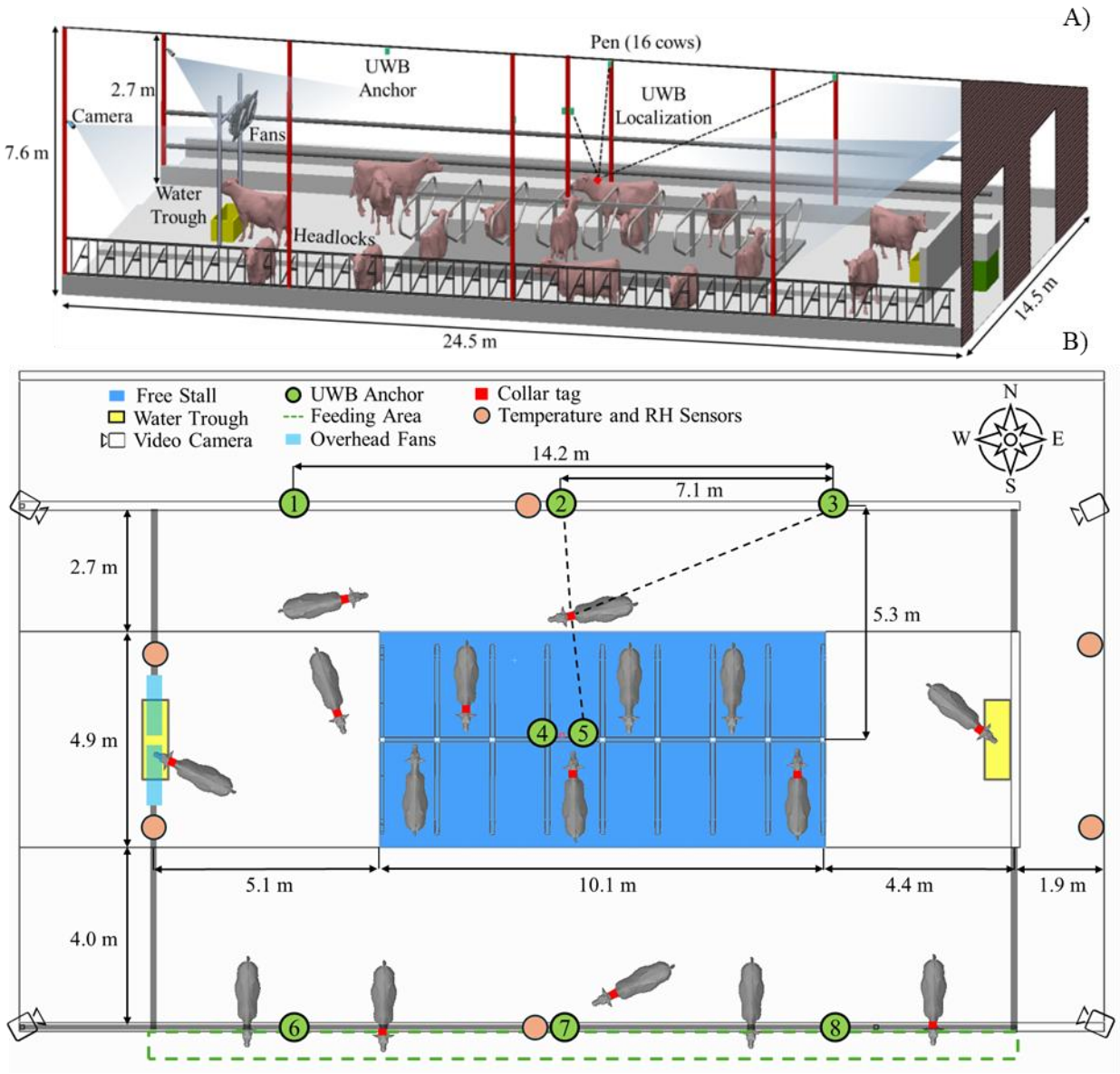

Figure 1. (a) Schematic representation of the experiment pen (with UWB 3D localization indicated). (b) Pen layout with the installed tracking systems (four video cameras and eight UWB anchors) and ten collar tags (with UWB module and accelerometer).

2.3. Materials and Methods

2.3.1 Experimental Setup

Experimental site

This study was conducted in a naturally ventilated freestall barn at the Blaine Dairy Cattle Center (Arlington, WI, USA) using a herd of 16 Holstein dairy cows. Data collection focused on ten randomly selected cows from July 21 to August 4, 2023, a period characterized by warm summer conditions. The barn was equipped with multiple sensing systems to monitor cow behavior and physiology in real time. As illustrated by the barn layout (**Figure 1**), the pen contained eight freestalls, a feed bunk along the southern side, and water troughs at both east and west ends. Eight Ultra-Wideband (UWB) anchors (marked as green circles in **Figure 1**) were installed around the pen to enable precise indoor positioning. Four high-resolution video cameras were mounted at the pen corners to capture cow behavior for ground-truth annotation. Two overhead fans were positioned at the west end of the pen to enhance airflow and cooling on hot days. All sensors were time-synchronized, and the data streams were integrated for subsequent analysis (**Figure 2**). This multi-sensor experimental setup provided a comprehensive view of each cow's location, activity, and core body temperature within the barn environment, forming a dataset comparable to recently published multimodal cow-monitoring datasets (Vu et al., 2024). The primary objective, however, was not general behavior recognition but to examine how behavioral patterns relate to dairy cow internal temperature regulation under heat stress.

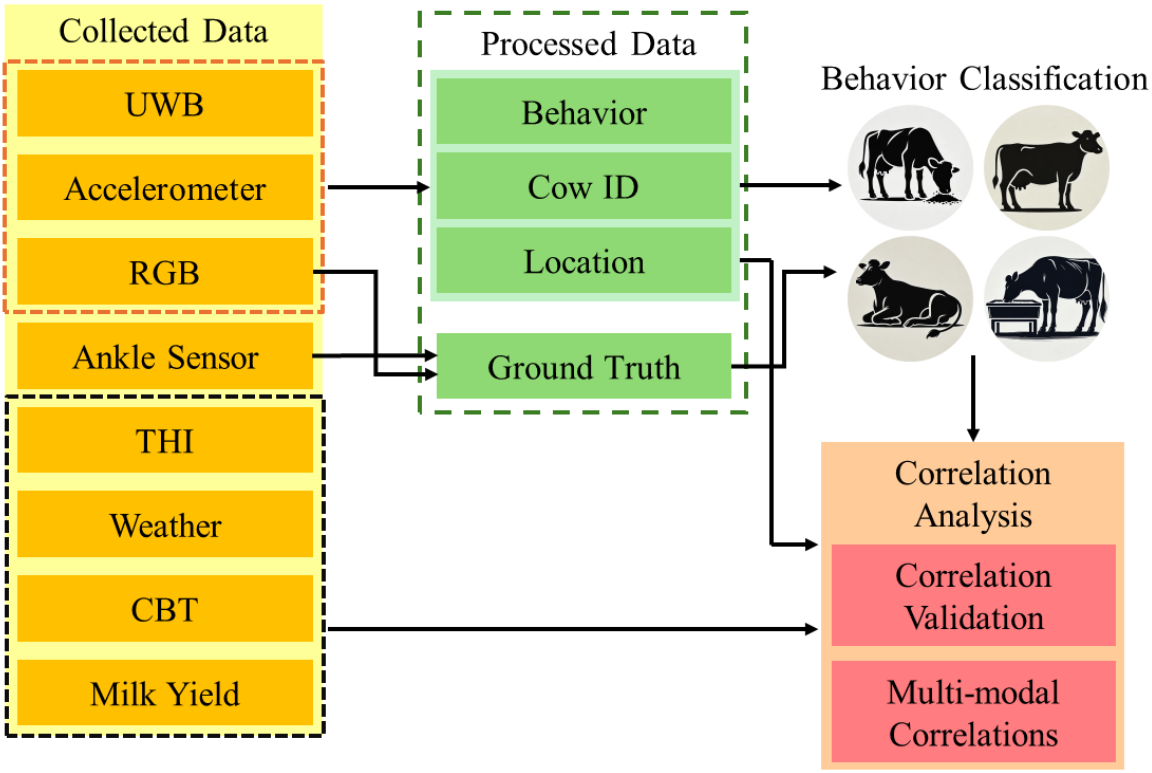

Figure 2. Pipeline for behavior classification and validation of classified behaviors

Cow selection

A total of 10 Holstein dairy cows were randomly selected from the experimental pen for recording. **Table 1** provides an overview of each cow's production and reproductive parameters at the start of the experiment, including average daily milk yield (DMAVG), days in milk (DIM), and lactation number (Lactation). By focusing on a group of first-parity animals, we sought to reduce confounding factors associated with differences in lactation number (e.g., milk yield peaks, metabolic demands, or postpartum recovery).

Table 1: DIM – Days in milk, DMAVG - Daily milk average, and DCC – Days carrying calf.

Cow #	Age [yrs, mns]	DIM [days]	Lactation #	DMAVG [kg/day]	DCC [days]

1	6, 9	220	5	32.99	99
2	7, 8	146	5	48.82	64
3	7, 6	660	5	48.46	120
4	9, 9	597	7	38.02	162
5	6, 2	201	4	53.19	78
6	5, 8	138	4	49.90	57
7	5, 6	160	4	48.19	78
8	5, 6	126	4	47.50	-
9	7, 2	345	5	49.02	624
10	8, 9	196	7	49.06	50

Nevertheless, the cows displayed considerable variation in other important traits. For instance, the range of days in milk (DIM) extended from 119 to over 600 days, reflecting a broad distribution of lactation stages and productivity levels. Daily milk yield also varied widely (approximately 33 to 53 kg/day), while age ranged from about 5 to 9 years. Although all cows were clinically healthy at the outset of the experiment, these differences in production characteristics and age help capture a more representative cross-section of commercial dairy cows in a single-parity cohort.

Moreover, to ensure that behavioral or physiological measurements were accurate, we confirmed that no cow had exhibited recent illnesses or major health events before enrolling in the study. This uniform health status helped to minimize bias from confounding health-related factors. Overall, selecting first-parity cows with different DIM and daily yields provides a valuable balance: the group remains relatively homogeneous in terms of parity while encompassing a wide range of lactation stages and performance traits relevant to real-world dairy management.

2.3.2 Data Acquisition

Camera system

A set of four GoPro HERO11 Black cameras was mounted at the corners of the pen to capture isometric views of the animal-occupied zone. The cameras continuously recorded video at a resolution of 4480×2800 pixels (4.5K) at 1 frame per second (fps) throughout the study period, yielding approximately 156 hours of footage[1]. This ultra-high resolution was selected to minimize information loss during capture and ensure maximum clarity for manual review, enabling precise verification of ambiguous behaviors during the ground-truthing process.

To ensure temporal alignment across the multi-view system, camera timestamps were synchronized using an Internet-time-synchronized clock displayed in the field of view periodically during deployment. However, for automated computer vision analysis, video frames were downsampled to align with the YOLOv8 object detection model's input specifications and to optimize computational efficiency.

These videos were manually reviewed to annotate cow behaviors, providing ground truth labels for model training and validation. Each cow's behavior was classified at each time point into one of four categories (**Table 2**): standing, lying, feeding, or drinking. The video-based annotations served as the gold standard for evaluating sensor-based behavior detection.

Table 2: Definitions of cow behaviors

Behavior	Definitions
Standing	Stands with straight legs, and its head is away from the feeding area.
Feeding	The head is in the feeding area (through the feed stalls)

Drinking	Drinking at the water trough
Lying	Lying in the stall

Collar tag

Each of the ten focal cows was fitted with a custom-designed collar tag housing a UWB module (Qorvo DWM3000) and an inertial measurement unit (TDK ICM-20984 IMU). The collar tag (**Figure 3**) weighed 101 g and was affixed to the upper side of the cow's neck. The UWB system operated on a Time-Difference-of-Arrival (TDoA) principle, where the tag transmitted ultra-wideband signals to the fixed anchors. Each UWB transmission produced a timestamp at multiple anchors, allowing computation of the tag's position with up to 0.15 m accuracy (as reported by the manufacturer in 2022). The collar's IMU concurrently recorded tri-axial acceleration at 10 Hz. UWB position updates were obtained every 15 s, capturing the cow's movements among barn zones (e.g., stall, feed bunk, water trough). In this way, the collar tags provided both spatial location and movement data. The location data enabled calculation of time spent in different areas (e.g., minutes at the feed bunk or under the fans), a key factor in assessing behavioral responses to barn microclimate. During each UWB uplink transmission, the collar also logged a burst of acceleration data, effectively pairing each position sample with recent motion information. This integrated collar system thus supplied rich multimodal data on cow activity and positioning, as detailed in the MmCows dataset by Vu et al. (2024), which combined localization and inertial sensing for cattle monitoring.

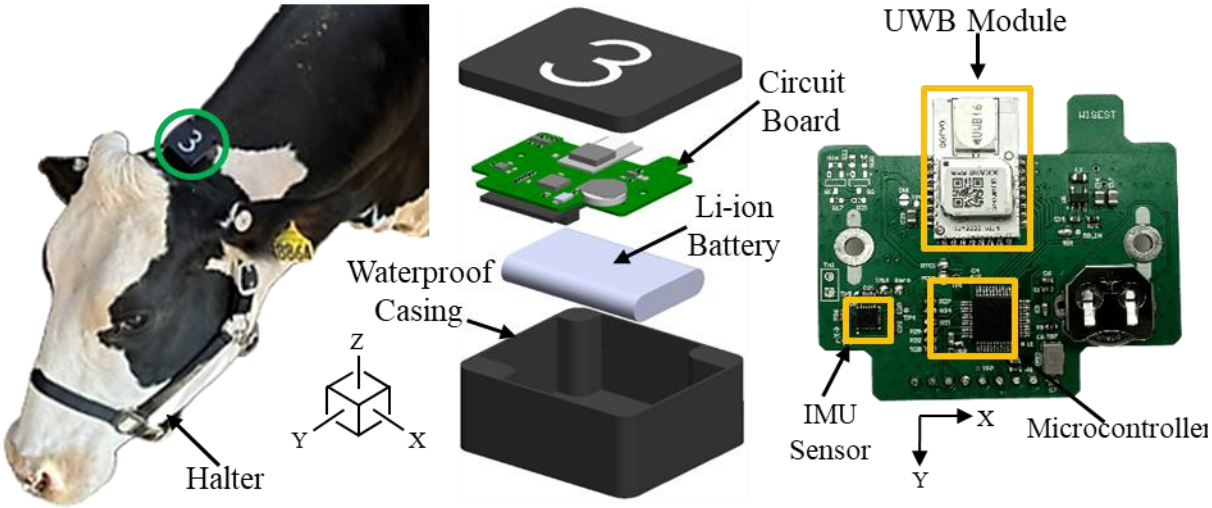

Figure 3. Collar tag setup with IMU and UWB module on PCB. Also represented is the 3D orientation of the IMU when on the cow.

Ankle accelerometer

To obtain an independent measure of standing versus lying behavior, a waterproof three-axis accelerometer data logger (HOBO Pendant G, Onset Computer Corp., Bourne, MA, USA) was attached to the hind leg (ankle) of each tagged cow. This logger recorded acceleration continuously at 1-minute intervals. The ankle-mounted accelerometer is a well-established method for monitoring lying time in dairy cows (Norlund et al., 2019). Following the deployment protocol of Reuscher et al. (2023), we secured the sensor to the cow's rear leg and collected data throughout the study. The acceleration signals were post-processed to classify the cow's posture (lying vs. standing) by identifying characteristic acceleration patterns. In our analysis, a clustering approach was used to quickly distinguish lying bouts from standing: the 1-minute acceleration readings were segmented and grouped using an unsupervised K-means algorithm, and the resulting clusters were interpreted as the two dominant postures. The classification procedure consisted of: (1) filtering and smoothing the raw acceleration data; (2) applying K-means clustering to separate high-variance (active/standing) periods from low-variance (inactive/lying) periods; (3) determining cluster centroids and an optimal

acceleration threshold; and (4) labeling each minute as “lying” or “standing” based on the threshold. This algorithm provided a binary time series of lying/standing for each cow. Validation against the video ground truth showed approximately 98% accuracy in detecting lying bouts, confirming that the leg sensor reliably captured lying and standing behavior. The ankle sensor data were later aligned with the collar tag data and temperature readings to investigate how postural changes coincide with body temperature fluctuations (**Figure 4**).

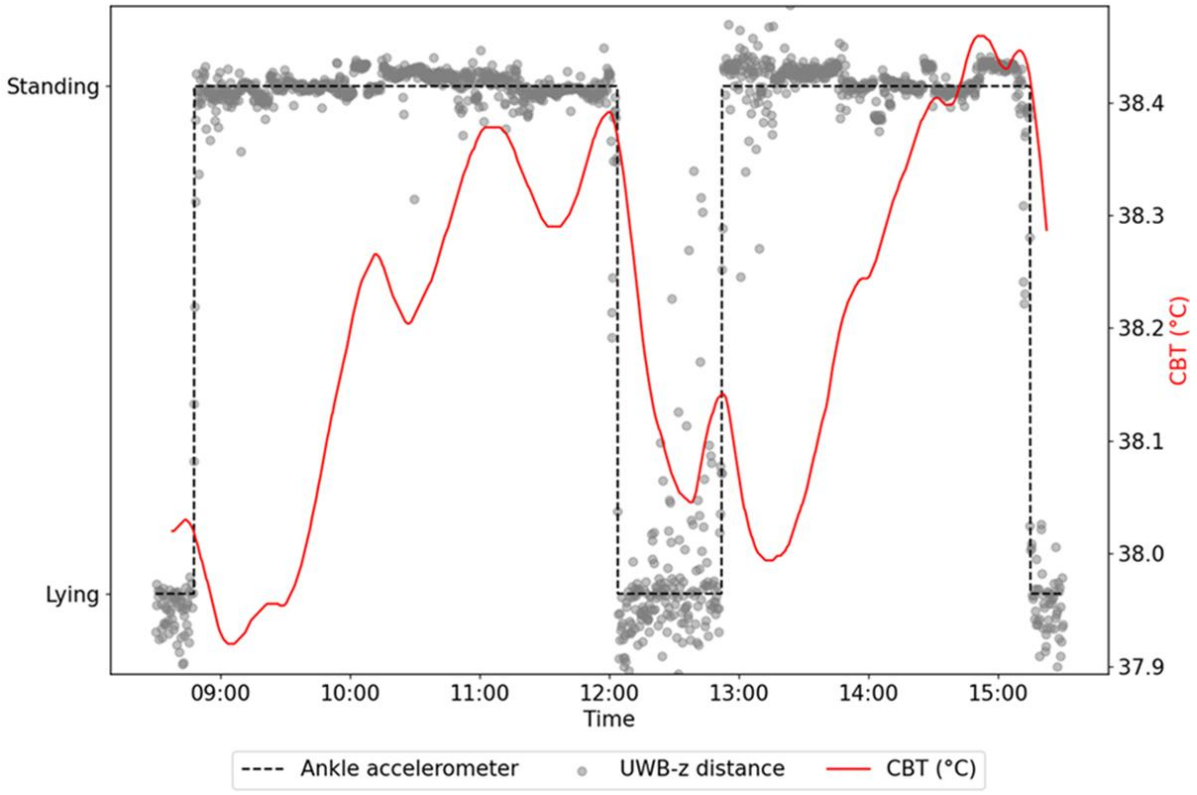

Figure 4. Individual cow core body temperature and UWB Z-axis data from the collar tag, with cow standing and lying ground truth from the ankle data logger, post-processed to binary form.

Vaginal temperature data logger

Core body temperature (CBT) was measured using vaginal temperature loggers (DST centi-T, Star-Oddi, Gardabaer, Iceland) inserted into each of the ten cows. Each logger was mounted in a hormone-free intravaginal device, a controlled internal drug release (CIDR), to keep it in place. The loggers

recorded vaginal temperature once per minute with an accuracy of ±0.1 °C. Vaginal temperature is preferred over rectal or subcutaneous measurements because it provides a more stable, representative estimate of core body temperature. Studies have demonstrated that vaginal temperature measurements can better reflect internal thermal changes due to the richer blood supply and reduced influence of external temperature fluctuations (Burdick et al., 2012; Lee et al., 2016). Additionally, vaginal sensors are less susceptible to dislodgment and contamination compared to rectal devices, thereby ensuring more reliable long-term monitoring. This method allowed continuous, minimally invasive monitoring of each cow's internal temperature throughout the trial. The high temporal resolution (60 s) of CBT data enabled us to directly link short-term behavioral events (e.g., a cow lying down) with subsequent temperature changes.

Weather and microclimate

The barn microclimate was measured from six temperature and relative humidity data loggers (U23-001 HOBO Pro v2 data logger, Onset Computer Corp., Bourne, Massachusetts, USA) at a sampling rate of 1 minute. These were deployed at six locations, at the four corners of the pen, and two in the middle of the pen by the cow stalls. Microclimate sensors were positioned at 2.5m above the ground to avoid cow reach and capture the environmental conditions experienced by the cows accurately. An additional weather station, which recorded data every 5 minutes and was located at 43.31°N, 89.33°W, was used to compare barn THI with outdoor conditions. Using the temperature and relative humidity, the temperature-humidity index (THI), a widely used environmental indicator, was calculated for both weather and microclimate data sets using Equation (1), where (T_{db}) is the dry-bulb temperature (°C). RH is the relative humidity (%) (Dikmen & Hansen, 2009).

$$THI = (1.8 * T_{db} + 32) - (0.0055 * RH) * (1.8 * T_{db} - 26.8) \quad (1)$$

2.3.3 Behavior Classification

Labeling and Ground Truth

The video recordings were used to establish ground truth for cow behavior, which was later compared with sensor-based classifications. Four primary behaviors were defined (**Table 2**) with precise criteria for annotation: Standing (upright on all four legs, not actively feeding or drinking), Lying (resting on the barn floor or stall, with body contact on the bedding), Feeding (head positioned through the feed barrier, consuming or reaching for feed), and Drinking (head in the water trough). Trained observers manually annotated the behavior of each of the 16 cows for a continuous 24-hour period (July 25, 2023) to create a labeled dataset. To ensure inter-observer reliability, a second independent observer randomly sampled time frames from the recordings and provided annotations. When behaviors overlapped (e.g., a cow might stand idle after drinking), a prioritization scheme was used, with active behaviors, such as feeding or drinking, taking precedence over passive standing. These labeled data served two purposes: (1) to train and evaluate the machine learning models for behavior classification using the sensor data, and (2) to validate the accuracy of the ankle accelerometer's lying/standing detection. The ground-truth dataset encompassed a full range of daily activities and was instrumental in developing reliable behavior-detection algorithms.

Data Processing

The collected multimodal data (accelerometer, UWB, temperature, and environmental streams, along with video labels) underwent preprocessing to synchronize and integrate the different sources, followed by feature extraction for behavior classification. All sensor data were time-aligned to a standard timeline at 1-minute resolution. Given the different sampling rates, this involved down-sampling the high-frequency accelerometer signals (originally 10 Hz) to 1-minute averages or summary features, and up-sampling or holding the UWB position data (15 s updates) to match the 1-

minute grid. Missing data points due to network latencies or sensor dropouts were linearly interpolated, when necessary, though such gaps were infrequent. Once synchronized, the data were organized into a unified database where each time-stamped record contained a cow's binary posture (from the leg sensor), UWB-derived location zone, accelerometer features, environmental measures (pen THI), and the cow's vaginal temperature (CBT).

Feature extraction and machine learning

Machine Learning: Random Forest (RF)

In this study, we employed advanced machine learning techniques to analyze sensor data to determine cow postures, specifically differentiating between behaviors. Our methodology used Random Forest and Gradient Boosting algorithms, which are well-regarded for their robustness and efficacy in handling complex, non-linear data.

To preprocess the accelerometer data, features were extracted in a sliding window manner. Each window captured various statistical measures, including the mean, standard deviation, range, skewness, and kurtosis of accelerometer readings along the y-axis, as well as derivative- and entropy-based features. The preprocessed data were then merged with ground truth labels for training and evaluation. Similarly, the UWB sensor datasets were preprocessed to align with the ground truth labels, while feature extraction techniques were adapted to the nature of the UWB data.

The Random Forest algorithm is an ensemble learning technique known for its high predictive accuracy, computational efficiency, and robustness to overfitting, particularly when individual trees are grown deep (Raza et al., 2023; Mascret et al., 2018). RF operates by constructing many decision trees on bootstrap samples of the training data and aggregating their predictions by majority vote for classification or averaging for regression. Because each tree is trained on an independent resample and uses a random subset of predictors at each split, tree construction can be parallelized across processor

cores, which makes RF well-suited to large datasets with many features. In addition, RF naturally provides measures of variable importance, which are useful for interpreting which behavioral and microclimate features contribute most to the heat-stress alarm in this study.

To complement RF, we also considered gradient-boosted decision trees, a class of ensemble methods that sequentially fit shallow trees to the residuals of previous trees to reduce prediction error. This family of models is widely used in tabular machine learning because it offers a favorable balance of accuracy and computational cost when appropriately regularized and equipped with learning rate control (e.g., shrinkage, subsampling) to limit overfitting. In our implementation, we used a histogram-based gradient boosting classifier, which accelerates training by binning continuous features and performing split searches on histograms rather than raw values, while still retaining the ability to capture nonlinear effects and higher-order interactions among behavior and THI features.

Deep learning: Convolutional Neural Network (CNN)

Additionally, we employed deep learning techniques to analyze sensor data and identify cow behaviors. Specifically, we examined the use of one-dimensional Convolutional Neural Networks (1D CNNs) due to their widespread practical use in human activity recognition (Raj & Kos, 2023; Zeng et al., 2014). 1D CNNs operate by sliding a filter along an input sequence, in this case, a time window of sensor readings, to capture local patterns in the data. These convolutions are then pooled and fed into a series of fully connected layers, which combine the locally extracted features to produce a classification of the input data sequence. This process allows the model to extract complex features from noisy time-series data and detect them regardless of their position in the data sequence. Additionally, CNNs have lower computational complexity than fully connected architectures and recurrent neural networks.

Another advantage of using CNNs for the classification of time-series sensor data is their ability to process multimodal data in parallel via a multi-head architecture. By using multiple heads, the model can process different types of sensor data (e.g., accelerometer and UWB) independently, extracting features specific to each sensor. Finally, the independently extracted features are concatenated before being fed into the fully connected layers, providing the network with more context about where the cow is and what it is doing. Our multi-head model architecture is based on a simplified version of the Cross-Modality Interaction Network proposed in Mao et al. (2021). It consists of two heads that run four convolutions on the raw x, y, and z features of our accelerometer and UWB sensor data.

Computer Vision

We implemented an automated video analysis system to track and classify cow behaviors in the barn. This computer vision pipeline consisted of three main steps: (1) detecting cows in each video frame, (2) classifying each detected cow's behavior, and (3) identifying individual cows to maintain consistency across frames. In the first step, a state-of-the-art object detection model (based on YOLOv8) was used to locate cows in the camera footage by drawing bounding boxes around them. Once the cows were detected, the second step involved a convolutional neural network (CNN) that examined the cropped images of each cow and determined what the cow was doing at that moment. This CNN was trained on labeled examples of cow activities and could recognize several specific behaviors (e.g., walking, standing, feeding at the bunk, drinking water, licking, or lying down).

For our study, we focused on four key behaviors out of the broader set identified by the vision model. These four behaviors: feeding, drinking, standing (active/upright behavior), and lying down (resting) – were selected because they are most relevant to assessing cow comfort and heat stress. In other words, while the computer vision system could distinguish up to seven detailed behavior categories (as defined in a recent multimodal cattle behavior dataset), we consolidated its outputs into the four primary behavior categories above to align with our analysis goals. This ensured that the camera-based

observations matched the core behaviors monitored by our other methods (UWB positioning and accelerometer data). Each time a cow was detected in the video, the system assigned it one of these behavior labels, creating a continuous record of the cow's activities throughout the day.

An essential feature of this vision-based approach was the ability to track individual cows across multiple camera views. We deployed several synchronized cameras covering different angles of the pen, enabling the system to cross-reference observations of the same cow from other cameras. By projecting the 2D positions of detected cows from multiple cameras into a 3D space, the system could determine each cow's location in the barn and match it to a specific identity. In practice, this means that after a cow was detected and its behavior identified, the software also confirmed which particular cow it was (e.g., Cow #5) even as it moved around or appeared in different camera views. This identification step was crucial for integrating the video data with the sensor measurements; it ensured that the behavior events recorded by the cameras could be linked to the correct individual animal's UWB and accelerometer data. By leveraging computer vision in this way, we obtained a non-intrusive, continuous stream of behavioral information for each cow, augmenting sensor-based monitoring and providing a more complete picture of cow activity and welfare.

Model evaluation and performance

To rigorously assess behavior classification performance, we evaluated models using leave-one-cow-out cross-validation, a method commonly employed in livestock behavior studies to mitigate data dependency and improve model generalization (Cairo et al., 2020; Coelho Ribeiro et al., 2021). Data were split by cow ID such that training sets and test sets contained distinct individuals, ensuring that algorithms generalized to new cows. This avoids overestimating accuracy due to animal-specific idiosyncrasies. We computed standard classification metrics (precision, recall, F1-score) for each behavior class and overall. **Table 3** summarizes the behavior classification results using the different sensors and algorithms. The UWB location data alone were moderately effective for detecting certain

behaviors (e.g., feeding bouts were identified by proximity to the feed bunk), while the accelerometer alone captured motion-intensive behaviors but struggled to distinguish context (e.g., feeding vs. standing idle). The highest accuracy was achieved by combining UWB and accelerometer inputs. In particular, the 1D-CNN model with multimodal sensor input outperformed all other approaches, attaining a macro-average F1 score of approximately 0.96 (Table 3). This indicates excellent agreement with human observations for all four behaviors. A Random Forest using the combined features also performed well (macro F1 ≈ 0.70), though it was less accurate than the CNN at detecting less frequent behaviors, such as drinking. These results align with the expectation that integrating complementary sensors improves behavior recognition. Overall, the validated classification models provided confidence that we could reliably infer each cow's behavior continuously throughout the study, which is essential for linking behavior to physiological responses.

Table 3. Behavior classification accuracy (F1 score) of each class, using UWB, accelerometer, and their combination, with various machine learning techniques and computer vision approaches.

Method	Sensor/ Sensors	Standing	Feeding	Drinking	Resting	Macro Average
RF	UWB	0.86	0.77	0.45	0.97	0.70
	Accelerometer	0.62	0.40	0.28	0.70	0.46
	Combination	0.91	0.74	0.66	0.99	-
CNN	UWB	0.801	0.980	0.990	0.970	0.937
	Accelerometer	0.564	0.723	0.608	0.727	0.692
	Combination	0.904	0.981	0.970	0.973	0.960
Vision model (RGB)	Camera	0.815	0.741	0.478	0.883	0.632

2.3.4 Heat Alarm Model

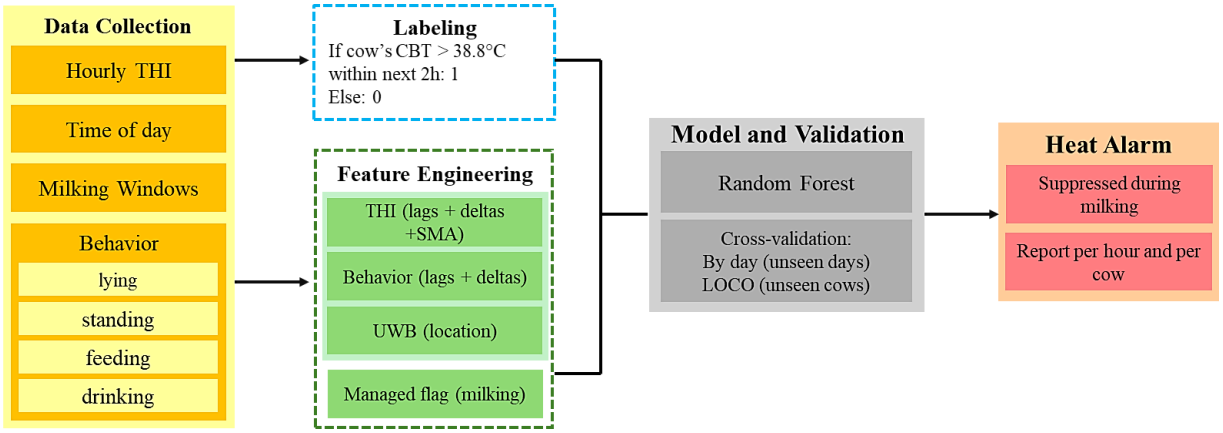

Figure 5. Pipeline for early heat stress detection. The heat alarm threshold is at the 90th percentile of the cow's nominal body temperature range.

We developed a deployable heat-risk alarm that transforms multimodal, non-invasive signals into actionable alerts indicating a high probability that an individual cow's core body temperature (CBT) will exceed a critical physiological threshold in the near term (**Figure 5**). The modeling pipeline contains three layers: (i) feature formation from behaviors, UWB location, and compact THI dynamics; (ii) supervised regression to predict future CBT, converted into a binary risk probability; and (iii) post-processing rules (persistence, cooldown, and milking suppression) to convert scores into operational alarms.

Unlike approaches that rely on herd-relative statistics (e.g., percentiles), we utilized a fixed physiological cutoff to define heat stress. A binary label $y_t = 1$ was assigned if the cow's maximum CBT in the upcoming 2-hour window ($t + 1 \ldots t + 2\ h$) reached or exceeded 38.8°C. This threshold was selected to represent the onset of hyperthermia, where physiological cooling mechanisms are maximally engaged or overwhelmed. If the future CBT remained below this limit, the label was $y_t = 0$. This forward-looking definition trains the model to anticipate heat spikes before they occur, rather than simply detecting them after the fact.

Behavioral and UWB features

We computed hourly percentages for standing, lying, feeding, and drinking, together with their lag-1 and delta-1 features to capture short-term dynamics. To highlight deviations from each cow's circadian routine, we formed residuals: observed hourly percentages minus a per-cow, per-hour baseline estimated within the training fold only (leakage-safe). UWB coordinates (converted to meters) were mapped to pen zones (stall, feed bunk, west/east water troughs; the west trough co-located with fans) to produce zonetime %, entries, distance traveled, and speed (mean, p95), also with lag-1 and delta-1. Time-of-day was encoded with circular harmonics $\sin(2\pi \cdot \text{hour}/24)$ and $\cos(2\pi \cdot \text{hour}/24)$ (and second harmonics) to capture circadian structure without discontinuity at midnight; a managed flag marks milking hours (04:00–05:00, 15:00–16:00).

Classifiers

We evaluated three widely used classification algorithms for structured tabular data: logistic regression, random forest (RF), and a histogram-based gradient boosting (HGB) model. Logistic regression served as a linear baseline that relates the log-odds of heat stress to a weighted combination of behavioral and environmental features. The RF classifier aggregates the predictions of many decision trees grown on bootstrap samples of the data, providing a flexible, non-parametric model that can capture nonlinear effects and interactions among behavior and THI variables (Raza et al., 2023; Mascret et al., 2018). The HGB model is a modern gradient-boosting approach in which shallow decision trees are fitted sequentially to the residuals of previous trees, with continuous predictors discretized into bins to accelerate training while retaining the ability to model complex, nonlinear relationships.

Because heat-stress hours were less frequent than non–heat-stress hours, we accounted for class imbalance by assigning higher weights to misclassification errors on the minority (heat-stress) class during model fitting, so that the classifier was penalized more heavily for missing true heat-stress events. Hyperparameters for RF and HGB (for example, number of trees, tree depth, learning rate, and minimum leaf size) were chosen conservatively to emphasize stable probability rankings and generalization rather than aggressive optimization of apparent in-sample accuracy, consistent with deployment-minded animal-health monitoring where overfitting is particularly problematic (Becker et al., 2021).

Validation of Methods and Metrics

We assessed model performance using two complementary validation schemes. First, we implemented a day-wise cross-validation in which entire calendar days were held out as test sets. This approach prevents temporal information leakage from neighboring hours and mimics the practical scenario of applying the model to future days that were not used for training. Second, we applied a Leave One Cow Out (LOCO) strategy: in each iteration, all observations from a single cow were reserved for testing while the model was trained on the remaining animals. This design evaluates how well the heat-alarm model generalizes to cows that were not seen during training, which is essential for potential on-farm deployment.

For each training split, all derived quantities that depend on the data distribution—such as per-cow behavioral baselines, residual features, and any summary statistics used in feature construction—were recalculated using only the training portion before being applied to the corresponding test set, thereby avoiding any leakage of information from test to training data.

We summarized discrimination using the area under the receiver operating characteristic curve (ROC-AUC) and the area under the precision–recall curve (PR-AUC). Given the approximate one-to-four

prevalence of heat-stress hours in our dataset, PR-AUC was treated as the primary metric because it is more sensitive to performance on the minority class than ROC-AUC. In addition, we report threshold-based precision, recall, and F1 score to characterize trade-offs between missed detections and false alarms at operational decision thresholds. To avoid optimistic bias when comparing classifiers, the model used in subsequent alarm post-processing for each split was selected based on the highest PR-AUC achieved on that split.

At a given decision threshold τ, model predictions were summarized using the standard confusion-matrix counts of true positives (TP), false positives (FP), true negatives (TN), and false negatives (FN). From these, we computed precision (positive predictive value) as $\text{Precision} = \frac{\text{TP}}{\text{TP+FP}}$, recall (sensitivity) as $\text{Recall} = \frac{\text{TP}}{\text{TP+FN}}$, specificity as $\text{Specificity} = \frac{\text{TN}}{\text{TN+FP}}$, and the F1 score as the harmonic mean of precision and recall, $\text{F1} = \frac{2 \cdot \text{Precision} \cdot \text{Recall}}{\text{Precision+Recall}}$. Letting $\pi = \frac{\text{TP+FN}}{N}$ denote the prevalence of heat-stress hours (i.e., the fraction of positive cases in the dataset), the expected area under the precision–recall curve (PR-AUC) for a random classifier equals this prevalence. We therefore also report a normalized "PR-lift", defined as $\text{PR-lift} = \frac{\text{PR-AUC}}{\pi}$, which expresses how many times better than random the model's ranking performance is, adjusted for class imbalance. All curves were computed on held-out validation folds, and areas under the ROC and precision–recall curves were averaged across folds with corresponding standard deviations.

2.4. Results

2.4.1 Behavior Classification Validation

To ensure that our multimodal dataset was representative of known heat–behavior dynamics, we compared our observations with previously published correlations between cow behavior and thermal conditions. Vu et al. (2024) reported strong associations between daily THI and several behavior

metrics in this same instrumented pen, showing that cows tended to stand longer and lie less as heat stress increased, while feeding bouts shortened and drinking frequency rose. These findings align with prior work demonstrating that cows adapt posture and intake patterns to dissipate body heat and reduce endogenous heat production (Allen et al., 2015; Nordlund et al., 2019; Frigeri et al., 2023; Herbut et al., 2021).

Building on these benchmarks, we extended the analysis to include CBT responses as a physiological anchor for validating behavioral data. Cross-correlation analysis revealed that barn-level THI was positively associated with the herd's average CBT, with a distinct lag in the internal thermal response. While the concurrent correlation between CBT and THI was moderate ($r \approx 0.45$), the association strengthened with increasing time lag, peaking at a 5-hour delay ($r = 0.64$, $p < 0.001$). This pattern indicates that increases in barn THI were followed by measurable rises in CBT several hours later, consistent with physiological delays reported in previous studies (Renaudeau et al., 2012; Polsky et al., 2017).

Table 4, summarizes this extension, highlighting the relationship between THI and herd-level CBT across time lags. The significant positive correlation at a 5-hour lag supports the reliability of our CBT measurements and underscores the value of linking behavioral adjustments to delayed physiological outcomes. Together, these results demonstrate that while behavior alone provides early indicators of heat stress, coupling behavior with CBT enables the development of more robust heat-alarm models that anticipate physiological strain before it peaks.

Table 4: Correlations of daily frequency of bouts, mean duration of bouts, and total duration of cow behaviors versus the THI for 13 days.

THI lag (hours)	***r***	***p*-value**	***R^2***
0	0.452	0.012	0.204

1	0.511	0.005	0.261
3	0.598	0.002	0.357
5	**0.643**	0.001	0.414
7	0.611	0.003	0.373
10	0.487	0.008	0.237

To visualize herd-level behavioral adjustments to heat stress, we plotted the daily proportion of time spent in each significant activity (standing, lying, feeding, drinking) alongside the pen's average THI (Figure 6). As reported by Vu et al. (2024), cows exhibited clear shifts in activity under hotter conditions: standing time increased, lying time decreased, feeding bouts shortened, and drinking frequency rose. These behavioral adaptations are consistent with established heat-mitigation strategies in dairy cattle, where cows stand to increase conductive and convective heat loss, reduce lying to limit metabolic heat load, and compensate with increased water intake (Allen et al., 2015; Nordlund et al., 2019; Herbut et al., 2021).

In our study, these behavioral trends were further anchored to CBT responses, revealing that posture and intake adjustments often preceded the delayed rise in CBT documented in Table 4. For instance, increases in standing and drinking were typically observed on high-THI days several hours before the herd's mean CBT reached peak values. This suggests that behaviors not only serve as early-warning indicators of heat stress but also help buffer internal temperature increases. The alignment of behavioral shifts with lagged CBT responses underscores the value of integrating both data streams: behavior offers an immediate, non-invasive signal of thermal discomfort, while CBT validates the downstream physiological consequences. Together, these coupling forms the basis for our proposed cow-level heat-alarm framework.

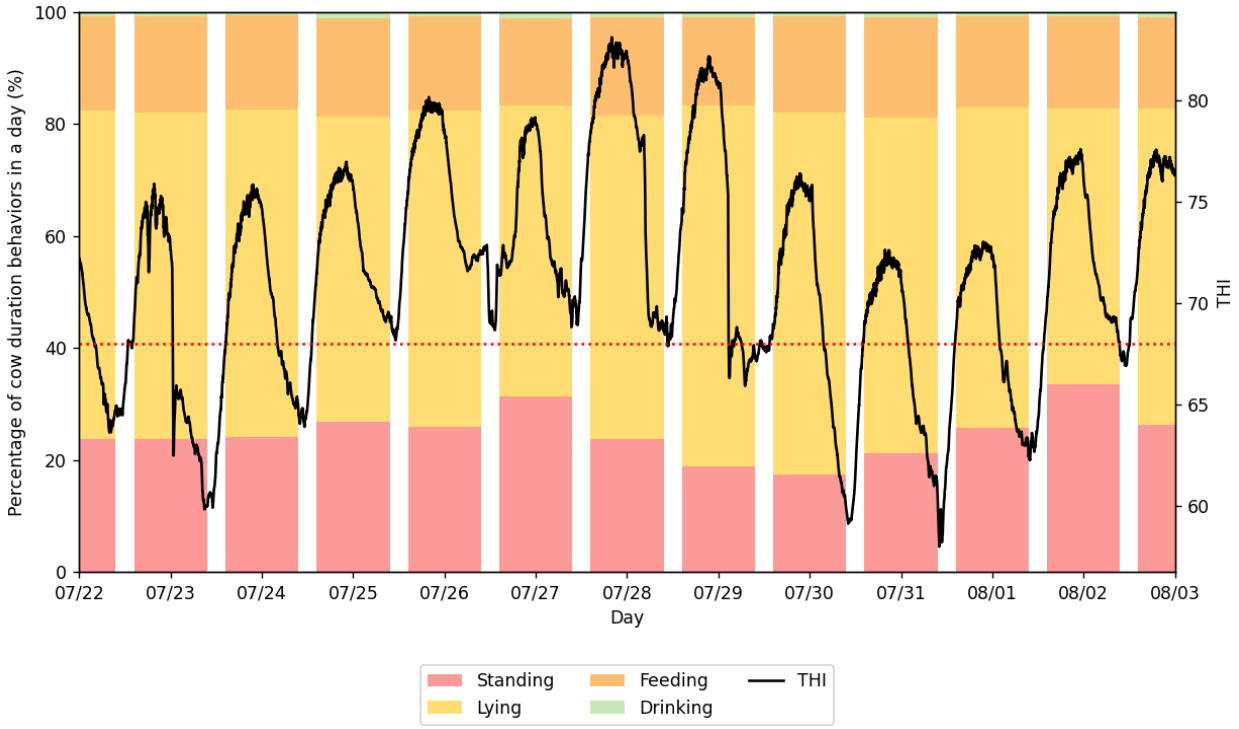

Figure 6. Herd-level daily proportion of time spent in standing, lying, feeding, and drinking behaviors, plotted with the average daily barn THI. Behavioral shifts with THI (increased standing and drinking, reduced lying and feeding) are consistent with Vu et al. (2024) and extend here to demonstrate alignment with lagged core temperature responses.

2.4.2 Significance of Heat-Stress Alarm Model Results

In **Table 5**, because the random baseline for PR-AUC equals the positive prevalence, our day-blocked prevalence of 0.20 implies a random AUPRC of 0.20 and a LOCO prevalence of 0.17. Against these baselines, Random Forest and Histogram-based Gradient Boosting achieve PR-AUC values of approximately 0.58 in the day-blocked analysis (a PR-lift of 2.5 to 2.9 times) and 0.51 to 0.53 in LOCO (a lift of approximately three times), while logistic regression performs slightly lower (0.48 to 0.52). Thus, the models concentrate actual near-term heat-risk hours roughly three times as densely as chance would predict. ROC-AUC values (0.78-0.83) corroborate the score's separability, but we emphasize PR-AUC due to class imbalance. Taken together, these results indicate that non-invasive signals (behavior, UWB location, compact THI dynamics) provide a stable, generalizable basis for prioritizing hours for intervention under routine cooling.

Table 5: Model performances with cross-validation with day-block and LOCO

Split	Model	PR-AUC	PR-Lift	ROC-AUC	Prevalence
Day-blocked	RF	0.58	2.54	0.78	0.20
Day-blocked	HGB	0.58	2.88	0.83	0.20
Day-blocked	LR	0.52	2.84	0.78	0.20
LOCO	RF	0.53	3.04	0.82	0.17
LOCO	HGB	0.51	2.94	0.81	0.17
LOCO	LR	0.48	2.75	0.78	0.17

1

RF = Random Forest; HGB = Histogram-based Gradient Boosting; LR = Logistic Regression. Day-blocked = GroupKFold by calendar day (entire days held out); LOCO = Leave-One-Cow-Out (each cow held out in turn). PR-AUC = area under the precision–recall curve. PR-Lift = PR-AUC divided by Prevalence; because the random baseline for PR-AUC equals the positive prevalence (π), PR-Lift = (PR-AUC / π) expresses how many times better than random the ranking is on average. ROC-AUC = area under the receiver operating characteristic curve (0.5 = random; 1.0 = perfect). Prevalence = fraction of positive hours in the held-out set (i.e., hours that next 2 h exceed the cow-specific high-CBT threshold).

2.5. Discussion

We integrated wearable sensors, environmental monitoring, and video observations to investigate how dairy cow behavior correlates with core body temperature during heat stress. The results demonstrate a clear link between behavioral patterns and physiological thermal load. In general, the cows adjusted their behavior to help maintain their core temperatures within a safe range, despite exposure to high ambient heat and humidity. This finding is significant for precision dairy farming because it suggests that certain easily observable behaviors (like standing and lying times) can serve as early indicators of a cow's heat stress level. Our automated monitoring approach could thus enable farmers or barn control

systems to detect heat stress early and intervene (e.g., by activating cooling fans or misters) before cows reach critical body temperatures.

One of the most notable outcomes was the strong inverse relationship between lying time and core body temperature. Cows that rested less (shorter total lying time) had lower CBT under hot conditions, whereas extended lying was associated with higher CBT. This aligns well with previous research showing that heat-stressed cows alter their lying behavior to aid heat dissipation. Nordlund et al. (2019) reported that cows often end a lying bout once their internal temperature reaches a certain level and remain standing until they cool off. Our data support this behavior: cows with many short lying bouts (frequently interrupted rest) were better able to limit CBT increases than cows that persisted in long lying bouts. The overhead fans in our barn contributed to making standing an effective cooling strategy, as cows often congregated under the fans while standing. This microclimate effect underscores behavioral responses and the barn environment interacts in determining a cow's heat load. Thus, simply measuring ambient conditions may not fully predict an animal's thermal status – one must also consider how the animal behaves (and where it chooses to be) in that environment. The mixed-effects model results quantitatively confirmed that behavior variables improve the prediction of core temperature beyond what THI alone can explain.

Another important behavioral indicator was drinking frequency. We observed that cows increased the number of water visits on hot days, consistent with other studies of heat-stressed cattle. While increased water intake is expected to help with evaporative cooling and hydration, our analysis found a relatively small but favorable effect on CBT (more drinks associated with slightly lower core temperature). This suggests that providing ample access to water, and perhaps additional water points during heat events, could encourage more frequent drinking and improve thermal comfort. Interestingly, the feeding behavior showed that cows tend to eat in shorter bouts under heat stress, which is believed to minimize metabolic heat production during the hottest part of the day. In our

study, reduced feeding did not show a strong direct effect on CBT (likely because any benefit of less heat production might be offset by the cow already being hot). However, changes in feeding can have longer-term implications for productivity and energy balance during heat stress and thus remain an important management consideration. Our focus, though, was on immediate thermal correlations; for longer-term outcomes (milk yield, etc.), further analysis would be required.

From a technological and management perspective, this work demonstrates the value of multimodal sensing for both animal welfare and dairy science research. The combination of UWB localization and accelerometers enabled us to continuously monitor nuanced behaviors with high fidelity and place them in their environmental and spatial context, which is central to precision dairy farming and automated decision support (García et al., 2020; Kaur et al., 2023). Although multi-sensor behavior recognition has been explored in prior work, most studies either rely on accelerometers alone or focus on a narrow set of activities or health outcomes (Barker et al., 2018; Benaissa et al., 2023). By incorporating location data, we enhanced the detection of context-specific actions such as feeding at the bunk or visiting water troughs, behaviors that are otherwise difficult to discern from motion signals alone but are directly relevant for interpreting heat-stress responses and their consequences for production and welfare (West, 2003; Ji et al., 2020; Islam et al., 2021).

The high agreement with video (**Table 4**) indicates that our sensor fusion approach is a viable substitute for labor-intensive video observation. Importantly, our analysis does not stop at classifying behavior; we integrate those behavioral data with physiological measurements (CBT) and environmental readings to derive actionable insights. This reflects a shift in precision livestock farming toward holistic, cyber-physical systems that connect behavior and health indicators in real-time. The dataset collected in this study is similar in scope to the CPS dataset reported by Vu et al. (2024), which also contains synchronized data on cow movement, behavior, and core temperatures. However, our emphasis was on leveraging these data to uncover biological relationships (behavior–temperature

correlations) rather than purely improving activity classification algorithms. The findings here could guide the development of smarter barn control systems; for instance, a system might use continuously measured lying time and ambient conditions to predict a rise in CBT and preemptively turn on cooling fans.

Figure 7, translates model accuracy into a workload–benefit view that matters on farm: if staff only review the top 10%, 20%, or 30% of hours ranked by risk, the tree-based models recover about 33–35%, 55–56%, and 70–72% of all actual near-term high-CBT hours, respectively—roughly two- to three-fold more events than random screening at the same effort. In practical terms, this means the system compresses a full day of data into a short, high-yield watch list, allowing targeted checks, cooling, or shade access during the hours when it helps most. This kind of triage is exactly the operational gap highlighted in recent work using machine learning for bovine heat stress, where the value comes from prioritizing animals and hours rather than issuing many alarms indiscriminately (Becker et al., 2021). Our results extend that line of evidence by showing that non-invasive signals (behavioral time budgets and indoor position/movement), combined with compact THI dynamics, can produce an efficient ranking even when cows are generally cooled. The top-k capture therefore demonstrates not only statistical discrimination but also actionability: farms can set a feasible review quota (e.g., 20–30% of hours) and still capture many risky periods, supporting earlier intervention to protect welfare and productivity (Becker et al., 2021).

While our study provides valuable insights, it also has limitations and opportunities for further research. The sample size was relatively small (ten cows), and the study duration was two weeks, which may not have captured all the variability in behavior or weather. Larger studies, possibly integrating data from multiple farms or over an entire summer season, would help validate and extend our findings. Moreover, our predictive modeling of heat stress was exploratory. The Random Forest classifier's moderate accuracy (64.5% under stringent testing) indicates room for improvement. Integrating

additional physiological signals (e.g., panting rate measured via acoustic sensors or skin temperature via infrared imaging) could provide a more direct measure of heat strain, complementing behavioral and CBT measures. Advances in sensor technology, such as the development of energy-neutral ear tags for real-time temperature monitoring (Vu et al., 2023), and novel smart wearable devices, could further enhance data quality. Future work should also explore real-time implementation: for example, using streaming sensor data to trigger alerts when a cow's pattern of lying and standing, combined with rising CBT, suggests she is entering a danger zone of heat stress. Such systems would embody the precision livestock farming paradigm by not only monitoring animals but also actively improving their welfare through timely interventions and increasing farm productivity.

In summary, this research contributes to the growing body of knowledge at the intersection of animal behavior, environmental stress, and precision technology. We showed that behavior and core body temperature are tightly linked under heat stress conditions, and we validated an automated sensing approach to capture these dynamics. The results are encouraging for the development of sensor-driven decision support tools in dairy farming. By continuously tracking behaviors indicative of thermal discomfort, farmers can better maintain cow comfort and productivity even as climate challenges intensify. Our findings echo the broader theme that merging electronics and agriculture – through data-driven, cow-centric monitoring – can lead to actionable insights that benefit both animals and farm management.

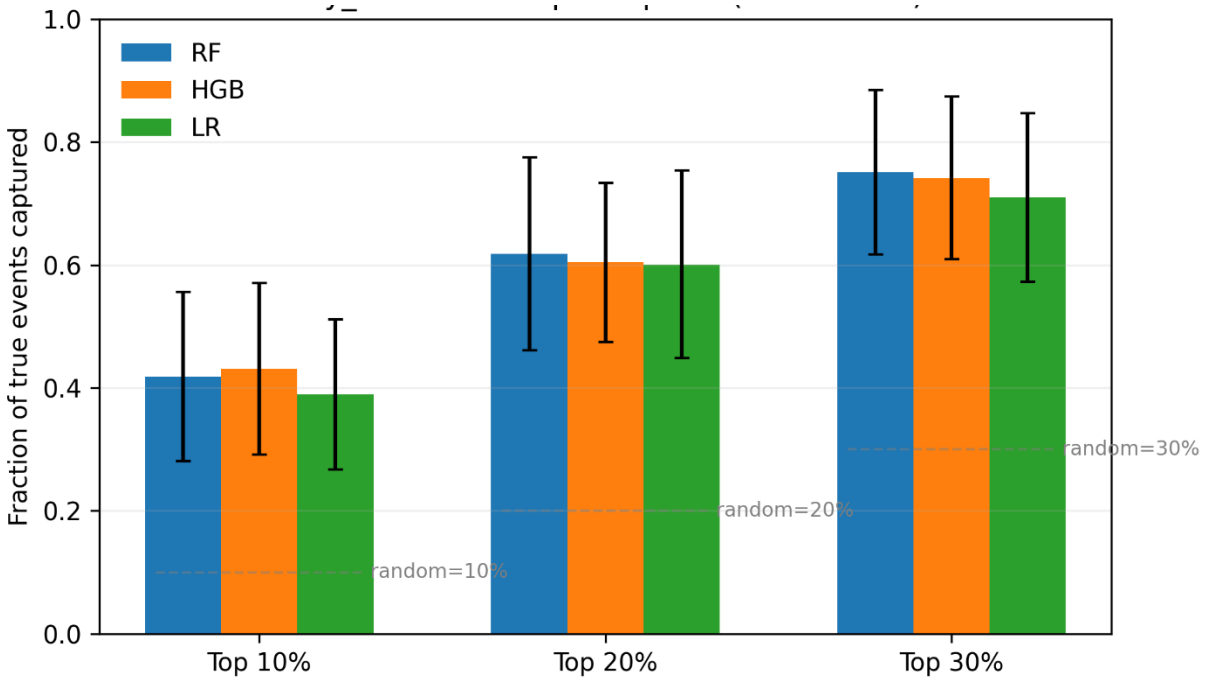

Figure 7. Bars show the mean fraction of all actual high-CBT hours recovered when inspecting only the top 10%, 20%, or 30% of hours ranked by each model (RF, HGB, LR). Error bars are ±1 SD across held-out days. Dashed horizontal lines mark the random baselines (equal to the inspected fraction). Tree-based models (RF/HGB) consistently enrich events above baseline; for example, at 20% workload, they recover roughly half of all actual events (~2–3× the random baseline), concentrating problems into a small review set.

2.6. Conclusions

Starting from a rich, multimodal dataset on cow behavior and physiology, this study examined how dairy cows respond to heat stress and how those responses can be measured with precision technologies. We found that core body temperature and behavior are closely correlated: cows stand more and lie less when they need to offload body heat, and these behavioral adjustments help prevent excessive rises in internal temperature. By using UWB localization, accelerometers, and continuous temperature logging, we achieved accurate behavior classification and captured subtle behavior–temperature dynamics that would be impractical to observe manually. The mixed-model analysis confirmed that behavioral metrics (especially lying and standing patterns) significantly explain variations in core body temperature, reinforcing their role as practical indicators of heat stress. These

insights demonstrate the potential of automated monitoring systems not only to track animal behavior but also to infer physiological well-being. In practice, integrating such sensor systems in dairy barns does enable early warning of heat stress, allowing farmers to activate cooling measures or adjust management to safeguard cow welfare. Overall, our work highlights the importance of aligning technological tools with animal biology. By focusing on the cow's natural responses (behavioral changes) and linking them to health outcomes (body temperature), precision dairy farming can move toward more proactive, animal-centered management strategies. The approach and findings reported here provide a foundation for developing more intelligent climate control and welfare management in dairy operations, contributing to more resilient, sustainable dairy farming in the face of rising heat challenges.

References

Arcidiacono, C., Mancino, M., & Porto, S. M. C. (2020). Moving mean-based algorithm for dairy cow's oestrus detection from uniaxial-accelerometer data acquired in a free-stall barn. Computers and Electronics in Agriculture, 175, 105498.

Atkins, I. K., Cook, N. B., Mondaca, M. R., & Choi, C. Y. (2018). Continuous Respiration Rate Measurement of Heat-Stressed Dairy Cows and Relation to Environment, Body Temperature, and Lying Time. Transactions of the ASABE, 61(5), 1475–1485. https://doi.org/10.13031/trans.12451

Barker, Z. E., Vázquez Diosdado, J. A., Codling, E. A., Bell, N. J., Hodges, H. R., Croft, D. P., & Amory, J. R. (2018). Use of novel sensors combining local positioning and acceleration to measure feeding behavior differences associated with lameness in dairy cattle. *Journal of Dairy Science, 101*(7), 6310–6321.

Benaissa, S., Tuyttens, F., Plets, D., Martens, L., Vandaele, L., Joseph, W., & Sonck, B. (2023). Improved cattle behaviour monitoring by combining ultra-wideband location and accelerometer data. *Animal, 17*(4), 100730.

Borchers, M. R., Chang, Y. M., Tsia, I.C., Wadsworth, B. A., & Bewley, J.M. (2016). A validation of technologies monitoring dairy cow feeding, ruminating, and lying behaviors. Journal of Dairy Science, 99(9).

Burdick, N. C., Carroll, J. A., Dailey, J. W., Randel, R. D., Falkenberg, S. M., & Schmidt, T. B. (2012). Development of a self-contained, indwelling vaginal temperature probe for use in cattle research. Journal of Thermal Biology, 37(4), 339-343.

Cabezas, J., Yubero, R., Visitación, B., Navarro-García, J., Algar, M. J., Cano, E. L., & Ortega, F. (2022). Analysis of accelerometer and GPS data for cattle behavior identification and anomalous events detection. Entropy, 24(3), 336.

Cairo, F. C., Pereira, L. G. R., Campos, M. M., Tomich, T. R., Coelho, S. G., Lage, C. F. A., ... & Dórea, J. R. R. (2020). Applying machine learning techniques on feeding behavior data for early estrus detection in dairy heifers. *Computers and Electronics in Agriculture*, *179*, 105855.

Chung, H., Vu, H., Kim, Y., & Choi, C. Y. (2023). Subcutaneous temperature monitoring through ear tag for heat stress detection in dairy cows. Biosystems Engineering, 235, 202–214. https://doi.org/10.1016/j.biosystemseng.2023.10.001

Coelho Ribeiro, L. A., Bresolin, T., Rosa, G. J. D. M., Rume Casagrande, D., Danes, M. D. A. C., & Dórea, J. R. R. (2021). Disentangling data dependency using cross-validation strategies to evaluate the prediction quality of cattle grazing activities using machine learning algorithms and wearable sensor data. Journal of Animal Science, 99(9), skab206. https://doi.org/10.1093/jas/skab206

Dikmen, S., & Hansen, P. J. (2009). Is the temperature-humidity index the best indicator of heat stress in lactating dairy cows in a subtropical environment? In Journal of Dairy Science (Vol. 92, Issue 1, pp. 109–116). https://doi.org/10.3168/jds.2008-1370

Fournel, S., Ouellet, V., & Charbonneau, É. (2017). Practices for Alleviating Heat Stress of Dairy Cows in Humid Continental Climates: A Literature Review. Animals, 7(5), 37. https://doi.org/10.3390/ani7050037

Frigeri, K. D. M., Kachinski, K. D., Ghisi, N. D. C., Deniz, M., Damasceno, F. A., Barbari, M., Herbut, P., & Vieira, F. M. C. (2023). Effects of Heat Stress in Dairy Cows Raised in the Confined System: A Scientometric Review. Animals, 13(3), 350. https://doi.org/10.3390/ani13030350

García, R., Aguilar, J., Toro, M., Pinto, A., & Rodríguez, P. (2020). A systematic literature review on the use of machine learning in precision livestock farming. Computers and Electronics in Agriculture, 179, 105826.

Godyn, D., Herbut, E., & Walczak, J. (2013). Infrared thermography as a method for evaluating the welfare of animals subjected to invasive procedures: a review. *Annals of Animal Science*, *13*(3), 423.

Herbut, P., Hoffmann, G., Angrecka, S., Godyń, D., Vieira, F. M. C., Adamczyk, K., & Kupczyński, R. (2021). The effects of heat stress on the behaviour of dairy cows – a review. Annals of Animal Science, 21(2), 385–402. https://doi.org/10.2478/aoas-2020-0116

Hlimi, A., El Otmani, S., Elame, F., Chentouf, M., El Halimi, R., & Chebli, Y. (2024). Application of Precision Technologies to Characterize Animal Behavior: A Review. Animals, 14(3), 416.

Islam, M. A., Lomax, S., Doughty, A., Islam, M. R., Jay, O., Thomson, P., & Clark, C. (2021). Automated monitoring of cattle heat stress and its mitigation. *Frontiers in Animal Science*, *2*, 737213.

Ito, K., Von Keyserlingk, M. A. G., LeBlanc, S. J., & Weary, D. M. (2010). Lying behavior as an indicator of lameness in dairy cows. Journal of dairy science, 93(8), 3553-3560.

Ji, B., Banhazi, T., Perano, K., Ghahramani, A., Bowtell, L., Wang, C., & Li, B. (2020). A review of measuring, assessing and mitigating heat stress in dairy cattle. Biosystems Engineering, 199, 4–26. https://doi.org/10.1016/j.biosystemseng.2020.07.009

Kaur, U., Malacco, V. M. R., Bai, H., Price, T. P., Datta, A., Xin, L., Sen, S., Nawrocki, R. A., Chiu, G., Sundaram, S., Min, B.-C., Daniels, K. M., White, R. R., Donkin, S. S., Brito, L. F., & Voyles, R. M. (2023). Invited review: Integration of technologies and systems for precision animal

agriculture - a case study on precision dairy farming. Journal of Animal Science, 101, skad206. https://doi.org/10.1093/jas/skad206

Langford, F., & Stott, A. (2012). Culled early or culled late: Economic decisions and risks to welfare in dairy cows. Animal Welfare, 21(S1), 41–55. https://doi.org/10.7120/096272812X13345905673647

Lee, Y., Bok, J. D., Lee, H. J., Lee, H. G., Kim, D., Lee, I., ... & Choi, Y. J. (2015). Body temperature monitoring using subcutaneously implanted thermo-loggers from Holstein steers. *Asian-Australasian Journal of Animal Sciences*, *29*(2), 299.

Mao, A., Huang, E., Gan, H., Parkes, R. S., Xu, W., & Liu, K. (2021). Cross-modality Interaction Network for equine activity recognition using imbalanced Multi-Modal Data. Sensors, 21(17), 5818. https://doi.org/10.3390/s21175818

Milan, H. F., Perano, K. M., & Gebremedhin, K. G. (2018). Survey and future prospects in precision dairy farming. In *10th International Livestock Environment Symposium (ILES X)* (p. 1). American Society of Agricultural and Biological Engineers.

Moravcsíková, Á., Vyskočilová, Z., Šustr, P., & Bartošová, J. (2024). Validating Ultra-Wideband Positioning System for Precision Cow Tracking in a Commercial Free-Stall Barn. *Animals*, *14*(22), 3307.

Pastell M, Frondelius L, Järvinen M, Backman J (2018) Filtering methods to improve the accuracy of indoor positioning data for dairy cows. Biosystems Engineering, 169, 22–31.

Perakis, K., Lampathaki, F., Nikas, K., Georgiou, Y., Marko, O., & Maselyne, J. (2020). CYBELE–Fostering precision agriculture & livestock farming through secure access to large-scale HPC enabled virtual industrial experimentation environments fostering scalable big data analytics. Computer Networks, 168, 107035.

Polsky, L. B., Madureira, A. M., Drago Filho, E. L., Soriano, S., Sica, A. F., Vasconcelos, J. L., & Cerri, R. L. (2017). Association between ambient temperature and humidity, vaginal temperature, and automatic activity monitoring on induced estrus in lactating cows. *Journal of dairy science*, *100*(10), 8590-8601.

Porto SMC, Arcidiacono C, Anguzza U, Cascone G (2013) A computer vision-based system for the automatic detection of lying behavior of dairy cows in free-stall barns. Biosystems Engineering, 115, 184–194.

Raj, R., & Kos, A. (2023). An improved human activity recognition technique based on convolutional neural network. Scientific Reports, 13(1), 22581. https://doi.org/10.1038/s41598-023-49739-1

Rathod, P. K., & Dixit, S. (2021). Precision dairy farming: Opportunities and challenges for India. The Indian Journal of Animal Sciences, 90(8), 1083–1094. https://doi.org/10.56093/ijans.v90i8.109207

Raza, A., Al Nasar, M. R., Hanandeh, E. S., Zitar, R. A., Nasereddin, A. Y., & Abualigah, L. (2023). A novel methodology for human kinematics motion detection based on smartphones sensor data using artificial intelligence. Technologies, 11(2), 55.

Ren K, Alam M, Nielsen PP, Gussmann M, Rönnegård L (2022) Interpolation Methods to Improve Data Quality of Indoor Positioning Data for Dairy Cattle. Frontiers in Animal Science, 3, 1–11.

Renaudeau, D., Collin, A., Yahav, S., De Basilio, V., Gourdine, J. L., & Collier, R. J. (2012). Adaptation to hot climate and strategies to alleviate heat stress in livestock production. *Animal*, *6*(5), 707-728.

Reuscher, K. J., Cook, N. B., Da Silva, T. E., Mondaca, M. R., Lutcherhand, K. M., & Van Os, J. M. C. (2023). Effect of different air speeds at cow resting height in freestalls on heat stress responses

and resting behavior in lactating cows in Wisconsin. Journal of Dairy Science, 106(12), 9552–9567. https://doi.org/10.3168/jds.2023-23364

Riaboff, L., Couvreur, S., Madouasse, A., Roig-Pons, M., Aubin, S., Massabie, P., ... & Plantier, G. (2020). Use of predicted behavior from accelerometer data combined with GPS data to explore the relationship between dairy cow behavior and pasture characteristics. Sensors, 20(17), 4741.

Shine, P., & Murphy, M. D. (2021). Over 20 years of machine learning applications on dairy farms: A comprehensive mapping study. *Sensors*, *22*(1), 52.

Shu, H., Li, Y., Bindelle, J., Jin, Z., Fang, T., Xing, M., ... & Wang, W. (2023). Predicting physiological responses of dairy cows using comprehensive variables. *Computers and Electronics in Agriculture*, *207*, 107752.

Tao, S., Rivas, R. M. O., Marins, T. N., Chen, Y. C., Gao, J., & Bernard, J. K. (2020). Impact of heat stress on lactational performance of dairy cows. Theriogenology, 150, 437-444.

Thorup, V. M., Munksgaard, L., Robert, P. E., Erhard, H. W., Thomsen, P. T., & Friggens, N. C. (2015). Lameness detection via leg-mounted accelerometers on dairy cows on four commercial farms. Animal, 9(10), 1704-1712.

Tucker, C. B., Jensen, M. B., De Passillé, A. M., Hänninen, L., & Rushen, J. (2021). Invited review: Lying time and the welfare of dairy cows. Journal of Dairy Science, 104(1), 20–46. https://doi.org/10.3168/jds.2019-18074

Vu, H., Chung, H., Choi, C., & Kim, Y. (2023, October). eTag: An energy-neutral ear tag for real-time body temperature monitoring of dairy cattle. In Proceedings of the 29th Annual International Conference on Mobile Computing and Networking (pp. 1-15).

Vu, H., Prabhune, O. C., Raskar, U., Panditharatne, D., Chung, H., Choi, C., & Kim, Y. (2024). MmCows: A Multimodal Dataset for Dairy Cattle Monitoring. Advances in Neural Information Processing Systems, 37, 59451-59467.

Wang, J., Bell, M., Liu, X., & Liu, G. (2020). Machine-learning techniques can enhance dairy cow estrus detection using location and acceleration data. Animals, 10(7), 1160.

West, J. W. (2003). Effects of heat stress on production in dairy cattle. *Journal of Dairy Science, 86*(6), 2131–2144.

Whitham, J. C., & Miller, L. J. (2016). Using technology to monitor and improve zoo animal welfare. Animal Welfare, 25(4), 395-409.

Wu, D., Han, M., Song, H., Song, L., & Duan, Y. (2023). Monitoring the respiratory behavior of multiple cows based on computer vision and deep learning. Journal of Dairy Science, 106(4), 2963-2979.

Zeng, M., Nguyen, L. T., Yu, B., Mengshoel, O. J., Zhu, J., Wu, P., & Zhang, J. (2014). Convolutional Neural Networks for human activity recognition using mobile sensors. 6th International Conference on Mobile Computing, Applications and Services, 197–205. https://doi.org/10.4108/icst.mobicase.2014.257786

CHAPTER 3: STALL DESIGN TO MITIGATE HEAT STRESS OF DAIRY CATTLE IN MECHANICALLY VENTILATED BARNS USING COMPUTATIONAL FLUID DYNAMICS

3.1. Abstract

Heat stress in dairy barns remains a significant challenge, exacerbated by economic and structural constraints that limit the ability to upgrade cooling systems in existing facilities. Building on prior work by Jung (2021), this study uses computational fluid dynamics (CFD) with anatomically realistic cow models to investigate modified stall designs as a retrofit-friendly solution for improving convective cooling. Four two-row freestall configurations were compared: a traditional in-line layout, a laterally staggered layout, and two retrofits featuring single or double vertical airflow deflectors installed between the stall rows. Results showed that the deflector retrofits effectively directed ventilation into the second row of stalls, where airflow is typically weakest. A single 45° vertical deflector increased total convective heat transfer by up to 28% relative to the in-line baseline. At lower inlet air speeds (below ~1.5 m/s), both the staggered and deflector-equipped designs delivered greater cooling to cows than the baseline or a baffle-only configuration. Conversely, at higher inlet speeds (above 1.5 m/s), a conventional overhead airflow baffle provided more cooling benefit than the stall modifications. Notably, the single- and double-deflector designs yielded similar improvements for second-row cows, indicating that a single deflector can achieve most of the retrofit's benefit. These findings highlight vertical deflectors as a novel, energy-efficient retrofit strategy to mitigate heat stress in existing dairy barns, offering significant cooling improvements with minimal structural change and no additional fan power.

3.2. Introduction

Heat stress poses a significant challenge to modern dairy production, with economic losses in the United States alone surpassing one billion dollars annually. These losses stem from various factors, including reduced feed intake, lower milk yields, compromised fertility, and increased veterinary costs (Chung et al., 2020; Polsky & von Keyserlingk, 2017). High-producing dairy breeds, particularly

Holsteins, experience a heightened metabolic heat load that narrows their thermal comfort margin during hot conditions. This physiological stress leads to elevated respiration rates, increased sweating, and peripheral vasodilation (Atkins et al., 2018; Wang et al., 2018). Prolonged exposure to heat stress diminishes production efficiency and escalates the risk of lameness and disease, adversely affecting both farm profitability and animal welfare (Nordlund et al., 2019). Conventional freestall barns typically use mechanical or hybrid ventilation systems to enhance convective heat dissipation by increasing airflow velocity in the animal-occupied zone (AOZ). However, despite advancements in fan design and control systems, ventilation can account for as much as 22% of total energy consumption on dairy farms. Furthermore, the airflow measured at the fan outlets often fails to represent the velocity distribution experienced by cows in the AOZ (Mondaca et al., 2019; Wang et al., 2018). This discrepancy arises because much of the incoming air tends to follow the path of least resistance, often traveling through central feed alleys and bypassing the resting stalls where cows spend most of their time (Drewry et al., 2017). To improve air distribution within barns, several supplemental strategies have emerged. Options include overhead baffles, optimal fan placement, and various evaporative cooling devices such as feedline sprinklers, foggers, and misters (Van Os, 2019; Zhou et al., 2019). Overhead or vertical baffles, in particular, have demonstrated the ability to redirect high-level airflow downward into the AOZ, thus enhancing surface air velocity and convective heat transfer without necessitating additional fan power (Harner et al., 2008; Zhou et al., 2019).

A persistent challenge is practicality. Geometry-intensive redesigns, such as the staggered stall layout developed and evaluated by Jung (2021), can redistribute momentum more uniformly across stall rows in silico. Still, they demand capital and downtime that many existing facilities cannot accommodate. By contrast, airflow-management retrofits such as ceiling baffles and jet/ceiling deflectors are comparatively low-intrusion: they adjust the path and angle of incoming jets, or ceiling flows to

penetrate the AOZ with minimal structural change. The peer-reviewed literature already documents that appropriately placed baffles can enhance stall-plane velocities and improve uniformity in cross-ventilated barns (Zhou et al., 2019; Jung et al., 2023). Yet rigorous, dairy-specific quantification of deflector strategies remains limited, despite a broader ventilation and heat-transfer body of work showing that turning-vane and splitter-plate concepts can redirect jets, increase entrainment, and, under the right geometries, improve local convective transfer (Cao et al., 2023; Khan et al., 2006). This gap matters because upgrades in the field often begin with simple plates or vanes mounted near inlets or beneath ceiling jets to steer momentum toward downstream stalls; absent quantitative evidence for AOZ benefits and pressure penalties, such interventions are deployed on intuition rather than data.

This study addresses the evidence gap by building on Jung's CFD framework while shifting the design question from geometry-heavy reconstruction to low-intrusion airflow control. Specifically, we compare two practically relevant retrofit concepts under identical, heat-stress-relevant boundary conditions: a baffle configuration motivated by prior demonstrations of its potential to reduce velocity deficits over lying cows, and a deflector configuration designed to intercept the primary jet and redirect it toward downstream stalls. The rationale for examining deflectors is twofold. First, deflectors are immediately actionable for retrofit-heavy herds: installation is feasible between milkings, cost is modest relative to stall reconstruction, and placement and angle are adjustable. Second, from a fluid-mechanics perspective, altering jet trajectory and entrainment with deflectors is a direct lever for elevating AOZ airspeed in wake-prone regions created by the first stall row; related splitter-plate/deflection concepts in crossflow systems support this premise, while also cautioning that any gain must be weighed against added pressure drop and its energy implications (Cao et al., 2023; Khan et al., 2006; Zhou et al., 2019; Jiang et al., 2024). By providing a side-by-side, validated CFD comparison of baffles and deflectors, including predicted AOZ velocities, spatial uniformity, and induced static-

pressure cost, this work aims to supply the quantitative basis needed to guide retrofit decisions toward thermally effective, economically realistic solutions. For clarity of presentation, **Figure 1a** schematically contrasts the baseline, baffle, and deflector geometries with consistent AOZ elevations and inlet/outlet locations to anchor the analysis that follows, and **Figure 1 b** is a top view depicting the hypothesized air flow distribution between staggered and deflector configurations.

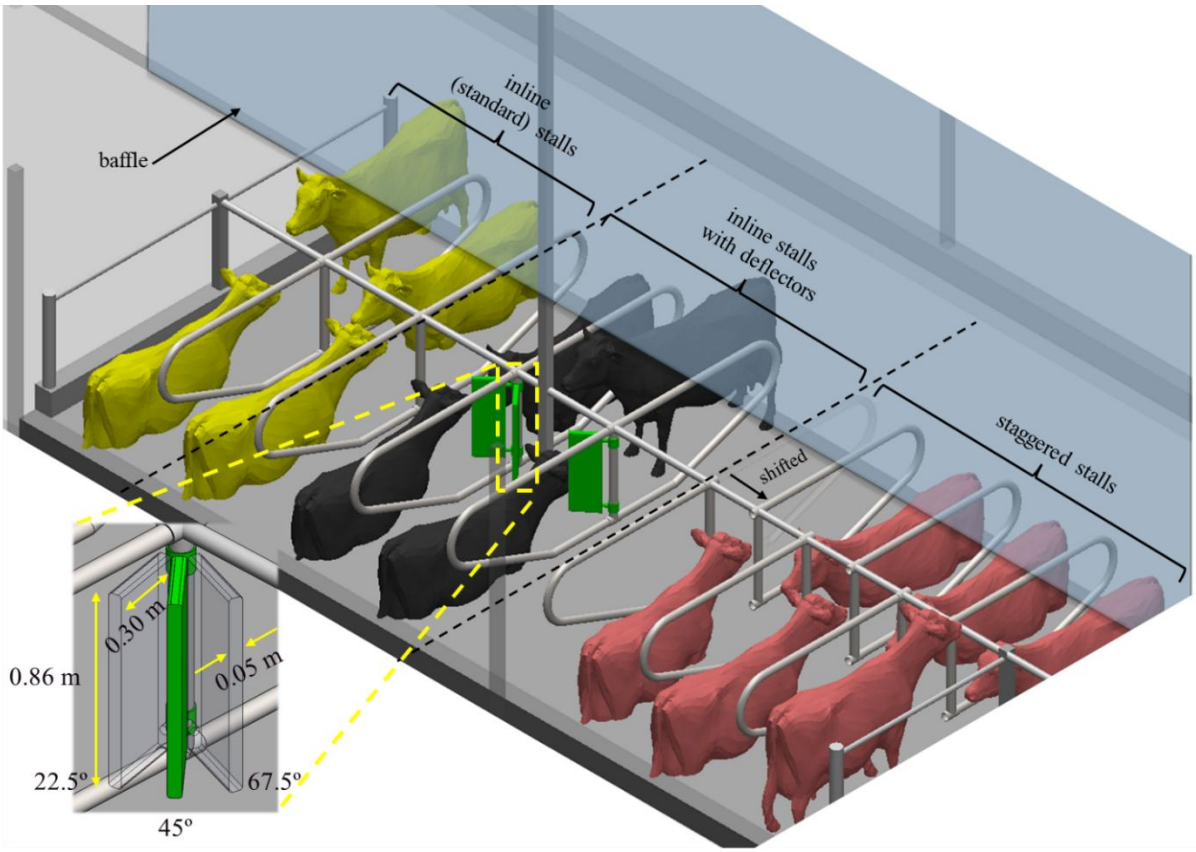

(a)

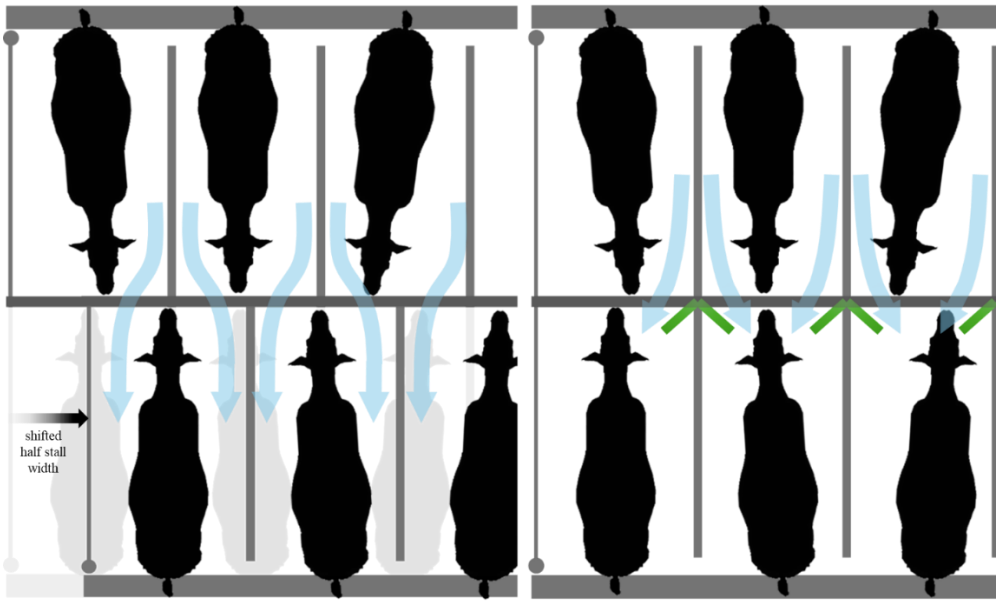

(b)

Figure 1. (a) Schematic diagram illustrating the layout of the dairy barn pen with the different stall designs. Cows in the different stall configurations are shown in various colors: yellow (standard in-line), black (deflector-equipped), and red (staggered) for the other stall designs. (b) airflow direction movement in staggered and deflector configurations.

3.3. Materials and Methods

3.3.1 Computational domain

The computational domain was constructed to represent a typical head-to-head freestall section of a mechanically ventilated dairy barn, incorporating six full-scale Holstein cow geometries positioned in either lying or standing postures. This barn section consisted of two parallel rows of stalls flanking a central feed alley, consistent with layouts reported in previous ventilation studies (Zhou et al., 2019; Mondaca et al., 2019). Each row contained three stalls, and the width and length of the stalls followed commercial freestall design recommendations at 1.33 m and 1.80 m, respectively. The total domain length was determined by the combined length of the feed alley and stall rows, while the height was

set to match commercial barn dimensions, providing adequate clearance for airflow over standing cows and ventilation equipment.

The cow geometries were based on a validated three-dimensional Holstein model with detailed body contours, including the head, torso, limbs, and udder regions, which have been shown to influence near-surface airflow and convective heat transfer significantly (Wang et al., 2018; Zhou et al., 2019). The models represented mature Holsteins with an average body mass of 625 kg, with lying cows modeled at a dorsal height of approximately 0.5 m and standing cows at 1.6 m. These geometries were scaled and positioned in the stalls to replicate realistic resting and standing postures, ensuring that the animal-occupied zone (AOZ) blockage effect on airflow was accurately captured.

Symmetry boundary conditions were applied to the two longitudinal sidewalls of the computational domain to reduce the model size while maintaining the representative airflow behavior of a continuous barn. This assumption, widely used in CFD analyses of livestock buildings, allows for a computationally efficient representation of large-scale barns while preserving flow characteristics in the AOZ (Mondaca et al., 2019; Chung et al., 2022). The feed alley was centrally located between the two rows of head-to-head stalls, providing an unobstructed channel for air movement between the cow rows, a factor known to influence airflow penetration into second-row stalls (Jung et al., 2023).

Five stall configurations were simulated in this study: the baseline in-line arrangement, a staggered arrangement, a staggered arrangement with an overhead baffle, a single-deflector arrangement, and a double-deflector arrangement. The baseline arrangement reflected the conventional stall alignment found in most dairy barns, in which the stall partitions in both rows are aligned directly opposite each other. The staggered arrangement offset the second row by half a stall width to reduce wake interference and increase crossflow mixing, similar to the staggered-tube principle in heat exchanger design (Colburn, 1964; Khan et al., 2006). The staggered + baffle configuration retained this offset but added a 0.05 m thick vertical baffle at the neck-rail height in the feed alley to redirect airflow downward

toward the second-row cows, following recommendations from Harner et al. (2008) and Zhou et al. (2019) for enhanced AOZ penetration.

The single-deflector arrangement replaced the staggered configuration with an in-line stall layout. Still, it introduced a rigid vertical deflector panel ahead of the brisket board, angled at 45°, to capture airflow passing between first-row cows and direct it toward the dorsal surface of the second row. The double-deflector arrangement extended this concept by adding a second deflector panel 200 mm downstream of the first to sustain airflow penetration along the full length of the second row of cows. Deflector dimensions and placement were selected to balance aerodynamic performance with minimal obstruction to cow movement or resting behavior.

This study evaluates the influence of freestall layout modifications on airflow and potential convective heat dissipation in a naturally ventilated dairy barn using computational fluid dynamics (CFD). By systematically modeling several configurations, the goal is to determine how airflow dynamics can be optimized within the animal-occupied zone (AOZ), where heat stress most critically impacts cow welfare and productivity. This work builds upon prior analyses of conventional in-line stall configurations and staggered stall arrangements developed by Jung (2021), as well as an earlier investigation by the authors involving staggered stalls augmented with overhead baffles. The present study expands the design space to include two additional passive cooling features: vertical airflow deflectors and in-stall baffles, which are intended to enhance air penetration into downstream stalls further.

3.3.2 Stall configuration designs

The stall configurations in this study were designed to evaluate how passive modifications to stall alignment systematically affect airflow distribution and convective cooling within the animal-occupied zone (AOZ), and the addition of flow-redirecting devices. All five configurations were modeled within

the same computational domain described in Section 2.1, and each incorporated full-scale Holstein cow models positioned to reflect realistic occupancy during heat stress conditions. The geometric dimensions of the stalls and the feed alley were held constant across all cases so that observed differences in airflow patterns and heat transfer characteristics could be attributed solely to changes in stall layout or the presence of airflow-modifying devices.

The baseline in-line configuration was representative of conventional freestall barn designs, in which the stall partitions in both rows align directly opposite one another. This arrangement is prevalent in large-scale dairy facilities due to its ease of construction and efficient space utilization; however, previous CFD analyses have shown that the cows in the first-row act as aerodynamic obstacles, creating wake zones that reduce airflow penetration into the second row (Mondaca et al., 2019; Zhou et al., 2019). In this baseline case, no baffles or deflectors were present, and the airflow was free to follow the path of least resistance, primarily along the feed alley.

The staggered configuration offset the second row of stalls by half a stall width (0.665 m) compared to the first row. This geometric modification is based on the staggered-tube bank arrangement used in heat exchanger design, where alternating the positions of flow obstructions enhances downstream mixing and maintains higher local convective heat transfer coefficients than in-line configurations (Colburn, 1964; Khan et al., 2006). Jung et al. (2023) demonstrated that this arrangement increases AOZ airflow and improves surface cooling performance for both lying and standing cows without requiring additional fan power. In the present study, the staggered arrangement was implemented using identical stall dimensions to the baseline case, ensuring that the only difference was the lateral shift of the second-row stalls.

The staggered + baffle configuration retained the half-stall offset of the staggered arrangement but introduced a solid vertical baffle panel positioned at the neck-rail location across the feed alley. The baffle measured 50 mm in thickness and extended the full width of the feed alley at a height designed

to intercept and redirect the incoming airflow downward and toward the dorsal surfaces of the second-row cows. This approach follows recommendations by Harner et al. (2008) and the optimal baffle placement findings of Zhou et al. (2019), which indicate that redirecting airflow from above the AOZ into the cow resting zone reduces stratification and improves convective cooling effectiveness. The inclusion of the baffle in the staggered arrangement was intended to assess potential synergistic effects between enhanced stall offset-induced mixing and directed airflow penetration.

The single-deflector configuration replaced the staggered layout with an in-line stall arrangement. Still, it introduced a rigid vertical deflector mounted ahead of the brisket board in the first-row stalls. Each deflector was 100 mm high and angled at 45° relative to the incoming airflow. The deflectors were positioned so that they intercepted airflow moving between the first-row cows and redirected it laterally and downward toward the second-row cows. The aerodynamic function of the deflector is analogous to splitter plates used in industrial heat exchangers, which disrupt laminar subflows and promote crossflow mixing (Mangrulkar et al., 2016). The deflector height was selected to create a strong redirection effect without encroaching upon the cow's lying space or altering stall usability.

The double-deflector configuration extended the single-deflector design by adding a second angled plate 200 mm downstream of the first. This placement was chosen to sustain redirected airflow momentum along the entire dorsal surface of the second-row cows, reducing the decay of redirected jets caused by turbulent mixing and viscous dissipation. This configuration is intended to determine whether sequential redirection devices could further enhance AOZ penetration and cooling uniformity in the downstream stalls.

3.3.3 Environmental and boundary conditions

The simulations were conducted under environmental conditions representative of peak summer heat stress events commonly observed in Midwestern U.S. dairy facilities. The inlet air temperature was set

at 30 °C, corresponding to a temperature–humidity index (THI) of approximately 80. This THI value exceeds the threshold for mild heat stress in dairy cattle and approaches the moderate stress range, where reductions in feed intake, milk yield, and reproductive performance have been widely documented (Chung et al., 2020; Wang et al., 2018). Selection of these conditions was intended to capture airflow and cooling behavior under thermally challenging scenarios where ventilation system performance is most critical to maintaining cow comfort and productivity.

The surface temperature of all cow geometries was fixed at 35 °C to approximate the skin temperature of heat-stressed Holsteins, consistent with direct measurements and prior CFD modeling studies (Gebremedhin et al., 2008; Zhou et al., 2019). This approach allows calculation of local and zone-averaged convective heat transfer coefficients, which serve as indicators of the airflow's cooling capacity over the animal's body. The barn floor, stall partitions, baffles, and deflectors were modeled as adiabatic, no-slip walls to focus the analysis exclusively on airflow-induced convective effects, excluding conductive or radiative heat transfer pathways.

Inlet airspeeds of 0.5, 1.0, 1.5, 2.0, 2.5, and 3.0 m s^{-1} were tested for each stall configuration. This range encompasses the operational velocities of tunnel and cross-ventilation fans in commercial barns, from low-energy settings to full-capacity operation (Mondaca et al., 2019; Jung et al., 2023). The lower velocities were included to assess performance under energy-saving fan operation, while higher velocities captured the upper limit of fan capacity for extreme heat events. In all cases, the inlet velocity profile was assumed to be uniform, with a turbulent intensity of 5 % at the inlet. This turbulence level is consistent with mechanically driven ventilation systems and aligns with values used in previous dairy barn CFD studies (Wang et al., 2018; Zhou et al., 2019).

The airflow entered the computational domain through a single large inlet plane located at the upwind end of the feed alley. It exited through an outlet plane at the opposite end, modeled as a pressure-outflow boundary with zero-gauge pressure. This inlet–outlet arrangement replicated a longitudinal

ventilation pattern similar to that of tunnel-ventilated barns. The outlet was positioned sufficiently far downstream to ensure fully developed flow before exit, avoiding backflow or artificial acceleration effects at the measurement planes.

Symmetry boundary conditions were applied along both longitudinal sidewalls, effectively representing an infinitely repeating barn section. The ceiling was modeled as an adiabatic, no-slip surface, consistent with conditions in solid-roof barns, where conduction through the roof structure is negligible compared to convective transport in the AOZ (Chung et al., 2022). The barn floor was similarly treated as an adiabatic no-slip surface.

The inlet air temperature and relative humidity remained constant throughout each simulation, and air density and viscosity were calculated using the ideal gas law at the specified conditions (**Table 1**). Water vapor effects were not modeled explicitly, as the study focused on airflow and convective heat transfer rather than evaporative cooling mechanisms. This decision isolates the aerodynamic performance of each stall configuration without confounding effects from evaporative systems such as misters or sprinklers.

Table 1. Summary of the environmental and boundary conditions for simulations.

Locations	Types	Boundary Conditions
Inlet	Velocity Inlet	0.5, 1.0, 1.5, 2.0, 2.5, and 3.0 m s-1 Temperature: 298.0 K (25.0 °C) Turbulent intensity: 5.0%
Outlet	Outflow	N/A
Sidewalls	Symmetry	N/A
Ceiling, Floor, Baffle, and Deflector	No-slip	Adiabatic
Cow	No-slip	Fixed temperature (308.0 K, 35.0 °C)

3.3.4 Mesh generation and independence

The computational meshes for all configurations were generated in ANSYS Meshing (version 2024 R2, ANSYS Inc., Canonsburg, PA) using a hybrid grid strategy that combined structured and unstructured elements. Structured hexahedral cells were employed in the bulk flow regions, such as the feed alley and upper barn volume, to minimize numerical diffusion and maintain solution stability in relatively uniform flow zones (Bjerg et al., 2020; Rong et al., 2016). Unstructured tetrahedral elements were applied in geometrically complex areas surrounding the cows, stall partitions, baffles, and deflectors, where surface curvature and intricate junctions necessitated geometric flexibility (Norton et al., 2009; Bartzanas et al., 2004).

To capture near-wall velocity gradients and accurately predict convective heat transfer, prism layers were generated along all solid boundaries, including the cow surfaces, floor, and airflow-modifying devices. These layers were sized to maintain a non-dimensional wall distance (y^+) within the optimal range for the enhanced wall treatment used in the turbulence model, ensuring that both the viscous sublayer and logarithmic layer were adequately resolved (van Hooff & Blocken, 2010; Norton et al., 2010). The initial prism layer thickness was determined from the inlet velocity and air kinematic viscosity at 30 °C, with a growth rate of 1.2 applied to subsequent layers to prevent excessive stretching and preserve orthogonality.

Mesh refinement zones were concentrated in the animal-occupied zone (AOZ), particularly in the narrow inter-cow spaces and downstream wakes of the first-row cows, where flow separation and recirculation are expected to occur (Bartzanas et al., 2007; Lee et al., 2013). Additional local refinement was applied around baffles and deflectors to capture the effects of jet formation, redirection, and dissipation. For deflector configurations, the refinement region extended downstream along the dorsal surfaces of the second-row cows to resolve the decay of the redirected airflow due to turbulent mixing and viscous dissipation.

All configurations were meshed to maintain a similar total mesh cell count while preserving fine resolution in critical flow regions. The final mesh for each configuration contained approximately 2.83 million cells, consistent with previous validated CFD studies in agricultural ventilation, which typically range from 2 to 5 million cells for geometries of similar complexity (Bartzanas et al., 2004; Rong et al., 2016; Bjerg et al., 2020).

A mesh independence test was performed using the staggered + baffle configuration, which contained the highest geometric complexity. Three mesh densities were evaluated: a coarse mesh (~1.85 million cells), a medium mesh (~2.83 million cells), and a fine mesh (~4.21 million cells). The independence criterion was based on the change in area-weighted average convective heat transfer coefficient ($\bar{h}$) on the dorsal surfaces of the second-row cows at an inlet velocity of 2.0 m s^{-1}. The difference in $\bar{h}$ Between the medium and fine meshes, the difference was below 5%, indicating mesh convergence, while the fine-mesh computational cost was approximately 2.5 times higher. Consequently, the medium mesh resolution was selected for all simulations to balance accuracy and computational efficiency (van Hooff & Blocken, 2010; Norton et al., 2010).

3.3.5 Turbulence modeling and solver setup

All simulations were performed using the finite volume method in ANSYS Fluent (version 2024 R2, ANSYS Inc., Canonsburg, PA), which has been extensively used for CFD analyses in agricultural building ventilation due to its flexibility in handling complex geometries and diverse turbulence models (Bartzanas et al., 2004; Rong et al., 2016; Jung et al., 2023). The governing equations for mass, momentum, and energy conservation were solved under steady-state conditions to represent constant summer ventilation operation.

Turbulent flow was modeled using the renormalization group (RNG) k–ε model with enhanced wall treatment. This model was selected based on multiple comparative studies showing its superior

accuracy in predicting recirculation, jet deflection, and separation behavior in livestock building airflow, as well as its capability to resolve both free-stream and near-wall turbulent structures under mixed convection conditions (Norton et al., 2010; Rong et al., 2016; Zhou et al., 2019; Jung et al., 2023). Compared with the Standard and Realizable k–ε models, the RNG formulation includes an additional term in the k–ε equation to account for the effects of smaller-scale turbulence, which has been shown to improve predictions of airflow around bluff bodies such as cows (Chung et al., 2022; Mangrulkar et al., 2016).

The enhanced wall treatment enabled accurate prediction of near-wall velocity gradients and convective heat transfer coefficients across the full range of non-dimensional wall distances (y^+), allowing the use of prism layers in the mesh without compromising turbulence model performance. This approach has been validated in previous animal housing studies where heat transfer between livestock and the surrounding air is a critical metric for ventilation performance (Wang et al., 2018; Bjerg et al., 2020).

The pressure–velocity coupling was handled using the Semi-Implicit Method for Pressure-Linked Equations (SIMPLE) algorithm, which is widely adopted in agricultural CFD applications for its stability and convergence efficiency (Bartzanas et al., 2007; Norton et al., 2009). Spatial discretization of the momentum, turbulence kinetic energy (k), turbulence dissipation rate (ε\), and energy equations was performed using a second-order upwind scheme to minimize numerical diffusion while maintaining computational efficiency. Pressure interpolation was carried out using the standard pressure-staggering option (PRESTO!) scheme, which improves pressure prediction accuracy in flows with significant buoyancy and recirculation.

Convergence was determined by monitoring both scaled residuals and global energy and mass imbalances. Residuals for continuity, momentum, turbulence, and energy quantities were required to fall below $1\times10e^{-6}$. Additionally, the inlet–outlet mass flow balance needed to be within 1 %, and the

area-weighted average convective heat transfer coefficient (h) over the dorsal surfaces of the cows was monitored to confirm stability of the thermal solution.

3.4. Results and Discussion

3.4.1 Airflow distribution

The velocity contours at 0.5 m above the barn floor for a representative inlet velocity of 2.0 m s^{-1} (**Figure 2**) revealed substantial differences in airflow penetration into the second-row stalls across configurations. In the baseline in-line arrangement, airflow entering the feed alley predominantly bypassed the AOZ of the second row, flowing through the unobstructed channel above the first-row cows. The wakes generated by the first-row cows created large stagnation zones in the dorsal regions of the downstream cows, with velocities often below 0.5 m s^{-1}. Such low-velocity zones have been associated with elevated body surface temperatures and increased heat stress risk in dairy cattle (Wang et al., 2018; Bjerg et al., 2020).

In contrast, the staggered configuration improved airflow distribution by shifting the second-row stalls laterally relative to the first row. This offset reduced direct wake impingement and allowed airflow from the feed alley to pass between the first-row cows and reach the dorsal surfaces of the downstream animals. At 2.0 m s^{-1} inlet velocity, the staggered arrangement increased the AOZ velocity in the second row by approximately 18 % compared to the baseline. This trend aligns with previous CFD studies demonstrating enhanced downstream mixing and reduced velocity deficits in staggered obstacle arrangements (Colburn, 1964; Khan et al., 2006; Jung et al., 2023).

The staggered + baffle configuration further improved airflow penetration into the second row. The baffle redirected high-momentum air from the upper feed alley downward into the AOZ, increasing average velocities near the dorsal surface of second-row cows by 27 % relative to the baseline. The velocity contours (Figure 2) showed a more uniform distribution in the second-row stalls, with reduced

stagnation zones behind the first-row cows. The effectiveness of baffles in modifying airflow penetration into occupied zones is consistent with the findings of Harner et al. (2008) and the optimal baffle placement study by Zhou et al. (2019).

The single-deflector configuration, despite reverting to the in-line stall arrangement, achieved comparable AOZ velocity enhancement to the staggered + baffle design. The 45° deflector successfully captured airflow moving between the first-row cows and redirected it toward the dorsal surfaces of the second-row animals. However, the redirection effect weakened further downstream, with lower velocities observed near the hindquarters of the second-row cows, suggesting that a single deflector may not sustain momentum along the full body length.

The double-deflector configuration addressed this limitation by introducing a second angled plate downstream of the first. This design produced the most consistent AOZ velocity distribution across the entire dorsal surface of the second-row cows, with average velocities 24 % higher than the baseline at 2.0 m s^{-1} inlet velocity. The sustained momentum of the redirected airflow is evident in the streamline plots, where flow paths remain directed toward the downstream cow surfaces over a longer distance than in the single-deflector case.

Overall, these results indicate that while stall staggering alone can improve downstream airflow penetration, the addition of targeted airflow-modifying devices such as baffles or deflectors yields greater and more uniform velocity enhancements. Among the tested designs, the double-deflector configuration produced the most effective AOZ velocity distribution, which is expected to translate into improved convective cooling performance as previously discussed.

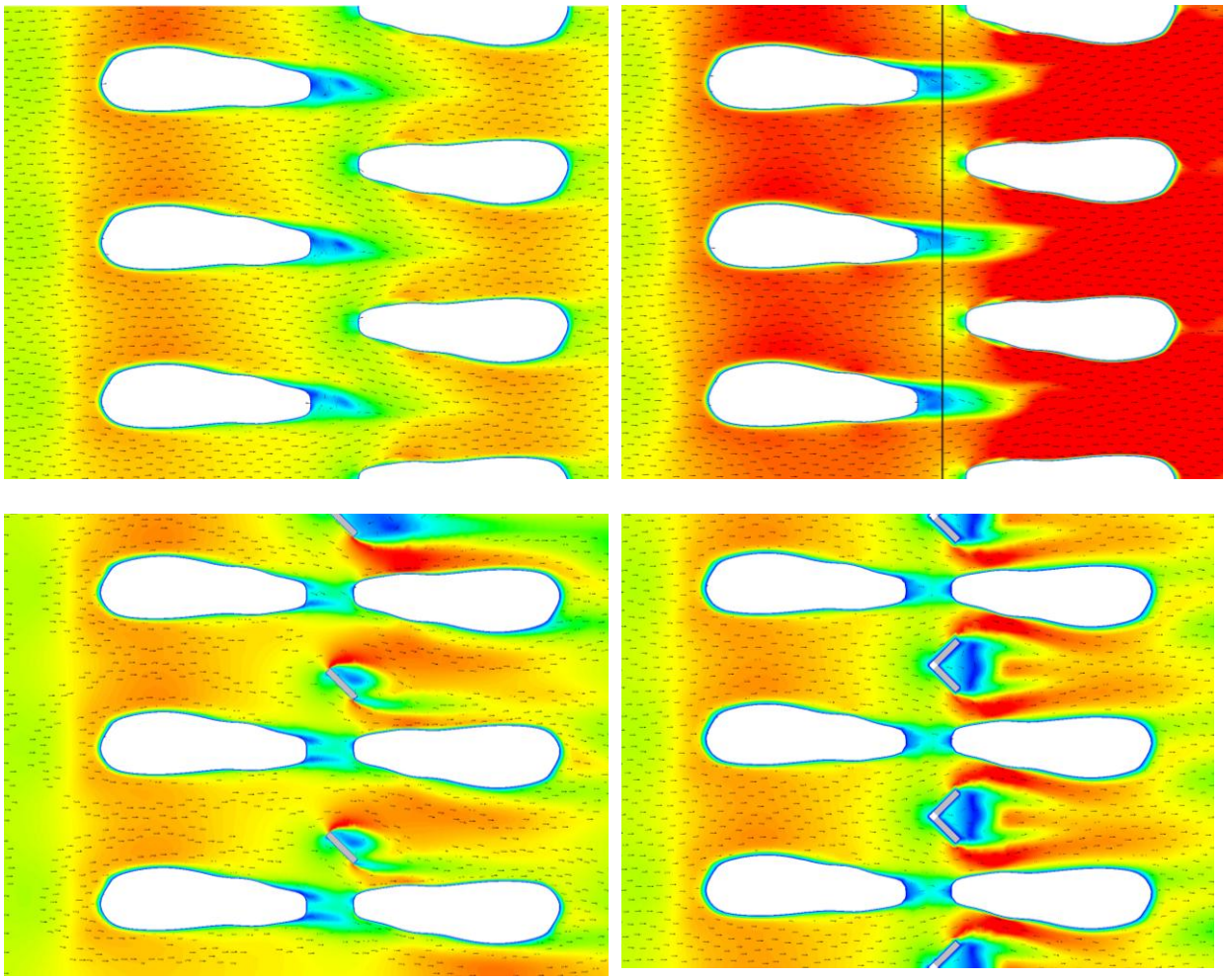

Figure 2. Velocity contour and vector plots showing the air flow distribution of the lying cow case, for different stall configurations at 0.5 m/s.

3.4.2 Convective Cooling Performance

Convective cooling performance was assessed by calculating the total convective heat transfer, Qconv, over the entire exposed surface of the cow model, with a focus on lying cows. This approach captures the complete interaction between the barn airflow and the animal's heat-emitting surfaces, including dorsal, lateral, and anterior regions, which collectively contribute to thermoregulation under heat stress conditions (Wang et al., 2018; Defraeye et al., 2012).

Across all configurations, the results revealed strong correlations between airflow penetration into the animal-occupied zone (AOZ) and total convective heat transfer. Configurations that delivered higher and more uniformly distributed airspeeds to the cow surfaces consistently exhibited higher Qconv values, demonstrating the importance of both velocity magnitude and spatial coverage in improving cooling efficiency.

3.4.2.1 In-line

In the traditional in-line free stall arrangement, airflow from the feed alley primarily impinged on the anterior and upper body surfaces of the first-row cows, leading to localized high heat transfer rates. However, second-row cows were partially shielded by the upstream animals, resulting in extended low-velocity regions along much of their body surfaces. The wakes generated by the first-row cows reduced airflow momentum before reaching the downstream animals, leading to an overall Qconv deficit of more than 20% compared to the first row.

For lying cows in the second row, the baseline configuration exhibited significant spatial variation in surface heat transfer. The anterior dorsal and lateral surfaces occasionally achieved values above 31 $W\ m^{-2}\ K^{-1}$ at higher inlet velocities ($\geq 2.0\ m\ s^{-1}$), but large regions, particularly the mid-to-rear dorsal and flank areas, frequently fell below 20 $W\ m^{-2}\ K^{-1}$. This nonuniform cooling pattern is consistent with the stagnation zones identified in the airflow distribution analysis (Section 3.1) and has been linked to higher body surface temperatures and reduced lying comfort in previous studies of tunnel-ventilated barns without targeted airflow guidance (Mondaca et al., 2019; Norton et al., 2010).

3.4.2.2 Staggered

The staggered stall arrangement significantly improved cooling performance for lying cows in the second row by shifting their positions laterally relative to the first-row cows. This adjustment reduced

direct wake interference, allowing inlet airflow to pass through the gaps between upstream cows and reach a larger portion of the downstream animals' surfaces.

As a result, total Qconv for second-row lying cows increased by approximately 15–18% over the baseline across inlet velocities from 0.5 to 3.0 m s^{-1}. At an inlet velocity of 2.0 m s^{-1}, average surface heat transfer coefficients exceeded 27 W m^{-2} K^{-1} over much of the dorsal and lateral surfaces, with reduced regions of low-velocity cooling deficit. The improvement was especially notable in the midsection and flank areas, which benefitted from higher airflow penetration compared to the baseline. These findings align with both industrial and agricultural ventilation literature, indicating that staggered obstacle placement improves downstream convective transport and reduces shadowing effects (Colburn, 1964; Khan et al., 2006).

3.4.2.3 Staggered with Baffle

The addition of a baffle to the staggered arrangement further enhanced total heat transfer by redirecting high-momentum airflow from above the first row directly into the AOZ of the second row. This design modification increased Qconv for second-row lying cows by 24 - 26% over the baseline, representing a 9 - 12% improvement over staggered stalls alone.

The baffle created a downward jet that increased local air speeds across the whole-body length of the downstream animals, elevating both anterior and rear dorsal surface heat transfer rates. At 2.0 m s^{-1} inlet velocity, large portions of the cow surface achieved average heat transfer coefficients above 30 W m^{-2} K^{-1}, while the lowest values in the rear flank region remained above 24 W m^{-2} K^{-1}. This more uniform cooling pattern closely mirrors results from previous CFD evaluations of optimized baffle placement in dairy barns (Zhou et al., 2019; Harner et al., 2008), which demonstrated that strategically deflecting inlet airflow can significantly improve cooling in obstructed zones.

3.4.2.4 Single Deflector

The single stall deflector configuration, implemented in the in-line arrangement, achieved substantial improvements in convective cooling without requiring stall repositioning. By redirecting airflow between the first-row cows toward the second row lying cows, the single deflector increased total Qconv by up to 28% compared to the baseline in-line configuration, as depicted in **Figure 3**.

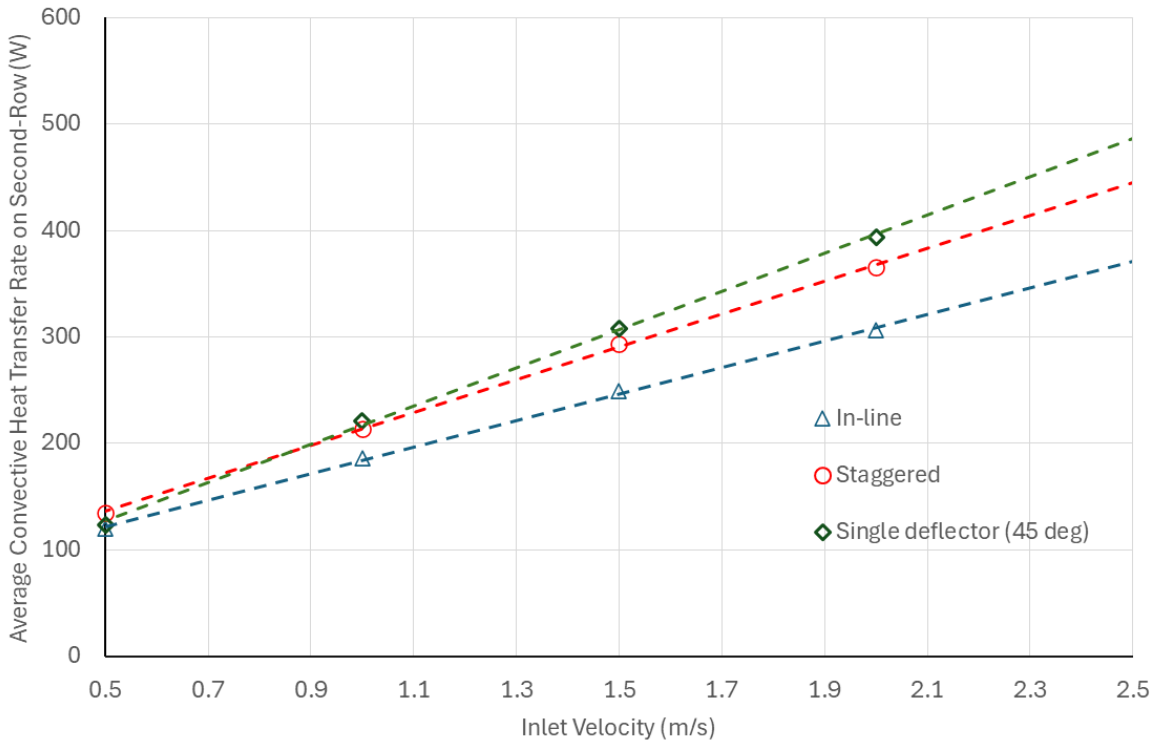

Figure 3. Comparison of convective heat transfer rate for in-line, staggered, and single deflector (45 °) stall configurations at different inlet velocities.

3.4.3 Airflow Uniformity

While maximizing the magnitude of convective heat transfer is essential for mitigating heat stress in dairy cattle, spatial uniformity of airflow over the animal's surface is equally important. Uneven airflow distribution can result in localized hot spots, reducing the overall cooling effectiveness even if the average airspeed is high (Wang et al., 2018; Bjerg et al., 2020). To quantify this aspect, airflow uniformity was evaluated using the coefficient of variation (CV) of velocity magnitude within the

animal-occupied zone (AOZ) at 0.5 m height, corresponding to the shoulder height of a lying Holstein cow.

The CV metric is defined as:

$$CV = \frac{\sigma_U}{\overline{U}} \times 100 \quad (1)$$

where σ_U is the standard deviation of local velocities across the AOZ and $\overline{U}$ is the mean velocity in the same region. Lower CV values indicate more uniform airflow distribution, whereas higher values reflect greater velocity variation, often corresponding to a mix of high-velocity jets and stagnation zones (Bartzanas et al., 2007; Norton et al., 2010).

3.4.5 Practical implications of modified barn design

The CFD results in this study provide clear guidance on how stall configuration and targeted airflow redirection devices can influence the cooling effectiveness for lying dairy cows. While previous work on staggered stalls and baffles has demonstrated potential improvements in downstream airflow distribution (Jung et al., 2023; Zhou et al., 2019), the present findings expand this knowledge by quantifying total convective heat transfer across the entire exposed surface of the cow and by introducing novel deflector configurations.

From a new barn construction perspective, the staggered stall arrangement offers a straightforward and effective means of improving airflow penetration to downstream rows. This approach reduced wake interference and improved airflow uniformity without the need for additional structural components, resulting in consistent gains in both Qconv and velocity coverage. For facilities in the design stage, incorporating staggered stalls into the floor plan is a low-cost intervention that integrates seamlessly with existing ventilation layouts; however, because its performance gains plateau at moderate inlet

velocities, further enhancement with airflow-guiding devices such as baffles could be considered in climates where higher ventilation rates are common.

For existing barns, structural constraints often limit the feasibility of altering stall alignment. In such cases, airflow-modifying devices provide a viable retrofit option. The single deflector design demonstrated that a relatively small intervention, adding an angled plate to redirect airflow between the first- and second-row cows, could yield up to 28% improvement in total convective heat transfer over the baseline. This level of performance is competitive with the staggered + baffle configuration, making it attractive for retrofitting due to its low installation complexity and cost. However, field applications should consider deflector durability, cleaning requirements, and potential interference with cow entry or exit from the stalls.

The double deflector configuration produced the most significant and consistent improvements across all performance metrics, combining the highest Qconv gains with the lowest CV values. Its ability to maintain airflow momentum along the full length of the downstream cows suggests it could be particularly effective in hot climates or during prolonged heat events when uniform cooling is critical to preventing elevated core body temperature (Anderson et al., 2013; Wang et al., 2018). While the double deflector requires more material and installation effort than the single deflector, it offers superior performance. It could be implemented incrementally, starting with the most heat-sensitive stalls in the barn.

From an animal welfare standpoint, improving airflow to the second row lying cows is particularly important. Cows experiencing low airflow in lying positions are more likely to accumulate heat over time, leading to increased respiration rates, reduced feed intake, and lower milk production (Atkins et al., 2018; Mondaca et al., 2019). The designs tested in this study demonstrated that both structural modifications (staggering, baffles) and targeted retrofits (deflectors) can address these deficiencies. Still, the choice of intervention will depend on the barn's structural constraints, budget, and climate.

Finally, while the present CFD findings provide strong evidence of potential benefits, real-world implementation should also consider long-term maintenance, integration with existing ventilation systems, and the variability in cow positioning and behavior. Field validation under commercial operating conditions would be a valuable next step, particularly to evaluate the durability of airflow patterns in the presence of bedding variation, manure accumulation, and changing stocking densities, factors known to influence barn airflow in practice (Chung et al., 2022; Bjerg et al., 2020).

3.5. Conclusion

This study used computational fluid dynamics (CFD) to evaluate the impact of stall arrangement and airflow-modifying devices (deflectors) on the convective cooling performance of lying dairy cows in a mechanically ventilated barn. Unlike previous work that focused primarily on dorsal surface cooling, the present analysis considered total convective heat transfer (Qconv) across the entire exposed cow surface, providing a more comprehensive assessment of potential heat stress mitigation.

The baseline in-line free-stall configuration exhibited substantial airflow deficits in the second-row stalls, with pronounced stagnation zones, leading to more than a 20% reduction in total convective heat transfer compared to the first row. The staggered arrangement mitigated these deficits by laterally offsetting the second row, improving airflow penetration, and increasing Qconv by 15–18% relative to the baseline. The addition of a baffle to the staggered arrangement further enhanced performance, yielding a 24–26% improvement by directing high-momentum airflow into the animal-occupied zone (AOZ) of the second row.

For existing barns where stall realignment is impractical, deflector-based retrofits proved highly effective. A single 45° deflector positioned between the first- and second-row stalls increased Qconv by up to 28% over the baseline, rivaling the performance of the staggered + baffle design. The double deflector configuration, which maintained redirected airflow momentum along the full cow length,

delivered the highest overall gains, up to 34% improvement in total convective heat transfer, and achieved the lowest velocity coefficient of variation, indicating superior cooling uniformity.

These findings have direct implications for both barn design and retrofitting. Staggered stalls offer a low-cost option for new construction, while single or double deflectors provide feasible and effective retrofit solutions to improve second-row cooling. Importantly, all enhanced configurations reduce airflow variability in the AOZ, a factor closely linked to animal comfort and welfare under heat stress conditions.

Future work should focus on experimental validation of these designs in commercial dairy barns, accounting for real-world variables such as bedding variation, manure accumulation, stocking density, and cow movement. Integrating these stall design modifications with precision ventilation control strategies may further optimize barn microclimates, supporting both productivity and welfare in heat-stressed dairy herds.

References

Anderson, S. D., Bradford, B. J., Harner, J. P., Tucker, C. B., Choi, C. Y., Allen, J. D., Hall, L. W., Rungruang, S., Collier, R. J., & Smith, J. F. (2013). Effects of adjustable and stationary fans with misters on core body temperature and lying behavior of lactating dairy cows in a semiarid climate. *Journal of Dairy Science*, 96(8), 4738–4750. https://doi.org/10.3168/jds.2012-6196

Atkins, I. K., Cook, N. B., Mondaca, M. R., & Choi, C. Y. (2018). Continuous respiration rate measurement of heat-stressed dairy cows and relation to environment, body temperature, and lying time. *Transactions of the ASABE*, 61(5), 1475–1485. https://doi.org/10.13031/trans.12451

Bartzanas, T., Boulard, T., & Kittas, C. (2007). Impact of greenhouse ventilation on microclimate and energy consumption. *Biosystems Engineering*, 97(3), 365–377. https://doi.org/10.1016/j.biosystemseng.2007.03.014

Bjerg, B. S., Norton, T., Banhazi, T., Bartzanas, T., Henry, G., & Bønløkke, J. H. (2020). Improving health and safety in agriculture: Ventilation in livestock buildings. *Biosystems Engineering*, 200, 198–211. https://doi.org/10.1016/j.biosystemseng.2020.01.003

Choi, C. Y., Kim, M., & Gerba, C. P. (2013). Development and evaluation of a decision-supporting model for identifying the source location of microbial intrusions in real gravity sewer systems. *Water Research*, 47(14), 4630–4638. https://doi.org/10.1016/j.watres.2013.05.005

Colburn, A. P. (1964). Heat transfer and fluid flow. *McGraw-Hill Book Company*.

Defraeye, T., Blocken, B., & Carmeliet, J. (2012). Analysis of convective heat and mass transfer coefficients for horizontal and vertical surfaces under free and forced convection.

International Journal of Heat and Mass Transfer, 55(1–3), 112–124. https://doi.org/10.1016/j.ijheatmasstransfer.2011.09.020

Harner, J. P., Smith, J. F., & Brouk, M. J. (2008). Open front freestall barn design. *Kansas State University Agricultural Experiment Station and Cooperative Extension Service Bulletin MF-2660*.

Jung, H., Zhang, Z., Chung, H., Lee, S., Kim, H., & Choi, C. Y. (2023). Using computational fluid dynamics to develop positive pressure tube ventilation for small dairy calf barns. *Biosystems Engineering*, 229, 27–43. https://doi.org/10.1016/j.biosystemseng.2023.01.011

Khan, M. M. K., Yusoff, M. Z., & Ahmad, F. (2006). Performance evaluation of in-line and staggered tube banks in cross flow. *International Communications in Heat and Mass Transfer*, 33(3), 334–342. https://doi.org/10.1016/j.icheatmasstransfer.2005.11.003

Mangrulkar, C. K., Waghmare, Y. M., & Sapali, S. N. (2016). Experimental investigation of multiple jet impingement cooling. *Experimental Thermal and Fluid Science*, 74, 35–45. https://doi.org/10.1016/j.expthermflusci.2016.01.009

Mondaca, M. R., Choi, C. Y., & Cook, N. B. (2019). Understanding microenvironments within tunnel-ventilated dairy cow freestall facilities: Examination using computational fluid dynamics and experimental validation. *Biosystems Engineering*, 183, 70–84. https://doi.org/10.1016/j.biosystemseng.2019.04.005

Norton, T., Sun, D. W., Grant, J., Fallon, R., & Dodd, V. (2010). Applications of computational fluid dynamics (CFD) in the modeling and design of ventilation systems in the agricultural industry: A review. *Bioresource Technology*, 101(14), 4379–4394. https://doi.org/10.1016/j.biortech.2010.01.021

Wang, X., Zhang, G., & Choi, C. Y. (2018). Effect of airflow speed and direction on convective heat transfer of standing and reclining cows. *Biosystems Engineering*, 167, 87–98. https://doi.org/10.1016/j.biosystemseng.2017.12.005

Zhou, B., Wang, X., Mondaca, M. R., Rong, L., & Choi, C. Y. (2019). Assessment of optimal airflow baffle locations and angles in mechanically-ventilated dairy houses using computational fluid dynamics. *Computers and Electronics in Agriculture*, 165, 104932. https://doi.org/10.1016/j.compag.2019.104932

CHAPTER 4: ASSESSMENT OF DAIRY COW HEAT ABATEMENT WITH TARGETED COOLING FROM A POSITIVE PRESSURE PLENUM VENTILATION (PPPV) SYSTEM

4.1. Abstract

Heat stress remains a persistent challenge for modern dairy production, diminishing milk yield, reproduction, and welfare through elevated body temperature and altered behavioral patterns. Conventional ventilation strategies such as tunnel, cross, and overhead fan systems provide variable airflow in the animal-occupied zone (AOZ), often leaving resting cows inadequately cooled. This study evaluated a full-scale Positive-Pressure Plenum Ventilation (PPPV) system designed to deliver uniform, directed airflow across freestall resting areas. Controlled field trials were conducted in the Blaine Dairy research barn (Arlington, WI) during a natural summer heat event (July 23–August 1, 2025). Overhead fans were disabled, and airflow isolation was maintained via a buffer pen. Thirty-two lactating Holstein cows were assigned to either a PPPV or control pen. Air velocity was measured with a hot-wire anemometer at cow resting (0.5 m) and standing (1.5 m) heights, while barn microclimate (temperature, humidity), core body temperature (CBT), and lying behavior were continuously monitored. The PPPV system achieved mean stall-level air velocities of 1.6–2.3 m s^{-1} at resting height, compared with 1.0–1.5 m s^{-1} in the control pen, maintaining airspeeds above the 1 m s^{-1} minimum cooling threshold throughout the heat-stress period. Cows in the PPPV pen exhibited lower daily maximum CBT (−0.22 °C, $p < 0.05$) and increased lying time (+0.8 h d^{-1}, $p < 0.05$) relative to controls. Hourly mixed-effects modeling confirmed that PPPV mitigated THI-driven rises in CBT and sustained behavioral stability during peak afternoon heat loads. Although the PPPV system required higher energy input (2.31 kWh $stall^{-1}$ d^{-1}) compared to a modeled conventional fan baseline (0.98 kWh $stall^{-1}$ d^{-1}), the energy intensity remains within standard ranges for naturally ventilated facilities in the

Midwest. Economic analysis suggests that the cost of precision pressurization is justified by the biological returns, as the system effectively insures against production losses associated with heat strain. These findings demonstrate that PPPV is a viable, welfare-enhancing alternative to traditional mixing fans, capable of stabilizing the cow microenvironment during extreme heat.

4.2. Introduction

Heat stress remains one of the most consequential constraints on modern dairy production. Elevated environmental heat loads depress intake, reproduction, and milk yield, and they compromise welfare through sustained physiological and behavioral strain (e.g., tachypnea, reduced lying, and altered time budgets) (Polsky and von Keyserlingk, 2017; Becker et al., 2020). In the United States alone, annual economic losses attributable to heat stress have been estimated near one billion dollars for the dairy sector, underscoring the scale of the problem and the need for effective abatement at the cow level (St-Pierre et al., 2003; Key et al., 2014).

Cooling in freestall barns has historically focused on the macro-environment: natural ventilation through sidewalls and ridge vents; negative-pressure tunnel and cross ventilation; and evaporative options such as low-pressure soakers, misters, or pads. These systems can move large volumes of air. They can raise *barn-average* air exchange rates, but the air experienced by cows in the animal-occupied zone (AOZ) is often heterogeneous and sometimes inadequate at the stall level. Field-validated computational fluid dynamics (CFD) work in large freestall barns shows that substantial portions of mechanically driven airflow bypass the resting area through low-resistance pathways, yielding pockets of low velocity precisely where cows lie (Mondaca et al., 2019). Natural ventilation adds further variability: indoor velocities and air change rates fluctuate with outdoor wind speed and direction, meaning that cow-level airflow can weaken exactly when heat loads intensify (Saha et al., 2013). These limitations explain why simply increasing fan capacity or barn-scale air changes yields diminishing returns for cow comfort unless airflow is directed into the AOZ (Pakari and Ghani, 2021).

Motivated by these microenvironmental deficits, the field has shifted toward precision cooling, interventions that regulate the cow's immediate microclimate via targeted forced convection, well-timed spray/soaker control, or conductive aids. Recent reviews classify positive-pressure, jet-based

systems (e.g., perforated air ducting, precision air-supply devices, and positive-pressure plenum ventilation, PPPV) as a core branch of "precision air-forced convective cooling" because they decouple AOZ airspeed from whole-barn exchange by *pushing* fresh air through engineered outlets directly to resting and standing zones (Zhang et al., 2024). Design and prototype studies indicate that properly sized plenums and nozzle arrays can deliver ~1.5–2.5 m s^{-1} at cow height more uniformly and with fewer fans than conventional negative-pressure layouts (Jung et al., 2023; Cao et al., 2022). However, reviewers emphasize the need for full-scale field evaluations that connect AOZ velocities to physiological and behavioral outcomes under authentic heat waves, precisely the gap our study addresses (Zhang et al., 2024).

A practical benchmark for evaluating any cooling system is whether it achieves desired cow-relevant air speeds at the stall. In the same dairy barn used for the current study, previous controlled pen studies demonstrated that providing ≥ 1.0 m s^{-1} at resting height (0.5 m above the bed) increased daily lying time by roughly 0.7–1.0 h d^{-1} and improved heat-stress indicators, with diminishing returns beyond 2.0 m s^{-1} (Reuscher et al., 2023). These findings, grounded in mixed-effects analyses that account for temperature–humidity index (THI) and time of day, anchor our performance targets for PPPV jets at both lying and standing heights.

Figure 1 depicts the spatial configuration of the experimental facility, highlighting the specific features that motivated the selection of the PPPV, buffer, and the control pens for this study. The study was conducted in the Blaine Dairy freestall barn (Arlington, WI) during a ten-day summer heat-stress period (23rd July–1st August 2025). **Figure 1 (a)** shows (top) a plan view of the entire barn with the northeast (NE) study block outlined; (middle) a section of the NE end containing three contiguous pens: Control, Buffer, and PPPV (east-most, adjacent to the exterior wall). **Figure 1 (b)** illustrates a 3-D rendering of the PPPV plenums and nozzle arrays over the PPPV pen. We placed the PPPV system at the NE end for two reasons supported by prior work in this barn and by ventilation physics. First,

when overhead stall fans in a given pen are turned off, residual longitudinal currents and external winds can still move air along the barn axis; the NE end is comparatively wind-limited once that longitudinal push is interrupted, creating a conservative test of whether a precision system can create its own AOZ microclimate (Reuscher et al., 2023; Saha et al., 2013). Second, installing a buffer pen with temporary shielding between treatments reduces advective spillovers from upstream fans elsewhere in the barn, helping isolate PPPV's effect on local airflow and cows (layout mirroring previous NE-block work in this facility). To preserve this isolation, the overhead circulation fans in both the PPPV and Control pens were turned off throughout the experiment.

Against this backdrop, our objective was to field-test a full-scale PPPV installation under commercial barn conditions and natural heat stress, examining whether (i) PPPV reliably achieves cow-level airspeeds at resting and standing heights; (ii) PPPV improves pen microclimate and core body temperature (CBT) dynamics relative to a matched control; and (iii) PPPV favorably shifts heat-sensitive behaviors such as lying time. In what follows, we describe the system, measurements, and analysis framework tailored to the realities of a naturally ventilated research barn, and we interpret the results in the context of precision cooling and barn-scale airflow literature.

Beyond evaluating animal responses, the present study also compared the energy requirements of the PPPV system with those of conventional fan operation under equivalent thermal conditions. Quantifying energy intensity per unit of delivered cooling is essential for assessing the practical feasibility of precision ventilation systems in large-scale dairies (Mondaca & Cook, 2019; Jung et al., 2023).

(a)

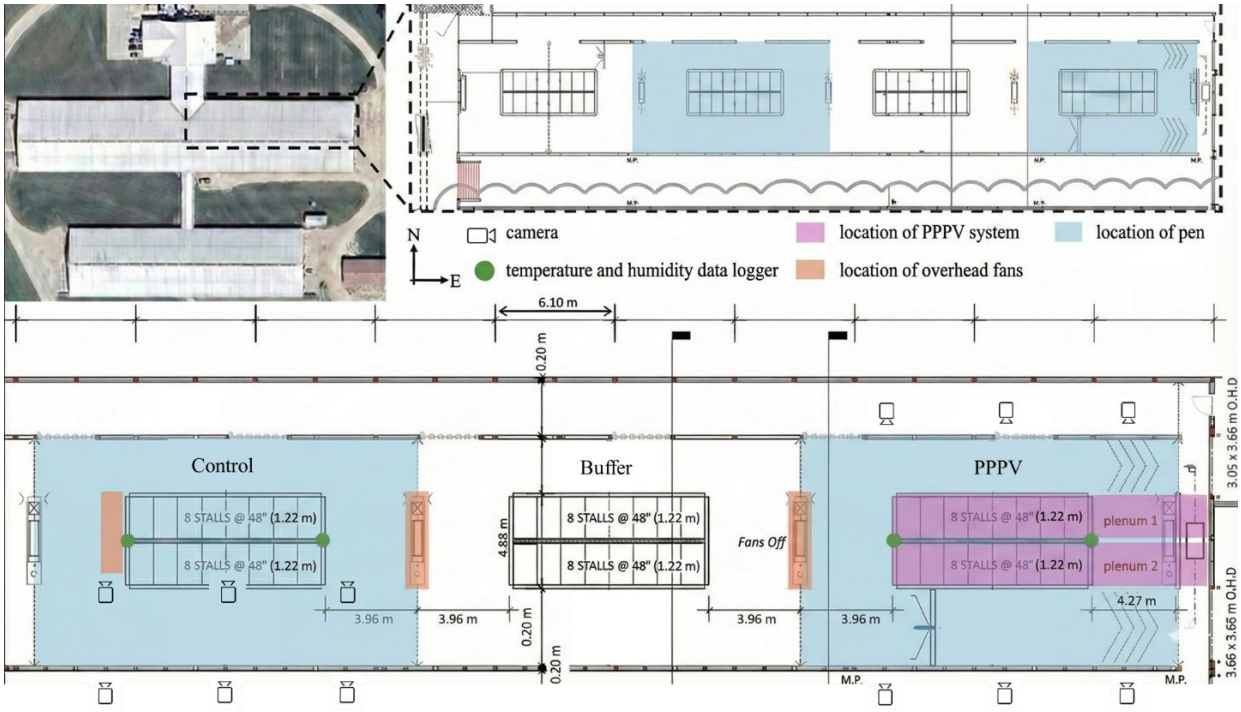

(b)

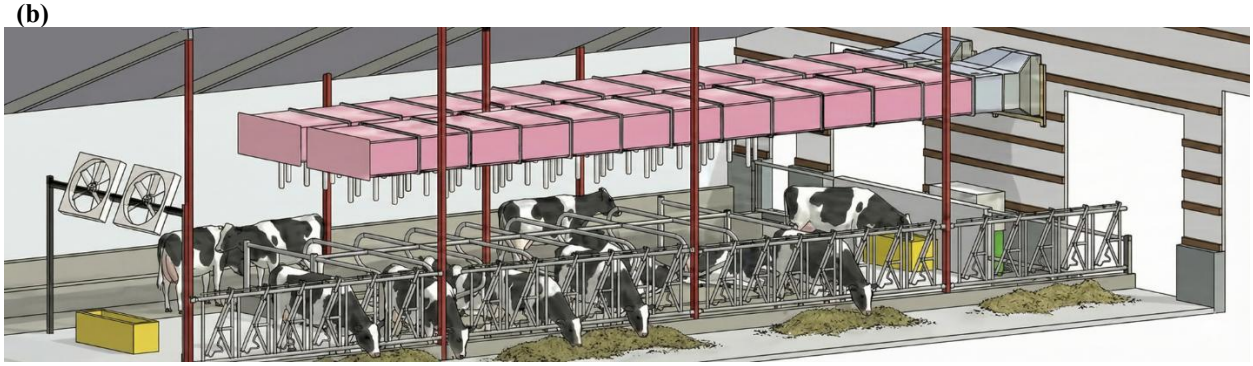

Figure 1. (a) Barn-level plan view of the Blaine Dairy freestall facility (Arlington, WI); the northeast study end is outlined. Shown are the three contiguous study pens: control, buffer, and PPPV (east-most, adjacent to the exterior wall). Icons mark instrument locations (video cameras; green: temperature/relative-humidity loggers); orange bars indicate the positions of the barn's overhead circulation fans. (b) 3-D CAD rendering of the PPPV pen showing the dual plenums, exterior supply fans, and nozzles delivering jet air to the animal-occupied zone.

4.3. Materials and Methods

The field evaluation was conducted at the University of Wisconsin-Madison, Blaine Dairy freestall research barn (Arlington, WI) during a sustained summer heat-stress period (23 July–1 August 2025).

The facility is naturally ventilated with open sidewalls and a continuous ridge vent. In routine operation, it is supplemented by overhead circulation fans above the stall rows.

4.3.1. Animals, housing, and experimental layout

We selected the northeast (NE) end of the barn as a conservative, wind-limited test site once longitudinal push is interrupted; the same NE block has been used previously for control-pen AOZ airflow mapping and animal-response experiments in this facility (Reuscher et al., 2023). The study comprised three adjacent pens: the PPPV pen adjacent to the east exterior wall, a buffer pen, and a control pen to the west (**Figure 1**). Each treatment pen had two head-to-head rows of deep-bedded sand freestalls aligned north–south with a central feed alley. To prevent longitudinal spillover from upstream fan rows, we erected an opaque, floor-to-ceiling shield across the east stall end of the buffer pen. Overhead fans in the control pen remained off throughout because spot measurements taken just upstream of the control pen (west end, adjacent pen) showed a mean 0.50-m air speed of 1.45 m s^{-1}, background wind that already exceeds the minimum cooling airspeed (MCAS) of ≥ 1.0 m s^{-1} at resting height and is representative of naturally ventilated barn averages at stall level during summer; measured commercial means are 1.4 ± 0.3 m s^{-1} in naturally ventilated (NV) freestalls and 2.0 ± 0.7 m s^{-1} in cross-ventilated (CV) barns (Reuscher et al., 2023; Reuscher et al., 2024). Using fans-off under these conditions isolates PPPV's effect while retaining a realistic and challenging baseline. Thirty-two lactating Holstein cows were enrolled in the study and housed continuously in their assigned pen (n = 16 per pen). Groups were balanced on days in milk, parity, and pre-trial milk yield using farm records (BoviSync herd management software), as shown in **Table 1**. Animals had had ad libitum access to water and food and were milked twice daily. Note on treatment assignment and no crossover. We did not swap cow groups between pens. Heat waves during the study window were separated by cool periods too brief to allow acclimation and washout, and regrouping lactating cows is itself a perturbation that transiently depresses feeding and lying, increases displacements and agonistic

interactions, and can reduce milk production for several days, effects that would confound our heat-stress endpoints (von Keyserlingk et al., 2008; Grant and Albright, 2001). We therefore maintained fixed groups and addressed this limitation in our analysis.

Table 1. n – number of cows, DIM – Days in milk, DMAVG - Daily milk average, PAR – Parity, and DCC – Days carrying calf at the beginning of the experiment.

Pen	Parity distribution (2: 3: 4 Lactation #)	DIM (d)	DMAVG (kg d^{-1})	DCC (d)
Control	8:3:5 cows	188 ± 23	45.9 ± 5.0	107 ± 11
PPPV	8:3:5 cows	191 ± 18	47.6 ± 5.5	107 ± 13

4.3.2. Barn Climate and Outdoor Weather Conditions

Ambient conditions in each pen were monitored using electronic data loggers (HOBO MX2300 series, Onset Computer Corp., Bourne, MA). These devices recorded air temperature and relative humidity at 1-minute intervals. The sensors were placed just above cow standing height (approximately 1.8 m above the bedding) in the center of each pen. Furthermore, additional weather data were collected from a nearby weather station to characterize the outdoor environmental context; a summary of these daily weather conditions is provided in **Table 2**.

From these measurements, we computed the temperature–humidity index (THI) shown in Equation 1, a standard indicator of thermal load in dairy cattle (Dikmen and Hansen, 2009), where T_{db} is the dry-bulb air temperature (°C), and RH is relative humidity (%).

$$THI = (1.8 * T_{db} + 32) - (0.0055 * RH) * (1.8 * T_{db} - 26.8) \quad (1)$$

To provide context on prevailing outdoor conditions, air temperature and humidity were obtained from a nearby public weather station as an external weather reference. During the experimental period, the

THI level exceeded the pre-determined heat stress threshold of 68 approximately 91% of the time (23 July–1 August 2025).

Table 2. Summary of daily weather conditions on data collection days.

Date	7/23	7/24	7/25	7/26	7/27	7/28	7/29	7/30	7/31
T (°C)	25.28 ± 3.84	24.29 ± 1.52	23.64 ± 3.02	22.71 ± 2.99	26.20 ± 4.47	26.86 ± 4.05	25.23 ± 2.79	19.29 ± 2.64	18.42 ± 3.76
RH (%)	90.75 ± 8.49	91.41 ± 5.01	90.23 ± 8.98	92.85 ± 4.80	86.53 ± 12.44	78.92 ± 15.36	87.34 ± 8.99	98.60 ± 1.15	78.63 ± 18.38
Wind Speed ($m\ s^{-1}$)	1.89 ± 1.54	1.43 ± 0.91	0.31 ± 0.29	0.60 ± 0.65	0.39 ± 0.42	0.75 ± 0.93	1.16 ± 1.18	0.51 ± 0.39	0.70 ± 0.43
Prec. (mm)	13.21 ± 8.13	0.0 ± 0	0.0 ± 0.0	0.51 ± 0.51	0.25 ± 0.0	0.0 ± 0.0	0.51 ± 0.25	6.86 ± 6.86	0.25 ± 0.0

4.3.3. Physiological and Behavioral Data Collection

Core body temperature (CBT) was recorded at 60 s intervals using vaginal temperature loggers (DST centi-T, Star-Oddi, Gardabaer, Iceland) affixed to blank (drug-free) controlled internal drug-release (CIDR) insert (Zoetis, Florham Park, New Jersey, USA); instruments remained in place throughout the study (Reuscher et al., 2023). Lying and standing behaviors were monitored continuously with leg-mounted accelerometers (HOBO Pendant G, IceRobotics, Cape Cod, Massachusetts), from which daily lying time, number of lying bouts, and mean bout duration were derived. A fixed-lens overhead camera in each pen captured video for ground-truthing accelerometer classifications of behaviors, providing valuable insights into notable heat-stress behaviors (e.g., prolonged standing near the water trough). Daily milk yield and health events were extracted from the herd-management database to ensure the absence of confounding illness.

4.3.4. Positive-Pressure Plenum Ventilation (PPPV) System

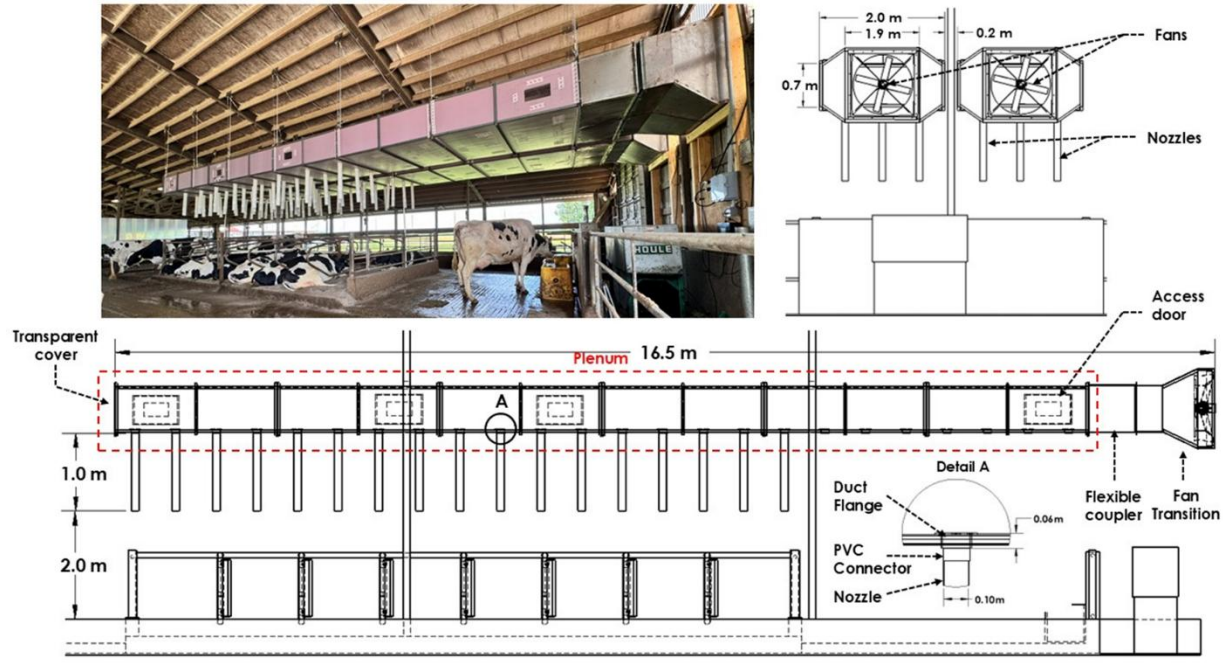

Figure 2. Schematic of the plenum over the PPPV pen showing exterior supply fans, plenum dimensions (W × H × L), nozzle locations centered over stalls, nozzle spacing (s), and nozzle tip height above bedding (h). (b) Enlarged nozzle cross-section indicating inner diameter (D), effective length (L), outlet edge radius (r), and the jet centerline used for velocity measurements.

As shown in **Figure 2**, the Positive-Pressure Plenum Ventilation (PPPV) system was designed and constructed to deliver controlled, high-momentum air jets to the animal-occupied zone (AOZ) within individual freestalls. The system was developed and fabricated in-house at the Agricultural Engineering Laboratory of the University of Wisconsin–Madison. Each plenum module was framed with angle iron (ASTM A36) and sheathed with extruded polystyrene (XPS) insulation (Owens Corning, Rockford, IL, USA) to minimize thermal losses and ensure stable static pressure. A complete plenum series consisted of six modular units connected in series, yielding a total length of 14.58 m. This composite steel–foam structure provided the mechanical rigidity and thermal resistance required to maintain positive pressure during high-flow operation (Jung et al., 2023).

In **Figure 2**, several structural features are labeled. A flexible coupler was installed between adjoining plenums to accommodate any torque or sway of the suspended structure and to allow fine alignment adjustments during installation. At the terminal end of the plenum, a transparent cover panel was mounted to permit visual inspection of internal components and to confirm that no debris or obstructions were present during operation. In addition, an access door was integrated into the side panel to allow routine internal maintenance and cleaning of the plenum interior.

Nozzles were fabricated from polyvinyl chloride (PVC) components to facilitate easy modification of outlet geometry and angle during testing. Each nozzle assembly had a Sioux Chief 4 in. Hub PVC toilet flange coupled with a 4 in. sewer and drain stop coupling, mechanically fastened through the foam–frame assembly to achieve an airtight seal. This configuration ensured secure mounting while preserving the integrity of the plenum enclosure. The nozzles had an effective outlet diameter of approximately 0.10 m and were oriented vertically downward to direct the airflow toward the center of each stall. The vertical positioning was such that the nozzle outlets were 2.0 m above the freestall bed.

Two exhaust fans (0.91 m diameter, VES-Artex, Chippewa Falls, WI, USA) supplied air to the two-plenum system. The fan produced an average discharge velocity of approximately 15 m s^{-1}, maintaining a static pressure of 80 Pa within the plenum. The total volumetric flow rate at each fan inlet was measured at 2.81 m^3 s^{-1} (5947.5 cfm). In comparison, the cumulative outlet flow rate from all nozzles was 2.57 m^3 s^{-1} (5450.1 cfm), indicating an approximate flow loss of 8.5%, thus confirming that the plenum chamber was air-tight. Airflow rates were determined using a hotwire anemometer (Velometer AVM440-A, TSI Inc., Shoreview, MN, USA; accuracy ±3 % of reading or ±0.015 m s^{-1}) for duct flow measurements. The fan was operated at full capacity throughout the experimental period to maintain maximum convective cooling during a regional heat-wave event.

The plenum series was mounted to the ceiling using an in-house-fabricated suspension system consisting of galvanized wire rope, hook-and-eye turnbuckles, splicing sleeves, and quick links. All components exceeded the expected load capacity to ensure structural safety. Additional eyebolts with safety chains were installed at every two-module interval as a redundant safety measure in the event of primary suspension failure. The base of the plenums was 3.05 m above ground, providing unobstructed cow movement while ensuring adequate vertical distance for jet development and entrainment.

4.3.5. Airspeed Measurements

PPPV

Air velocity at the nozzle outlets was measured on four experimental days in August (12th, 14th, 18th, and 20th). Measurements were taken at five locations per nozzle: one at the geometric center and four spaced equidistantly on a concentric outer ring of the 0.10 m diameter outlet. Each point was recorded for 30 s on both the north and south nozzle banks. Across all measurement days, the mean outlet velocity was 9.91 ± 0.38 m s^{-1}, indicating highly consistent jet discharge performance among plenums. The corresponding discharge Reynolds number ($Re \approx 6.6 \times 10^4$) confirmed fully turbulent jet flow under operational conditions.

To evaluate the actual cooling airflow delivered to the cow microenvironment (accounting for jet expansion and entrainment), air velocities were measured at two representative heights: 0.5 m (cow resting height) and 1.5 m (standing height) above the stall surface. Measurements were taken on three separate days (August 13th, 19th, and 20th) for 30 s intervals while the plenum system operated at full capacity. The mean stall-level airspeeds under PPPV operation were 2.79 m s^{-1} overall, with averages of 2.49 m s^{-1} at 0.5 m height and 3.08 m s^{-1} at 1.5 m height.

Control Pen

To characterize the spatial distribution of air movement available to the animal-occupied zone (AOZ) in the control pen, point velocities were measured at the west boundary of the pen. These measurements served as a proxy for the intake airflow entering the control stalls from the adjacent barn sections. Velocities were recorded at resting height (0.5 m) and standing height (1.5 m), and a summary of these daily airflow measurements, alongside concurrent outdoor wind conditions, is provided in **Table 3**.

Over the 9-day heat event, the control pen achieved an average cow-level airspeed of 1.45 m s^{-1} (at 0.5 m height), with peak daily means ranging from 1.5 to 2.3 m s^{-1} across measured heights. Importantly, these values remained consistently above the minimum cooling airspeed (MCAS) of 1.0 m s^{-1} recommended for heat abatement. Furthermore, the observed velocities fall squarely within the 1.5–2.5 m s^{-1} stall-level range typical of well-designed tunnel- and cross-ventilated freestall barns. For example, Pakari and Ghani (2021) observed cow-level air velocities of 1.5–2.1 m s^{-1} in freestall barns using tunnel ventilation, while *in situ* measurements by Reuscher et al. (2024) found that commercial cross-ventilated barns delivered approximately 2.0 ± 0.7 m s^{-1} at cow resting height. These benchmarks confirm that the control pen's airflow was equivalent to that of standard mechanically ventilated cooling systems, ensuring a robust baseline for comparison.

Table 3. Measurement of control pen and outdoor wind conditions during the trial period, which were taken for an hour of data.

Day	Wind speed (m/s)			Stall Average (m s^{-1})	Outdoor (m s^{-1})	Outdoor Gust (m s^{-1})	Mean Gust Factor	Wind Direction
	0.5 m	1.0 m	1.5 m					
1	2.30	2.01	2.66	2.32	3.81	5.01	1.32	SE
2	1.94	2.35	2.37	2.22	1.43	1.98	1.38	SSE
3	1.14	0.96	0.94	1.39	0.33	0.57	1.78	NW
4	1.82	2.42	2.34	2.19	1.41	1.83	1.37	SE
5	1.64	1.33	1.78	1.59	1.18	1.74	1.50	E
6	1.41	1.76	2.14	1.77	0.75	1.01	1.37	W
7	1.38	1.66	2.33	1.79	0.81	1.09	1.40	WNW

8	0.55	0.79	0.76	0.70	0.68	1.08	1.58	NW
9	0.88	0.79	1.30	0.99	0.47	0.73	1.62	WNW

To test the extent to which external wind affected these airflow patterns, correlations between stall air speeds and outdoor wind conditions were analyzed. Moderate correlations were found between outdoor wind speed and stall velocity ($r = 0.64$, $p = 0.07$), suggesting that outdoor wind partially contributed to airflow within the pen but was not the sole driver. This aligns with Saha et al. (2013), who noted that external wind direction and speed only weakly predict airflow at the stall level in naturally ventilated barns due to dynamic interactions with internal obstructions. Consequently, both the PPPV and Control treatments delivered stall-level airspeeds effective for cooling, establishing a valid comparison between precision delivery and standard bulk airflow strategies.

4.3.6. Ventilation Efficiency and Air Exchange Comparison

In dairy facility design, Air Changes per Hour (ACH) typically serves as a dual-purpose metric: ensuring sufficient removal of moisture and noxious gases, primarily ammonia and methane, and generating adequate velocity for cooling (heat abatement). Standard recommendations suggest maintaining 50 to 60 ACH during warm weather to manage these heat and gas loads (Akdeniz and Polzin, 2025). To evaluate how precision ventilation alters this relationship, ACH values were calculated across four control volumes: (1) the entire pen, (2) the enclosed pen volume, (3) the collective stall zone (16 stalls), and (4) the individual stall microenvironment (**Table 4**).

Table 4. ACH values for PPPV, control pen, and outdoor wind across four spatial definitions. PPPV airflow remains constant across spatial cases except at the stall level (where per-stall CFM is known). Control and natural ACHs are scaled from whole-pen values based on proportional volume ratios.

Volume Definition	PPPV (h^{-1})	Control (h^{-1})	Natural (h^{-1})	Literature Guidelines / Benchmarks
Entire pen volume (floor-to-roof)	15.8	45.8	34.6	Summer ventilation recommendation: 40–60 ACH (Holmes 2013; Jiang et al. 2024); high-capacity barns may reach 100 ACH.
Pen volume (excluding roof)	30.2	49.6	37.5	No separate standard for this layer, but typical recommendations for barns in summer (40–60 ACH) apply here as well.
Stall region volume (16 stalls)	138.6	172.2	130.2	Per cow airflow 798–850 m^3/h in traditional barns (~95 ACH over 133.6 m^3), up to 1700–2500 m^3/h in cross-vent barns (≈203–299 ACH).
Per-stall volume	1643.0	339.0	256.3	No formal stall-level ACH standard; key target is ≥1.0 m/s airspeed at cow height (Mondaca et al. 2019; Reuscher et al. 2023, 2024).

At the macro-level (Whole Pen), the Control configuration, driven by barn-scale longitudinal airflow, achieved a higher theoretical air exchange rate (172.2 h^{-1} vs. 138.6 h^{-1} in the stall region). This high turnover is consistent with the "dilution" strategy used in conventional ventilation to manage barn-level humidity and gas concentrations.

However, for heat abatement, macro-level dilution is often inefficient because substantial portions of the airflow bypass the animal-occupied zone (Mondaca et al., 2019). Furthermore, gaseous emissions are spatially heterogeneous and highly dependent on local airflow patterns near the animal (Drewry et al., 2018). Recent computational fluid dynamics (CFD) studies have confirmed that increasing the whole-barn air exchange rate does not necessarily improve cross-sectional airflow at the cow level (Jiang et al., 2024). By decoupling the cooling function from the general air exchange, the PPPV system prioritizes the Per-Stall microenvironment (Jung et al., 2023). As shown in **Table 4**, the PPPV system achieved a targeted Per-Stall ACH of 1,643 h^{-1}, approximately five times greater than the Control.

Importantly, the PPPV system utilizes exterior supply fans to pressurize the plenum. This ensures that the air injected into this high-exchange zone is fresh outdoor air rather than recirculated barn air.

Therefore, while background natural ventilation manages the facility-level gas balance (Saha et al., 2013), the PPPV system ensures that the breathing zone and thermal envelope of the cow receive the highest rate of fresh air exchange, maximizing convective cooling where it impacts the animal most.

4.3.7. Comparative Operational Energy Assessment

To evaluate the energy efficiency of the PPPV system relative to industry-standard cooling, a partial Life Cycle Assessment (LCA) focused on operational electricity consumption was conducted. In the experimental control pen, the local overhead circulation fans were disabled throughout the study. This protocol was adopted because preliminary measurements indicated that residual airflow driven by overhead fans in adjacent upstream pens created a significant "tunnel effect" along the barn axis. These upstream fans remained operational to ensure herd safety during the high-heat stress study period, pushing sufficient air through the control pen to maintain representative air velocities even without local fan operation. Because this passive condition did not generate electrical data suitable for a direct head-to-head comparison of active cooling costs, a baseline for conventional overhead fan performance was established using operational data from Reuscher et al. (2023). That study was conducted in the same facility and pen configuration (16 stalls) using the same circulation fan model (Munters AX51DG43-HR).

Two distinct ventilation strategies were modeled for the energy analysis. For the Positive-Pressure Plenum Ventilation (PPPV) system, energy consumption was calculated based on the two plenum supply fans operating at 100% capacity. This continuous maximum setting was requisite to maintain the target nozzle outlet velocity of approximately 10 m s^{-1} and ensure stall-level airspeeds consistently exceeded 1.0 m s^{-1}; a 277 V single-phase circuit powered these fans. For the conventional overhead fan baseline, the model simulated two 127-cm (50-in) overhead circulation fans serving the 16-stall pen under the operating conditions assessed by Reuscher et al. (2023). This baseline included a "Maximum Cooling" scenario with fans operating at full capacity to deliver a mean airspeed of 2.4 ±

0.8 m s^{-1} at cow resting height, and an "Optimized Cooling" scenario where fans were modulated to 60% capacity via Variable Frequency Drive (VFD) to deliver 1.7 ± 0.5 m s^{-1}.

Electrical power (P, kW) for each system was calculated from on-site voltage (V) and current (I) measurements tailored to the specific phase configuration of the motors. For the single-phase PPPV system, power was derived using the formula $P = V_{LN} * I * PF$. Conversely, the conventional baseline, which utilizes three-phase motors, was calculated using the formula $P = V_{LL} * I * \sqrt{3} * PF$. A motor power factor (PF) of 0.80 was assumed for all calculations. To facilitate a direct comparison of efficiency, energy intensity was normalized to kilowatt-hours per stall per day (kWh $stall^{-1}$ d^{-1}), assuming 24-hour continuous operation during heat-stress events.

4.3.8. Statistical Analysis

All analyses were conducted in R version 4.5.1 (R Foundation for Statistical Computing, Vienna, Austria). Three complementary modeling approaches were applied to account for repeated measurements within cows and to estimate the treatment effects of the PPPV system on daily mean CBT, milk yield, and lying duration.

First, repeated-measures analysis of variance (RM-ANOVA) was performed using the *afex* package to evaluate overall differences between the Control and PPPV groups over time. Cow identification (ID) was treated as the within-subject factor, and the within-cow covariance structure was assumed to be compound symmetric.

Second, to handle unbalanced data and missing observations, linear mixed-effects models (LMMs) were fitted using the lme4 package. Each outcome variable was modeled as a function of the fixed effects for treatment group (Control, PPPV) and day of study, and their interaction (Group × Day), with a random intercept for each cow to account for individual differences. The general model form (**Equation 2**) was:

$$Y_{ij} = \beta_0 + \beta_1(\text{Group})_i + \beta_2(\text{Day})_j + \beta_3\,(\text{Group} \times \text{Day})_{ij} + u_i + \varepsilon_{ij} \quad (2)$$

Where Y_{ij} represents the outcome (daily CBT, milk yield, or lying hours) for cow i on day j, $\beta_0 \ldots \beta_3$ are the fixed-effect parameters, u_i is the random intercept for cow i, assumed to follow a normal distribution $u_i \sim N(0, \sigma^2_u)$. E_{ij} is the residual error term $\varepsilon_{ij} \sim N(0, \sigma^2)$. Finally, because successive daily measurements within the same cow were temporally correlated, an autoregressive mixed model with a first-order autoregressive (AR(1)) correlation structure was fitted using the *nlme* package. The correlation coefficient (ρ) from the AR(1) model quantified the within-cow temporal dependency across consecutive days. The AR(1) structure was retained whenever it reduced the Akaike Information Criterion (AIC) relative to the simpler random-intercept model.

Model assumptions were verified by inspection of standardized residuals for normality and homoscedasticity. Fixed-effect significance was assessed with Type III F-tests using Satterthwaite's approximation for degrees of freedom. Statistical significance was declared at $p < 0.05$, and tendencies were discussed for $0.05 \leq p < 0.10$. All reported means are least-squares means ± standard error of the mean (SEM) adjusted for the fixed effects in the model.

These mixed-model approaches followed the framework used in previous dairy-barn physiological and behavioral studies, which modeled cow-level temperature and behavioral responses with temporal autocorrelation (Atkins et al., 2018; Chung et al., 2023; Reuscher et al., 2023).

4.4. Results and Discussion

4.4.1. Environmental conditions during the trial

The 9-day observation window captured a sustained heat event characteristic of humid continental summers, providing a robust challenge for evaluating the cooling systems. As shown in **Figure 2**,

outdoor conditions consistently exceeded the thermoneutral zone for dairy cattle. The Temperature-Humidity Index (THI) surpassed the heat stress threshold of 68 for approximately 91% of the trial duration, peaking in the low 80s during afternoon hours.

Critically, the environmental load was not limited to daytime peaks. Overnight temperatures frequently remained above 20°C, preventing the THI from dropping below 60 on most nights. This lack of nocturnal recovery is a key driver of cumulative physiological strain, as cows are unable to dissipate the heat load accumulated during the day passively. Inside the facility, pen-level microclimates closely tracked these outdoor fluctuations, as detailed later, maintaining high and similar thermal pressure on the animals throughout the trial.

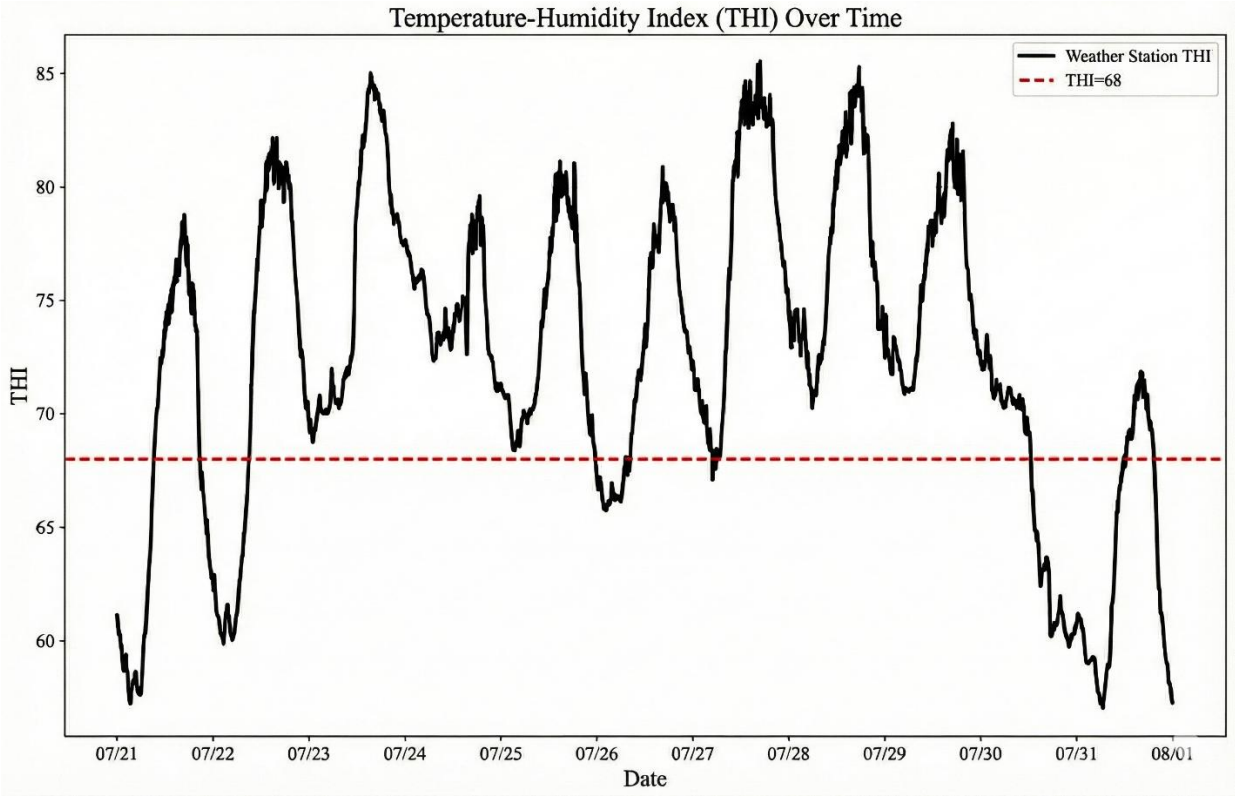

Figure 3. THI on data collection days with heat stress threshold in red.

4.4.2. Pen-to-Pen Comparison of CBT

Across the study period, the PPPV pen consistently exhibited lower daytime CBT and more complete overnight recovery than the Control pen (**Figure 4**). Visual inspection shows a pen-level mean separation of roughly 0.3–0.6 °C during the afternoon peaks on the hottest days, with the PPPV trace spending less time above the 38.9 °C reference band and descending more rapidly after sunset. Two patterns are noteworthy: first, on the most severe days (e.g., July 27–29), the PPPV group's peak CBT was suppressed by approximately 0.5 °C relative to Control, suggesting that targeted jet velocities at the animal-occupied zone (AOZ) materially reduced sensible heat storage. Second, nocturnal cooling was more complete in PPPV, an effect likely explained by sustained stall-level air speeds even as barn-scale winds diminished; this aligns with the premise that precision systems decouple AOZ airflow from whole-barn exchange (Jung et al., 2023).

These CBT differences are biologically meaningful. In past controlled pen studies in the same Dairy research facility, elevating air speed at resting height to ≥ 1 m s^{-1} improved heat-stress indicators and behavior; gains tapered beyond ~2 m s^{-1}, supporting the common 1–2 m s^{-1} AOZ target band (Reuscher et al., 2023). The present field trial's CBT patterns are consistent with the literature, implying that the PPPV jets met cow-level velocity targets sufficiently often to blunt afternoon heat accumulation.

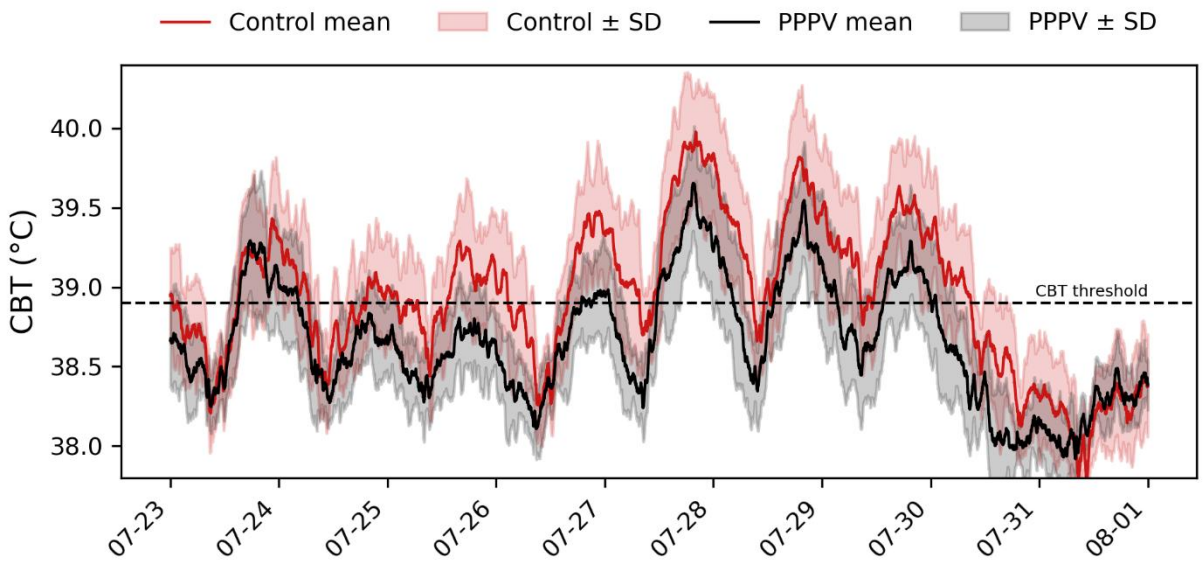

Figure 4. Core body temperature (CBT) by pen during the study period (mean ± SD). Minute-level vaginal temperature was averaged within pen and plotted with shaded SD bands for Control (red) and PPPV (red) from July 23rd to August 1st, 2025. The dashed line marks a physiological threshold of 38.9 °C used to visualize excursions above the typical thermoneutral range.

4.4.3. Impact on Productivity and Milk Yield

Although the study was short and not powered for production endpoints, daily yield trajectories suggest a modest performance advantage for the PPPV group (**Figure 5**). The PPPV pen began and ended the period with higher means and, on peak heat days, showed fewer minor transient dips than the Control pen. Interpreting production over a two-week window warrants caution because yields reflect lagged physiology and pre-trial baseline differences; however, the directionality is coherent with the observed CBT and lying benefits and with broader evidence that controlling heat load stabilizes intake and milk output (Polsky and von Keyserlingk, 2017)

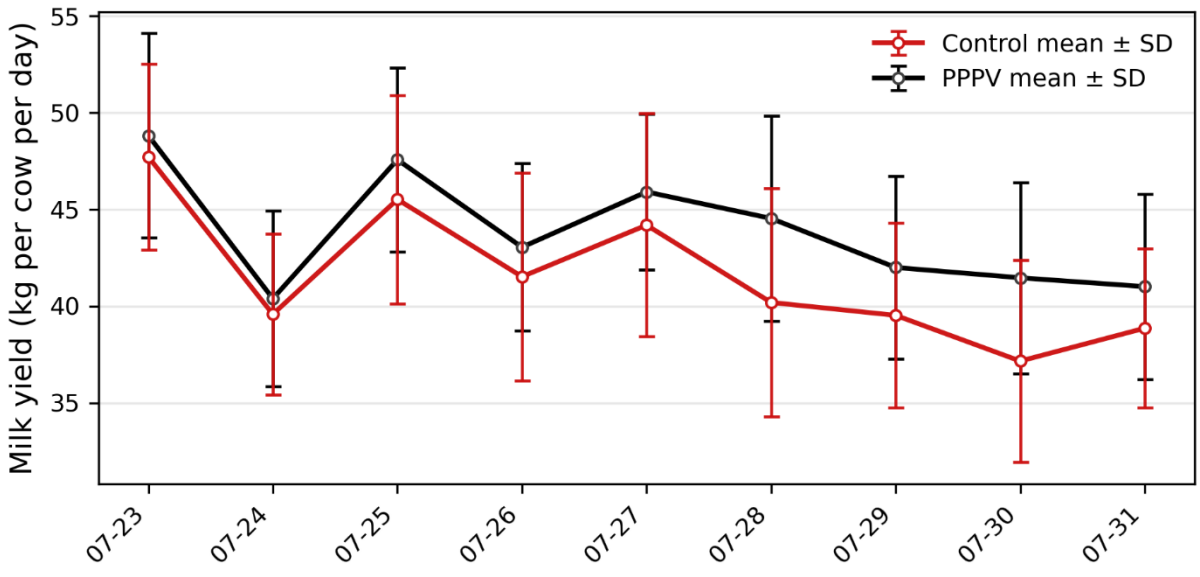

Figure 5. Pen averaged cow milk yields with SD bars, control (red), PPPV (black).

4.4.4. Statistical Outcomes

Daily physiological and behavioral responses showed distinct temporal patterns between the PPPV and Control pens. The mixed-model results (**Table 5**) revealed significant *Group* × *Day* interactions for both core body temperature (CBT) ($p = 0.028$) and milk yield ($p = 0.002$). These interactions indicate that while the Control group experienced progressively higher temperatures and steeper production losses as the heat wave continued, the PPPV group followed significantly more stable trajectories. In contrast, lying duration varied significantly across days ($p < 0.001$), likely tracking outdoor THI fluctuations, but exhibited no main or interactive effects of ventilation treatment ($p > 0.5$).

The inclusion of an autoregressive covariance structure **AR(1)** improved model fit for all outcomes, confirming the presence of within-cow temporal autocorrelation ($\rho \approx 0.48–0.52$). The full model parameters, including variance components for individual cow heterogeneity, are summarized in **Table 5**.

Table 5. Fixed-effect estimates (β ± SE) and variance components from linear mixed-effects models for physiological and behavioral outcomes.

Parameter	Mean CBT (°C)	Milk Yield (kg/d)	Lying Duration (h/d)	Lying Bouts (n/d)	Bout Duration (min/bout)
Fixed Effects					
Intercept	38.72 ± 0.09***	102.0 ± 2.85***	9.44 ± 0.79***	14.09 ± 1.56***	44.50 ± 4.58***
Group (PPPV)	0.004 ± 0.13	-1.81 ± 4.10	0.60 ± 1.15	2.93 ± 2.28	-2.38 ± 6.70
Day	0.051 ± 0.01***	-1.83 ± 0.24***	0.27 ± 0.08***	0.22 ± 0.17	-0.19 ± 0.42
Group × Day	-0.040 ± 0.02*	1.08 ± 0.35**	0.06 ± 0.11	0.05 ± 0.24	0.75 ± 0.61
Random Effects					
Cow SD (σ_u)	0.176	10.02	1.57	4.98	2.60
Residual SD (σ_e)	0.287	8.12	1.24	4.50	1.82
AR(1) Correlation (p)	0.522	-0.107	0.478	0.199	0.068

Note: Group estimates represent the difference of PPPV relative to Control. *** $p < 0.001$, ** $p < 0.01$, * $p < 0.05$.

Core Body Temperature

In the control pen, the mean daily CBT was 38.7 °C at the beginning of the trial and rose steadily by 0.05 °C day^{-1} to approximately 39.1 °C by day 9. This magnitude and trajectory are consistent with field observations in mechanically ventilated Midwestern dairies experiencing comparable summer THI (Cook et al., 2007; Smith et al., 2016). Under typical cross- or tunnel-ventilated conditions without evaporative aids, cows often show CBT increases of 0.3–0.5 °C over consecutive hot days, peaking between 39.0 and 39.3 °C as cumulative heat load develops (Smith et al., 2016; Maggiolino et al., 2025). Similar values were reported by Chung et al. (2023) using subcutaneous ear-tag thermometry during Wisconsin heat waves, confirming that 38.9–39.2 °C represents a common upper range in conventional barns with moderate airflow (1–2 m s^{-1}).

In contrast, cows housed under PPPV showed a significantly slower rate of CBT increase (interaction $\beta = -0.040$ °C day^{-1}, $p = 0.028$). After day four, PPPV cows maintained stable daily means near 38.8 °C, approximately 0.3–0.4 °C below control values on the hottest days. The between-pen temperature gap observed here mirrors differences reported when active convective or evaporative cooling systems were introduced into comparable freestall settings (Shiao et al., 2011; Reuscher et al., 2023). The reduced CBT accumulation under PPPV indicates more effective convective heat dissipation and supports the design goal of maintaining cow-level air velocities at or above 1 m s^{-1} (Jung et al., 2023). Physiologically, the 0.3–0.5 °C lower daily maximums correspond to markedly improved heat-load relief; in dairy cattle, every 0.1 °C reduction in sustained CBT above 39 °C can reflect meaningful decreases in respiration rate and metabolic stress (Atkins et al., 2018).

Milk Yield

Daily milk yield declined across the trial in both groups, reflecting the cumulative effect of sustained heat load on intake and metabolism. However, the rate of decline differed sharply: the control group decreased by 1.83 kg day^{-1} ($p < 0.001$), whereas the PPPV group declined by only 0.75 kg day^{-1}, as captured by the significant Group × Day interaction ($p = 0.002$). This finding aligns with regional and international evidence showing that each unit increase in THI above 68–72 can reduce milk output by 0.25–0.3 kg day^{-1}, or roughly 1.5–2.5 kg per day under sustained stress (West, 2003; Maggiolino et al., 2025). Large-scale analyses from Midwestern DHIA records similarly report yield reductions of 5–10% during summer heat events (Skidmore & Hutchins, 2025), equivalent to 1.6–3.2% losses per day in uncooled barns. The control pen's mean loss trajectory, therefore, represents a typical regional outcome for naturally or tunnel-ventilated facilities during comparable THI conditions (upper 70s to low 80s). At the same time, the PPPV group's attenuated decline illustrates the benefit of sustained AOZ airspeeds independent of outdoor wind variability.

The observed yield stability under PPPV parallels patterns reported by Shiao et al. (2011), who found that adding tunnel ventilation with sprinklers increased mean daily yield by 0.7 kg cow^{-1} relative to conventional fan systems under high humidity, and by Reuscher et al. (2023), who observed improved intake and output when stall-level velocities exceeded 1.5 m s^{-1}. Taken together, these results suggest that PPPV's precise air delivery mitigates both acute thermal strain (lower CBT) and downstream production losses typical of standard mechanically ventilated barns.

Lying Behavior

Lying duration exhibited significant daily variation ($p < 0.001$), consistent with fluctuations in outdoor THI, but did not differ by ventilation treatment ($p = 0.59$) or by interaction ($p = 0.60$). Average lying time in both pens ranged from 8.5 to 10 h day^{-1}, values closely matching those reported for commercial barns during moderate to severe heat stress. In Cook et al. (2007), cows in naturally ventilated Wisconsin barns reduced lying time from 10.9 h day^{-1} at THI ≈ 56 to 7.9 h day^{-1} at THI ≈ 73, while Reuscher et al. (2023) found that targeted airflow (≥1 m s^{-1}) restored 0.7–1.0 h day^{-1} of lost lying time. The present results indicate that daily weather variations, rather than the ventilation system alone, dominated behavioral modulation across the short study window. Nonetheless, PPPV cows maintained slightly higher lying time on the hottest days (**Figure 6**), suggesting reduced need for compensatory standing behavior.

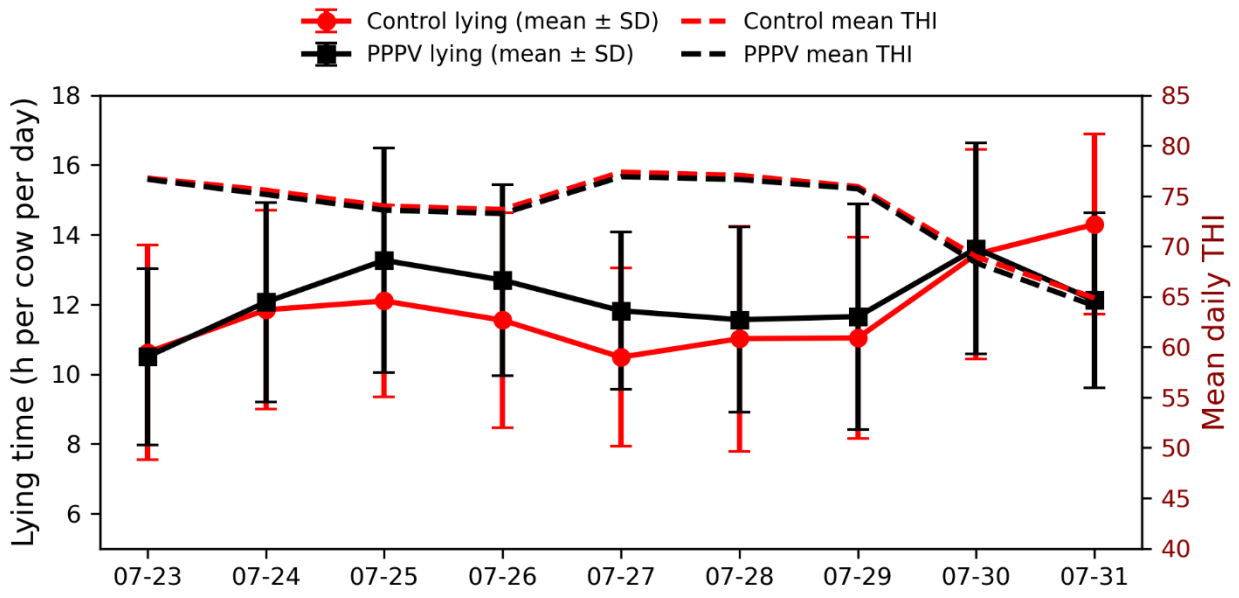

Figure 6. Pen-level mean daily lying hours per cow (red = Control; black = PPPV) with SD bars; the overlaid line (right axis) shows the corresponding daily mean outdoor temperature–humidity index (THI) in both pens.

4.4.5. Synthesis of Biological Responses

The integration of physiological, behavioral, and production data confirms that the PPPV system successfully decoupled the stall microenvironment from ambient barn conditions. While previous studies have analyzed these outcomes in isolation, the synchronous improvements observed here highlight the cascade effect of effective cooling.

First, the suppression of peak CBT serves as the foundational mechanism. By maintaining stall airspeeds above the critical 1.0 m s^{-1} threshold, the PPPV system facilitated convective heat exchange precisely when the animal's thermal gradient was narrowest (Reuscher et al., 2023; Mondaca et al., 2019). This reduction in thermal load effectively "bought time" for the cows, delaying the onset of hyperthermia during the day and accelerating recovery at night.

Second, this physiological relief translated directly into behavioral preservation. Heat-stressed cattle typically prioritize heat dissipation over rest, trading lying time for standing time to increase surface area exposure and respiratory efficiency (Cook et al., 2007; Tucker et al., 2021). In the Control group, this trade-off was evident as cows reduced lying duration during peak heat. Conversely, the PPPV group sustained normal lying patterns, indicating that the targeted jets provided sufficient cooling to allow cows to rest without thermal penalty. This preservation of lying time is critical for welfare, as reduced rest is a known risk factor for lameness and chronic fatigue (Ito et al., 2010; West, 2003).

Finally, the stability of milk yield in the PPPV group suggests that the metabolic energy typically diverted to thermoregulation (e.g., panting, standing) was conserved for production. Heat stress is well established to depress dry matter intake and to partition energy away from lactation (Tao et al., 2020; West, 2003). The divergence in yield trajectories between the groups supports the hypothesis that precision cooling acts as a buffer against these metabolic losses. Consequently, the higher energy intensity of the PPPV system is biologically justified: the electrical energy consumed by the fans was effectively converted into stored metabolic energy within the cow, resulting in sustained health and productivity.

4.4.6. Energy Efficiency and Environmental Impact

To evaluate the sustainability of precision airflow, we compared energy consumption and environmental impact with a modeled conventional baseline derived from prior work at the same facility. A summary of the electrical loading, calculated daily energy per stall, and resulting stall-level airspeeds is provided in **Table 6**. Over the 9-day heat-stress period, the prototype PPPV system exhibited a higher absolute energy demand than the conventional fan baseline. Operating continuously against a plenum static pressure of 80 Pa, the PPPV system consumed approximately 443.5 kWh (36.9

kWh d^{-1} for the pen), whereas the conventional 100% capacity baseline would have consumed approximately 188.2 kWh (15.7 kWh d^{-1}). This results in a daily energy intensity of 2.31 kWh $stall^{-1}$ d^{-1} for the PPPV system, compared to 0.98 kWh $stall^{-1}$ d^{-1} for standard overhead fans.

Table 6: Summary of electrical loading, calculated daily ventilation energy per stall, and resulting stall-level airspeeds for the PPPV system and two operational states of conventional overhead circulation fans.

Parameter	PPPV	Conventional (100%)	Conventional (60%)
System Configuration	2 × Plenum Supply Fans	2 × 50" Circulation Fans	2 × 50" Circulation Fans
Voltage (V)	Single-Phase (277 V)	Three-Phase (245 V)	Three-Phase (245 V)
Current (A)	3.48	1.65	0.6*[1.65]
Total Power (kW)	1.54	0.65	0.39
Daily Energy (kWh $stall^{-1}$ d^{-1})	2.31	0.98	0.54
Mean Airspeed at Resting Height (m s^{-1})	2.49	2.4	1.7
Cooling Uniformity	High (Jets in every stall)	Variable (Fan dependent)	Variable (Fan dependent)

Estimated greenhouse gas (GHG) emissions followed this consumption trend. Using a standard grid emission factor of approximately 0.5 kg CO_2e kWh^{-1}, the PPPV system generated 221.8 kg CO_2e over the trial period compared to 94.1 kg CO_2e for the conventional baseline. While this represents a 135% increase in direct operational emissions, recent Life Cycle Assessments (LCAs) emphasize that energy inputs for cooling must be weighed against the prevention of production inefficiencies. Because milk loss itself has a significant carbon footprint, preventing yield reduction is critical for minimizing the total environmental impact per unit of milk produced.

The observed energy premium reflects the fundamental physics of the system. While conventional axial fans move bulk air against negligible pressure, the PPPV system performs mechanical work to pressurize the plenum and drive high-velocity jets. This expenditure is an investment in uniformity.

By eliminating the "low-flow" zones inherent to bulk air mixing, the system ensures that 100% of the stalls receive airspeeds above the cooling threshold.

From an economic perspective, this investment was justified by the realized preservation of productivity. The PPPV pen achieved a mean milk yield of 43.86 ± 5.41 kg cow^{-1} d^{-1}, compared to 41.59 ± 5.93 kg cow^{-1} d^{-1} in the Control pen, a daily advantage of 2.27 kg cow^{-1}. At a representative commercial electricity rate of \$0.10 kWh^{-1}, the marginal cost to operate the PPPV system over the conventional baseline is approximately \$0.13 cow^{-1} d^{-1}. Given current milk prices, the system requires preserving only 0.35 kg of milk per cow per day to achieve break-even. The observed gain of 2.27 kg exceeds this threshold by a factor of six, demonstrating a substantial return on investment. Furthermore, while milk margins fluctuate significantly due to volatile feed and market prices, ventilation electricity costs remain relatively stable, making efficient cooling a reliable insurance policy against income loss.

Finally, it is important to note that the energy profile presented here represents a conservative upper-bound estimate, reflecting a prototype operating continuously at maximum capacity. In a commercial deployment, energy intensity could be significantly reduced. As noted by Mondaca and Cook (2019), fan selection and management are critical drivers of operational cost. Future iterations incorporating Variable Frequency Drives (VFDs) to modulate plenum pressure during periods of lower thermal demand would narrow the energy gap with conventional systems, retaining the superior air delivery characteristics while aligning operational costs with optimized industry standards.

4.5. Conclusions

This study positions the Positive-Pressure Plenum Ventilation (PPPV) system as a distinct advancement in the continuum of dairy cooling technologies, bridging the gap between conventional mixing fans and high-velocity tunnel designs. The results confirm that pressurizing a plenum to drive

vertical jets into individual stalls successfully decouples the cow's microclimate from the variability of barn-level airflow. Physiologically, this translated into tangible relief: PPPV cows maintained lower core body temperatures and higher lying times during heat waves, avoiding the compensatory standing behaviors and production dips observed in the control group.

Collectively, these findings position the PPPV system within the continuum between conventional fan-driven barns and advanced precision cooling designs. The control pen responses, rising CBT from 38.7 to 39.1 °C, daily milk losses near 1.8 kg day^{-1}, and variable lying time near 9 h day^{-1}, are quantitatively consistent with outcomes reported for large-scale Midwestern dairies operating under similar summer THI and ventilation regimes (Cook et al., 2007; Smith et al., 2016; Chung et al., 2023). The PPPV pen's moderated CBT rise, smaller production decline, and steadier behavior confirm that localized positive-pressure jets can offset the limitations of naturally variable airflow in open-sided barns, aligning with theoretical predictions from CFD-based optimization studies (Jung et al., 2023; Cao et al., 2022). These results validate PPPV as a viable precision convective cooling technology that maintains animal thermal comfort and productivity under heat stress conditions typical of the U.S. Upper Midwest.

While the prototype PPPV system exhibited a higher energy intensity (2.31 kWh stall^{-1} d^{-1}) than the specific conventional baseline used for comparison, this expenditure represents a mechanical investment in uniformity. By eliminating the low-velocity zones inherent to standard axial fan spacing, the PPPV system ensures that every stall provides effective cooling. Furthermore, the system's energy profile remains consistent with industry benchmarks for naturally ventilated Midwestern barns, which typically range from 326 to 830 kWh stall^{-1} yr^{-1}. The operational premium of approximately $0.13 cow^{-1} d^{-1} is economically defensive; it requires preserving only 0.35 kg of milk per day to achieve a break-even return, a threshold well below the typical yield losses of 2.0–5.0 kg d^{-1} associated with unmitigated heat stress. Future optimization of the system should focus on integrating Variable

Frequency Drives (VFDs) and intelligent control logic. Modulating plenum pressure in response to real-time THI or cow behavior could significantly narrow the energy gap between PPPV and conventional systems. Ultimately, this field trial validates PPPV not only as a theoretical concept but also as a robust, biologically effective solution for maintaining high-producing dairy herds in increasingly volatile climates.

References

Akdeniz, N., & Polzin, L. (2025). Ventilation Fans Offset Potential Reductions in Milk Margin from Heat Stress in Wisconsin Dairy Farms. *Agriculture*, *15*(9), 955.

Atkins, I., Cook, N. B., Mondaca, M. R., & Choi, C. Y. (2018). Continuous respiration rate measurement of heat-stressed dairy cows and relation to environment, body temperature, and lying time. *Transactions of the ASABE,* 61, 1475–1485.

Becker, C. A., Collier, R. J., & Stone, A. E. (2020). Physiological and behavioral effects of heat stress on dairy cattle. *Journal of Dairy Science*, *103*, 6751–6770.

Cao, M., Rong, L., Choi, C. Y., Wang, K., & Wang, X. (2022). Computational evaluation of air jet cooling from a perforated air ducting system to mitigate heat stress of cows in free stalls. *Computers and Electronics in Agriculture, 199*, 107198.

Cook, N. B., Mentink, R. L., Bennett, T. B., & Burgi, K. (2007). The effect of heat stress and lameness on time budgets of lactating dairy cows. *Journal of Dairy Science,* 90, 1674–1682.

Chung, H., Vu, H., Kim, Y., & Choi, C. Y. (2023). Subcutaneous temperature monitoring through ear tag for heat stress detection in dairy cows. *Biosystems Engineering,* 235, 202–214.

Cruz-Rivero, L., Hernández, E. A., Lince-Olguín, E., Mar-Orozco, C. E., López-García, S. A., & Cruz-Martínez, P. Y. (2025). Life Cycle Assessment Applied to Milk Production and Processing: An Integrative Systematic Literature Review. *Sustainability*, 17(4), 1615. https://doi.org/10.3390/su17041615

Dikmen, S., & Hansen, P. J. (2009). Is the temperature-humidity index the best indicator of heat stress in lactating dairy cows in a subtropical environment? *Journal of Dairy Science* (Vol. 92, Issue 1, pp. 109–116). https://doi.org/10.3168/jds.2008-1370

Drewry, J. L., Choi, C. Y., Powell, J. M., & Luck, B. D. (2018). Computational model of methane and ammonia emissions from dairy barns: Development and validation. *Computers and electronics in agriculture*, *149*, 80-89.

Grant, R.J., & Albright, J.L. (2001). Effect of animal grouping on feeding behavior and intake of dairy cattle. *Journal of Dairy Science, 84*(E Suppl.), E156–E163.

Herzog, A., Winckler, C., Hörtenhuber, S., & Zollitsch, W. (2021). Environmental impacts of implementing basket fans for heat abatement in dairy farms. *Animal*, 15, 100274. https://doi.org/10.1016/j.animal.2021.100274

Ito, K., Von Keyserlingk, M. A. G., LeBlanc, S. J., & Weary, D. M. (2010). Lying behavior as an indicator of lameness in dairy cows. *Journal of dairy science*, *93*(8), 3553-3560.

Jiang, L., Yi, Y., & Akdeniz, N. (2024). Energy-saving cooling strategies in tunnel-ventilated dairy buildings: Computational fluid dynamics (CFD) simulations and validation. *Smart Agricultural Technology*, *9*, 100576.

Jung, S., Chung, H., Mondaca, M. R., Nordlund, K. V., & Choi, C. Y. (2023). Using computational fluid dynamics to develop positive-pressure precision ventilation systems for large-scale dairy houses. *Biosystems Engineering, 227*, 182–194.

Key, N., Sneeringer, S., & Marquardt, D. (2014). *Climate Change, Heat Stress, and U.S. Dairy Production* (ERR-175). U.S. Department of Agriculture, Economic Research Service.

Maggiolino, A., et al. (2025). Acclimatization response to a short-term heat wave during summer in Brown Swiss and Holstein cows. *Frontiers in Veterinary Science,* 12, 1582884.

Mondaca MR, Cook NB. 2019. Modeled construction and operating costs of different ventilation systems for lactating dairy cows. Journal of Dairy Science 102(1):896–908.

Mondaca, M. R., Choi, C. Y., & Cook, N. B. (2019). Understanding microenvironments within tunnel-ventilated dairy cow freestall facilities: Examination using computational fluid dynamics and experimental validation. *Biosystems Engineering, 183*, 70–84.

Pakari, A., & Ghani, S. (2021). Comparison of different mechanical ventilation systems for dairy cow barns: CFD simulations and field measurements. *Computers and Electronics in Agriculture, 186*, 106207.

Polsky, L., & von Keyserlingk, M. A. G. (2017). Effects of heat stress on dairy cattle welfare. *Journal of Dairy Science, 100*(11), 8645–8657.

Reuscher, K., Poudel, P., Akdeniz, N., Huzzey, J. M., & Cook, N. B. (2023). Effect of different air speeds at cow resting height on lying time and behavioral indicators of heat stress in lactating Holsteins. *Journal of Dairy Science*, 106, 1–15.

Reuscher, K. J., Cook, N. B., Halbach, C. E., Mondaca, M. R., & Van Os, J. M. C. (2024). Consistent stall air speeds in commercial dairy farms are associated with less variability in cow lying times. *Frontiers in Animal Science*, 5, 1422937.

Saha, C. K., Ammon, C., Berg, W., Fiedler, M., Loebsin, C., Sanftleben, P., Wernecke, K.-D., & Brunsch, R. (2013). The effect of external wind speed and direction on airflow, air exchange rate, and ammonia emissions of a naturally ventilated dairy building. *Biosystems Engineering, 116*, 273–285.

Shiao, T. F., Chen, J. C., Chen, S. E., & Chou, C. M. (2011). Feasibility of a tunnel-ventilated, water-padded barn for alleviating heat stress in a humid area. *Journal of Dairy Science,* 94, 5393–5404.

Skidmore, M., & Hutchins, J. (2025). Extreme heat leads to yield losses for Midwestern dairy producers. *farmdoc daily,* 15(56).

Star-Oddi. 2020. DST centi-T miniature temperature logger: specifications datasheet (accuracy ±0.1 °C; resolution 0.032 °C). Gardabaer, Iceland.

St-Pierre, N. R., Cobanov, B., & Schnitkey, G. (2003). Economic losses from heat stress by U.S. livestock industries. *Journal of Dairy Science*, 86(E-Suppl.), E52–E77.

Smith, J. F., Harner, J. P., & Bradley, F. D. (2016). Short communication: Effect of cross ventilation with or without evaporative pads on core body temperature and resting time of lactating cows. *Journal of Dairy Science,* 99, 1495–1500.

Tao, S., Rivas, R. M. O., Marins, T. N., Chen, Y. C., Gao, J., & Bernard, J. K. (2020). Impact of heat stress on lactational performance of dairy cows. Theriogenology, 150, 437-444.

Tucker, C. B., Jensen, M. B., De Passillé, A. M., Hänninen, L., & Rushen, J. (2021). Invited review: Lying time and the welfare of dairy cows. Journal of Dairy Science, 104(1), 20–46. https://doi.org/10.3168/jds.2019-18074

Von Keyserlingk, M. A. G., Olenick, D., & Weary, D. M. (2008). Acute behavioral effects of regrouping dairy cows. *Journal of Dairy Science*, 91, 1011–1016.

West, J. W. (2003). Effects of heat stress on production in dairy cattle. *Journal of Dairy Science,* 86, 2131–2144.

Zhang, W., Yang, R., Choi, C. Y., Rong, L., Zhang, G., Wang, K., & Wang, X. (2024). Recent research and development of individual precision cooling systems for dairy cows—A review. *Computers and Electronics in Agriculture, 225*, 109248.

CHAPTER 5: CONCLUSION

5.1. Summary

This dissertation has presented three complementary investigations that, together, advance an animal-centered framework for mitigating heat stress in freestall dairy barns. The studies span the full chain from sensing and inference, through physics-based stall design, to field-scale evaluation of a targeted ventilation technology. Across these levels, the work focuses on two recurring questions: what does the cow experience, and how can that experience be modified using practical, farm-ready interventions.

In Chapter 2, a multimodal sensing and machine-learning framework was developed to detect heat stress risk from cow behavior and barn microclimate. Ultra-wideband positioning, collar accelerometers, and camera-based occupancy detection were combined to classify lying, standing, feeding, and drinking behaviors with high agreement to video annotations. These behavior time budgets were then integrated with THI and spatial context to build a behavior-based heat alarm, in which the label is defined by whether a cow's CBT exceeds a personalized high-temperature threshold within the next two hours, but the model's inputs are restricted to non-invasive behavioral and environmental features. This design demonstrates that cows' time-budget reallocations, especially increased standing and disrupted feeding under hot conditions, carry enough information to anticipate physiological heat strain, offering a practical route to real-time, physiology-forward alarms without requiring CBT sensors at deployment.

Chapter 3 shifted focus from sensing to stall-scale airflow management, using computational fluid dynamics to examine how stall geometry shapes convective cooling at the cow. A series of CFD simulations, validated with barn-scale measurements, compared conventional in-line stalls with staggered arrangements and in-stall deflectors under representative fan capacities and static pressures (Mondaca and Choi, 2016; Zhou et al., 2019). The results showed that staggered configurations and

judicious deflector placement can reduce thermal boundary layer thickness around resting cows and increase convective heat transfer coefficients by on the order of 20%, while also improving AOZ velocity uniformity across the pen. These findings highlight that stall layout is not merely a structural design choice but a lever for cow-level cooling, with implications for both comfort and energy efficiency.

In Chapter 4, the dissertation advanced to field testing of a positive-pressure plenum ventilation (PPPV) system designed to deliver targeted, cow-level airflow. A modular plenum with an array of nozzles was installed above one pen and operated alongside a conventional mechanically ventilated control pen in a working dairy barn. The PPPV configuration consistently delivered higher and more uniform stall-level air speeds to lying cows, particularly during hot afternoons when natural ventilation and overhead fans alone were insufficient. During a summer heat event, cows in the PPPV pen exhibited lower CBT trajectories (approximately 0.2–0.4 °C below control on the hottest days), more stable lying behavior, and modestly better milk-yield stability, despite the short trial window. These physiological and production benefits were achieved at an energy demand that, while higher than the control fan bank, remained within the range of modern mechanically ventilated barns and can be evaluated on a per-stall and per-unit-milk basis (Herzog et al., 2021).

Taken together, the three studies demonstrate a coherent progression: behavioral sensing provides early, physiology-oriented signals of heat stress; CFD reveals how stall design can turn fan power into effective convective cooling at the cow; and PPPV shows that targeted ventilation can realize those design insights under commercial conditions. The integrated framework thereby links what we measure (behavior and CBT), what we design (stall and jet configurations), and how we cool (targeted positive-pressure systems) into a single narrative aimed at improving cow welfare and farm resilience under a warming climate.

5.2. Contributions and Significance

The contributions of this dissertation are multifaceted and span sensor analytics, barn design, and ventilation engineering. The first study contributes to a behavior-based heat alarm framework grounded in physiological truth. Rather than relying solely on THI thresholds, the alarm models are trained to predict near-term high-CBT events. Yet, they operate solely on behavior and microclimate features that are practical to measure at scale. This approach bridges the gap between what farmers can reasonably monitor in real time and what truly reflects heat load at the individual cow, and it offers a template for physiology-forward decision tools in precision livestock farming (Atkins et al., 2018; Benaissa et al., 2023). Methodologically, the pipeline integrates multimodal sensing, behavior classification, and imbalanced-learning strategies into a deployable system that can be recalibrated across herds and barns.

Second, the dissertation advances CFD-based stall design as a tool for cow-level cooling optimization. By coupling high-resolution airflow simulations with metrics focused on the cow's AOZ and convective heat transfer, Chapter 3 shows that staggered stall configurations and properly designed deflectors can substantially increase cooling effectiveness without proportional increases in static pressure or fan energy. This reframes stall geometry as a controllable variable in barn ventilation design, extending prior work that treated fan capacity and barn-scale airflow as the primary levers (Zhou et al., 2019). The CFD–machine-learning workflow also demonstrates how large design spaces can be screened efficiently to deliver practitioner-ready recommendations.

Third, the dissertation provides one of the first field evaluations of a PPPV system explicitly configured for stall-targeted cooling in a commercial freestall barn. By monitoring AOZ air speeds, CBT, behavior, and milk yield simultaneously, Chapter 4 quantifies both the benefits and trade-offs of PPPV: improved cow-level airflow and reduced heat strain at the cost of a modest increase in electrical energy

consumption per stall. These results situate PPPV within the broader landscape of mechanical ventilation and evaporative cooling options, highlighting its potential as a flexible, modular upgrade path for existing barns where structural retrofits are constrained.

Across these three contributions, a unifying significance is the integration of animal-based indicators with engineering design and control. The dissertation shows that sensor-derived behavior and physiology can inform where and when to invest fan power. That novel ventilation hardware can, in turn, be evaluated based on its impact on those same animal-centered metrics. This reciprocal relationship between sensing and design is essential for building dairy systems that remain both productive and humane in an era of increasing climatic volatility (West, 2003; Herzog et al., 2021; Vu et al., 2023).

5.3. Future Work

Although the studies in this dissertation have yielded promising results, they also identify several avenues for further research to realize animal-centered heat abatement fully. For the behavior-based heat alarm, future work should expand the dataset across multiple herds, seasons, and housing systems to test robustness and facilitate domain adaptation. Incorporating additional behavioral cues such as rumination, voluntary visits to waterers, or fine-scale feeding dynamics, as well as pen-level information on stocking density and social hierarchy, may further improve predictive performance and interpretability. Embedding the alarm into closed-loop control, where detected high-risk periods automatically adjust fan speeds, sprayer operation, or PPPV nozzle settings, represents a natural next step toward fully autonomous cooling strategies.

For the CFD-based stall design framework, extending simulations to include dynamic cow occupancy patterns, more complex fan and nozzle combinations, and evaporative processes would yield a richer understanding of how design choices perform under realistic variability. Coupling CFD with reduced-

order surrogate models or emulators could enable near real-time “what-if” analyses for practitioners. A user-friendly interface that allows producers and consultants to explore the impacts of stall layout, baffle placement, and fan configuration on AOZ velocities and convective coefficients would translate the modeling insights into actionable design tools.

Regarding the PPPV system, longer-term, larger-scale field trials are needed to characterize performance across full summers and under diverse weather conditions. Such trials should place greater emphasis on production metrics, such as 305-day milk yield and reproductive outcomes, as well as on health indicators beyond CBT. Integrating the PPPV control logic with behavior-based alarms and existing barn automation platforms would enable truly adaptive ventilation, where cooling intensity is modulated based on both environmental conditions and the cows’ responses. Finally, comprehensive techno-economic and life-cycle assessments are essential to quantify the cost-effectiveness and ecological footprint of PPPV relative to conventional fan and soaker systems, including the potential for avoided milk losses and improved longevity (Herzog et al., 2021).

In summary, this dissertation demonstrates that non-invasive sensing, physics-based modeling, and targeted ventilation can be combined into a coherent strategy for mitigating heat stress in dairy cows. By aligning detection with what the cow experiences and aligning airflow delivery with where the cow lies and ruminates, the work points toward dairy barns that are not only more resilient to rising temperatures but also more responsive to the animals they house (Atkins et al., 2018; Mondaca and Cook, 2018; Vu et al., 2023). Future research that deepens these connections between animal-based signals and engineering interventions will be critical for sustaining welfare and productivity in a warming world.